MECHANISM UNDERLYING DYSREGULATED CEREBRAL VESSEL GROWTH IN ALZHEIMER'S DISEASE

by

Chaahat S.B. Singh

B.Sc., Guru Nanak Dev University, 2008

M.Sc. (Hons.), Guru Nanak Dev University, 2010

A THESIS SUBMITTED IN PARTIAL FULFILLMENT OF

THE REQUIREMENTS FOR THE DEGREE OF

Doctor of Philosophy

in

THE FACULTY OF GRADUATE AND POSTDOCTORAL STUDIES

(Medical Genetics)

THE UNIVERSITY OF BRITISH COLUMBIA

(Vancouver)

April 2019

The following individuals certify that they have read, and recommend to the Faculty of Graduate and Postdoctoral Studies for acceptance, the dissertation entitled:

MECHANISM UNDERLYING DYSREGULATED CEREBRAL VESSEL GROWTH IN ALZHEIMER'S DISEASE

submitted by **Chaahat S.B. Singh** in partial fulfillment of the requirements for the degree of **Doctor of Philosophy** in **Medical Genetics**

Examining Committee:

Dr. Wilfred A. Jefferies

Supervisor

Dr. Jan Friedman

Supervisory Committee Member

Dr. Peter Soja

Supervisory Committee Member

Dr. Haakon Nygaard

University Examiner

Dr. Stanley Floresco

University Examiner

Additional Supervisory Committee Members:

Dr. Wolfram Tetzlaff

Supervisory Committee Member

Abstract

Alzheimer's disease (AD), a neurodegenerative disorder of the elderly, causes loss of memory leading to dementia. The exact cause of this disease is still unknown, and the mechanism of pathogenesis highly debated. Amyloid beta (Aβ) peptide is central to the disease along with the cerebrovascular dysfunction and impaired cerebral blood flow (CBF). A strong link exitsts between brain vascular dysfunction and AD. This link was established due to evidence of reduced blood-brain barrier (BBB) integrity preceding various AD neuropathologies. Furthermore, BBB dysfunction could influence CBF, which in turn influences blood vessel growth. Current dogma holds that BBB leakiness is likely due to vascular deterioration. Inflammatory changes in the AD brain lead to up-regulation of mediators like, VEGF and Tie-2, that initiate angiogenesis. Studies indicate pathological angiogenesis and BBB disruption occur as a compensatory response to impaired CBF. Aβ-induced neuroinflammatory responses promote the generation of reactive oxygen species and further endothelial damage. Aβ is shown to be a modulator of blood vessel density and vascular remodeling via angiogenic mechanisms. Studies on the cerebrovascular integrity in AD model mice showed a significant increase in the incidence of disrupted tight junctions which is directly linked to an increase in microvascular density. This strongly supports amyloidgenesis-triggered angiogenesis as the basis of BBB disruption.

This thesis aims in attempting to curb vascular damage seen in the brains of AD mice and improve cognition by treating them with anti-angiogenic drugs providing scope for these to modulate cerebral angiogenesis to ameliorate Aβ load, reduce vasculature damage and reverting cognitive decline. This may facilitate new preventive and therapeutic interventions for not only AD but also related vascular diseases such as small vessel disease. As a part of the study, a mechanism for

vascular dysfunction in AD is proposed as follows: Aβ triggers dysregulated blood vessel growth via Angiopoietin-2 mediated activation of the Tie-2 receptor of the angiogenesis pathway. Also demonstrated in this thesis is that AD pathology can be established by a bone marrow transplant from an AD mouse model into an *APP* knockout mouse suggesting the role of soluble Aβ in AD pathogenesis.

Lay Summary

Alzheimer's disease is a condition where patients experience loss of neurons in the brain causing memory loss. It is shown that AD brains have deposits, comprised of a protein called amyloid. Amyloid is thought to be responsible for neuronal death. We reported that amyloid causes an increase in blood vessel growth in AD mouse brains. Uncontrolled sprouting of blood vessels leads to the breakdown of a barrier that protects the brain from disease causing microorganisms and unwanted products from the blood to enter the brain. We examined how blood vessels change throughout the course of AD, looking at the loss or reorganization of proteins that form the structural basis of the blood-brain barrier. We attempt to curb the damage seen in AD mouse brains and improve cognition by treating them with drugs that prevent the formation of new blood vessels and try to understand the mechanism of the disease pathology.

Preface

All *in vivo* experiments were approved and were performed in accordance with The University of British Columbia Animal Care Committee: Ethics Application number A17-0094 and A16-0299.

Chapter 3
A version of Chapter 3 is under preparation for two separate publications.

Anti-cancer drug Sunitinib reverses pathogenesis in a model of Alzheimer's disease (Manuscript in preparation)

Chaahat S.B. Singh, Lonna Munro, and Wilfred A. Jefferies

I was responsible for the experimental design, execution, and data analysis. Lonna Munro helped with experimental design and mouse perfusions. I was responsible for writing the manuscript, and Lonna Munro, Cheryl G. Pfeifer, and Wilfred A. Jefferies helped with editing and revisions. Wilfred A. Jefferies supervised the project.

Anti-VEGFR2 antibody: a therapeutic intervention towards Alzheimer's disease (Manuscript in preparation)

Chaahat S.B. Singh, Lonna Munro, and Wilfred A. Jefferies

I was responsible for the experimental design, execution, and data analysis. Lonna Munro helped with experimental design and mouse perfusions. I was responsible for writing the manuscript, and Lonna Munro, Cheryl G. Pfeifer, and Wilfred A. Jefferies helped with editing and revisions. Wilfred A. Jefferies supervised the project.

Chapter 4
A version of Chapter 4 is ready for submission for publication

Modulating vessel growth: a mechanistic explanation of dysregulated cerebral pathology in Alzheimer's disease

Chaahat S.B. Singh, Kyung Bok Choi, Grace Wang, Lonna Munro, Cheryl G. Pfeifer and Wilfred A. Jefferies.

I was responsible for experimental design, execution, and data analysis.
KB Choi helped with the experimental designs. Grace Wang helped with the execution of western blots. Lonna Munro helped with the perfusions.

I was responsible for writing the manuscript, and Lonna Munro, Cheryl G. Pfeifer, and Wilfred A. Jefferies helped with editing and revisions. Wilfred A. Jefferies supervised the project.

Chapter 5
A version of Chapter 5 is under preparation for publication

Haematopoietic stem cell transplant from AD mouse model produces Alzheimer's disease pathology in APP-KO mouse model

Chaahat S.B. Singh, Lonna Munro, Franz Fenninger, Cheryl G. Pfeifer and Wilfred A. Jefferies.

I was responsible for experimental design, execution, and data analysis.
Lonna Munro and Cheryl G. Pfeifer helped with the experimental design. Lonna Munro also helped with the perfusions. Franz Fenninger helped with the bone marrow isolations and helped with the FACS analysis.
I was responsible for writing the manuscript, and Lonna Munro, Cheryl G. Pfeifer, and Wilfred A. Jefferies helped with editing and revisions. Wilfred A. Jefferies supervised the project.

Table of Contents

List of Tables

List of Figures

List of Abbreviations

Aβ	Amyloid-beta peptide
Aβ 1-40	Amyloid-beta 1-40
Aβ 1-42	Amyloid-beta 1-42
AD	Alzheimer's disease
AJ	Adherens junction
Ang-1	Angiopoetin-1
Ang-2	Angiopoetin-2
APLP1	APP-like protein-1
APLP2	APP-like protein-2
ApoE	Apolipoprotein E
APP	Amyloid precursor protein
APP-KO	APP knockout
BBB	Blood-brain barrier
BACE1	β-secretase enzyme
CAA	Cerebral amyloid angiopathy
CBF	Cerebral blood flow
CNS	Central nervous system
CSF	Cerebral spinal fluid
CT	Computerized tomography
CVL	Cerebrovascular lesions
DNA	Deoxyribonucleic acid

EDTA	Ethylenediaminetetraacetic acid
EOAD	Early-onset Alzheimer's disease
GIST	Gastrointestinal stromal tumor
HAD	HIV associated dementia
HBEC-5i	Human brain endothelial cells-5i
HUVEC	Human umbilical vein endothelial cells
i.p.	Intraperitoneal
i.v.	Intravenous
KPI	Kunitz protease inhibitor
LDL	Low-density lipoprotein
LOAD	Late-onset Alzheimer's disease
LRP	Low density lipoprotein receptor-related protein
MAO	Monoamine oxidase
MRI	Magnetic resonance imaging
MVD	Microvessel density
NFT	Neurofibrillary tangle
NVU	Neurovascular unit
PBS	Phosphate buffered saline
PCR	Polymerase chain reaction
PD	Parkinson's disease
PDGFβ	Platelet derived growth factor-β
PET	Positron emission tomography
PFA	Paraformaldehyde

PrP	Prion protein
PSEN1	Presenilin 1
PSEN2	Presenilin 2
RAGE	Receptor for advanced glycosylation products
rCBF	Resting cerebral blood flow
RCC	Renal cell carcinoma
ROS	Reactive oxygen species
SEM	Standard error of the mean
SNPs	Single-nucleotide polymorphisms
Tf	Iron transferrin
TFA	Total fluorescence area
Tg2576	Transgenic heterozygous Tg2576 AD mouse
Tie2	Tyrosine kinase with immunoglobulin-like and EGF-like domains-2
TJ	Tight junction
TJP	Tight junction protein
TKI	Tyrosine kinase inhibitor
TNFα	Tumor necrosis factor α
VD	Vascular disease
VEGF	Vascular endothelial growth factor
VEGFR2	Vascular endothelial growth factor receptor 2
ZO1	Zona occludin 1

Acknowledgements

My special gratitude to my mentor and Supervisor, Dr. Wilfred Jefferies for taking me on in his lab and encouraging me to find my own path to swim and reach my goals in research. Wilf, thanks for this opportunity and the guidance.

To my committee members; Dr. Soja- you believed in me in the darkest hours especially during my first year at UBC. I can never thank you enough for that. Dr. Friedman- I have learnt so much from you. You were always so generous with your availabilities and your willingness to help and giving sound research advice. Dr. Tetzlaff- I thank you for coming on board in the last leg of this journey of mine. I thank you all for sharing your knowledge, time and support.

I am especially grateful to Hitesh, Samantha, Brett, Sarah, Shawna, Franz, KB, Pablo, Maria, Grace and all the other, present and former, lab members from the Jefferies' group who I interacted with. Most of you were the recipients of my tears, joys, failures and resilience- your support and assistance made the lab 'a home away from home'. It was great sharing the lab and this journey with each of you.

To Dr. Cheryl Pfeifer, thank you for your constant encouragement and advice. Agreeing to order all the expensive materials and kits to help me do my experiments, but most of all for putting up all those jokes on the white board to help us cope with our long days of experiments and lighten our moods.

To Lonna Munro, my heartfelt gratitude to you for being a constant friend, for all your help, your true support and for your positive vibrations. You have always silently helped all of us

in the lab. Thank you for being there during my emotional outbursts in general but specifically due to the animals that were sacrificed during the course of this study. Thank you for being that voice of reason. I would not have been able to work as much as I did with the mice if it weren't for you supporting me emotionally besides doing all the perfusions for me.

Friends are anchors in the stormiest seas and I've weathered these storms because of Varun, Rupinder, Ansu, Vishakha and all my friends. To Kanwaljit Kaur, thank you for helping me on my spiritual journey and for the healing and for your prayers.

Finally, and by no means the last- my family-My brother, Urvash Bir, my friend, my rock, who remains in the shadows but is always at hand. You have always been my pillar of support through everything in life. Thank you for being my 4 am friend, that one person I can lean on anytime.

My father Shivinder Bir, you always jumped with joy at any experiment that went right, even if it was beyond your understanding and pushed me on. I can never forget the hours spent explaining my research to you, only to find you forgetting it the very next moment. How that would crack us up.

Last but not least, my mother, Manpreet, you have been my life coach, my eternal friend and cheerleader, always interested, encouraging and positive. The one who taught me to dream big and to be a confidant and an independent woman.

My angel, my little Beagle, Mischief, you have been my beacon of light, whenever I am down and out, your spirit lifts we back up and tells me that you have faith in me. Thank you for your unconditional love.

To all- it is said 'When your mentor and God, both stand side by side, choose to supplicate before your mentor, as he shows you the path to God'. Thank you all.

Dedication

This thesis is dedicated to:

Late. Col. Surinder Singh (my paternal grandfather)
Dadaji, you gave me the strength and the reason for perusing research in Alzheimer's disease.

Late. Col. Inderbir Bawa (my maternal grandfather)

Nanaji, your interest and encouragement made all the difference along this journey. The heaviness in my heart will always remain knowing that I was so close to completion when you passed away.

Late. Laj Bawa (my maternal grandmother)

Nanima, you taught me 'no mountain is impossible to climb'. Your spirit is with me always, guiding me and loving me. I have missed you every single day since you left us.

Balbir Surinder Singh (my paternal grandmother)

Dadima, you are ever enthusiastic, encouraging and full of life. I owe it to you and your support for my research. It was painful to lose Dadaji the way we did to this horrid disease.

Chapter 1 Introduction

1.1 Alzheimer's disease

Alzheimer's disease (AD) presents itself as a progressive neurological disorder, which is the major cause of dementia leading to deaths in the elderly. It affects thinking, orientation and memory, causing impairment in cognition, social behaviour and motivation [1]. Approximately 47.5 million people worldwide have dementia, of which the most common contributor is AD at 60-70% [1]. According to the World Alzheimer Report of 2015, the total global societal costs were estimated to be 818 billion USD, corresponding to 1.0% of the worldwide gross domestic product and estimated to surpass 1 trillion USD by 2018 [2]. It is estimated that the annual cost associated is going to balloon to over 2 trillion USD by 2030.

1.1.1 History of Alzheimer's disease: the inception

The year 1901 saw one Auguste Deter, a 50-year-old patient at the Frankfurt mental institution, examined by Dr. Alois Alzheimer for her mental issues. He described her condition as having a severe cognitive impairment related to memory, language and social interactions. In 1906, after her death, Dr. Alzheimer [3] began characterization of her brain and noted two microscopic neuropathological findings: senile neuritic plaques, which are aggregates that are primarily composed of β-amyloid (Aβ) peptides; [3-5] and neurofibrillary tangles (NFTs), which are primarily composed of intraneuronal hyperphosphorylated aggregates of 'tau protein' [6]. In 1910, psychiatrist Emil Kraepelin, Dr. Alzheimer's colleague, coined the name "Alzheimer's disease" for this disorder. Following the discovery of the electron microscope, detailed study of the brain

was possible, and in 1984 β amyloid protein and in 1986 NFTs were isolated and further characterized [4, 5]. Aβ plaques and NFTs were eventually established as the hallmarks of AD.

1.1.2 Alzheimer's disease: an abridged account

AD is described as a form of 'dementia', which is an umbrella term that encompasses a collection of non-specific symptoms associated with cognitive functioning where memory, attention, personality, language and problem-solving abilities are affected. It is a complex neurodegenerative disorder, progressive in nature, and is known to be the most common form of dementia, presenting itself as the leading cause of deaths in the elderly. Neurodegeneration is defined as the loss of structure and function and probably including cell death of neurons which are the specialized type of cells of the central nervous system (CNS) that communicate information electrically and chemically throughout the body. These signals relate information regarding movement, the senses and memory. With the escalation of neuronal degeneration, the survival of patients affected with AD is typically 3-10yrs [7].

There are two known forms of AD: familial and sporadic. The familial form also referred to as early-onset Alzheimer's disease (EOAD), accounts for <5% of the diagnosed cases [8]. It has an overriding genetic component and tends to strike at an early age (prior to ages 60-65yrs). Sporadic AD also referred to as late-onset Alzheimer's disease (LOAD), has a complex and multifactorial etiology but generally strikes an aging brain (>65yrs) [8].

The diagnosis of AD is labyrinthine, and a singular test does not yet exist. A patient displaying "noticeable" gradual cognitive decline is put through a battery of imaging such as CT scans, PET scans and/or MRI procedures or neurological, blood and psychological tests like the mini-mental

state examinations [8]. Furthermore, other forms of dementia, such as Parkinson's disease (PD), vascular dementia (VD) or secondary forms like HIV-associated dementia (HAD) must be ruled out. Upon a probable diagnosis, a patient is categorized according to the severity of their disease and symptomatic treatment options will be given. A cure for AD currently does not exist.

1.1.3 Disease pathology

The two neuropathologies observed by Dr. Alzheimer that were eventually established as the hallmarks of the disease bearing his name were: amyloid plaques and neurofibrillary tangles (NFT) [9]. These can be described as pathologies that are a result of protein aggregation. Amyloid plaques are the embodiment of the aberrant extracellular aggregation of a peptide called amyloid-β (Aβ). NFTs are the intracellular neuronal aggregation of a microtubule stabilizer protein called tau. It is yet to be demonstrated whether Aβ plaques and/or NFTs are a cause or an outcome of AD. Both pathologies are believed to contribute to a cascade of events that leads to pathological alterations in the CNS and eventual symptoms of AD. The pathogenesis is a highly debated subject. Several factors like angiogenesis, inflammation and oxidative stress, which may contribute to the development of AD, have been examined and are discussed later in the chapter.

1.1.3.1.1 Amyloid β: The culprit and its genesis

In 1984, researchers George Glenner and Caine Wong isolated a peptide from AD senile plaques and reported, for the first time, the identification of "a novel cerebrovascular amyloid protein," known as β-amyloid (Aβ). This was established as the chief component of AD brain plaques and a crucial candidate for triggering nerve cell damage. Subsequently, similar plaque deposits were noted in the brains of individuals with Down's syndrome [5, 10, 11]. Upon detailed molecular

evaluation, it was found that Aβ, a 4 KDa peptide, is a product of proteolytic cleavage of the amyloid precursor protein (APP) by the action of β and γ secretase enzymes [12, 13]. Mutations either in the *APP* gene or the secretase enzyme complex lead to β secretase cleavage, forming a pathogenic Aβ species (Aβ42). These Aβ molecules aggregate to form oligomers, which multimerize into protofibrils, followed by the formation of dense core amyloid plaques [14-16]; this cleavage pathway has been extensively characterized in Figure 1.1 (reviewed by [17]).

The connection of Aβ to Down's syndrome eventually led to genetic analysis and the cloning of the *APP* gene which became the first deterministic gene for AD [18]. APP is a type 1 integral membrane protein belonging to an evolutionarily conserved gene family [19] found on chromosome 21 in humans. In mammals, three major isoforms of the *APP* gene are known to exist: *APP695*, *APP751* and *APP770*. Although *APP* is ubiquitously expressed, certain isoforms are predominantly tissue specific. *APP695* is primarily expressed in the brain [18], while *APP751* and *APP770* are mostly found in platelets [20, 21]. All the isoforms of *APP* have a large extracellular N-terminal portion and a shorter cytoplasmic C-terminal sequence [22]. The presence or absence of a Kunitz protease inhibitor (KPI) domain is the major difference between these isoforms. The *APP695* is devoid of this domain, which is known to be capable of inhibiting blood clotting [23-26]. Homologs of *APP* have also been identified and are termed as APP-like protein-1 [27] and -2 [28] (*APLP1* and *APLP2*). Although these have similar protein structures and similar predicted proteolytic cleavage patterns to APP, they are not involved in the production of Aβ. The relevance of the *APP* isoforms to AD is ambiguous.

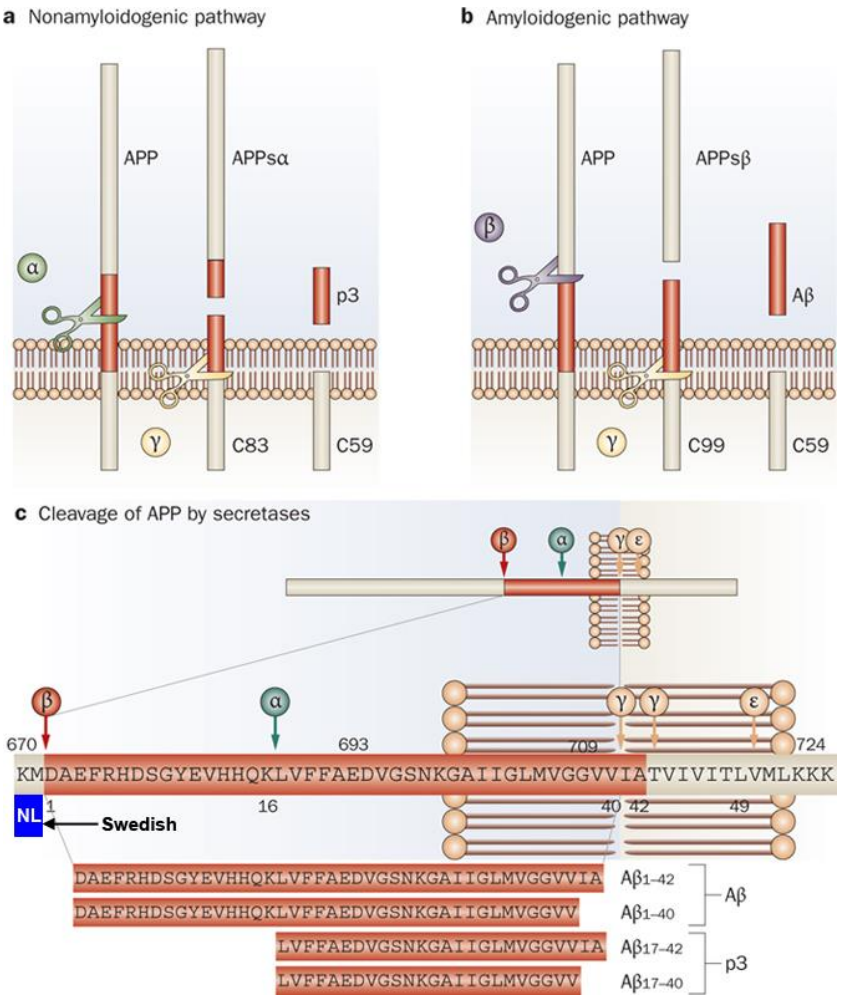

Figure 1.1: Processing of APP by the secretases.

APP can undergo two distinct proteolytic cleavage functional pathways. (a) **The nonamyloidogenic pathway**: α-secretase initially cleaves APP within the Aβ sequence. This releases the APPs-α ectodomain. The next stage is the γ-secretase processing the carboxyl terminal of the Aβ domain culminating in the release of the neuroprotective fragment called p3 fragment. (b) **The amyloidogenic pathway**: initiates with the β-secretase cleavage of APP at the amino terminus of Aβ domain, releasing the APPs-β ectodomain. Further processing at the carboxy-terminal fragment of the Aβ domain, by γ-secretase which results in the release of Aβ. (c) **The target amino acid residues where various secretases cleave APP.** Either p3 fragments or Aβ of differing lengths is produced by processing of APP at two different sites by γ-secretase. The blue box depicts the location of the familial Swedish mutation (KM670/671NL). Abbreviations: Aβ, amyloid-β peptide; APP, amyloid precursor protein; APPs-α, soluble amyloid precursor protein-α; APPs-β, soluble amyloid precursor protein-β; C83, carboxy-terminal fragment 83; C59, carboxy-terminal fragment 59; C99, carboxy-terminal fragment 99 [Figure is taken from open access review of De Strooper et al., 2010 [29]].

1.1.3.1.2 The road from APP to amyloid-β plaques

A sequential proteolytic breakdown of APP into its various products occurs as a result of a combination of three distinct secretase enzymes (γ and α or β) [17]. Depending on the action of a combination of these secretase enzymes, two major APP processing pathways can result. The involvement of the α and γ-secretases precludes the production of Aβ; this is known as the 'non-amyloidogenic' pathway (**Figure 1.1a)**, whereas, the activity of β and γ-secretases together liberate soluble Aβ and hence constitute the 'amyloidogenic' pathway as shown in **Figure 1.1b**. It is approximated that under normal physiological conditions, 90% of APP is processed by means of the non-amyloidogenic pathway [30]. A mere 10% of the APP undergoes cleavage to small amounts of Aβ peptide in physiological conditions. Although the physiological functions of the various cleavage products of either pathway are not clear, some like the soluble APP α-secretase cleavage product (APPs-α) in **Figure 1.1a** is thought to be neuroprotective [30, 31]. It is unclear what the definitive physiological function of APP is, however, APP and its homologs may have a physiological function in processes like neuronal growth and survival, cell adhesion and insulin-glucose homeostasis (reviewed briefly by Jacobsen *et al.* (2009) [19]).

Knocking out the *APP* gene in mice is not lethal, and APP null mice are viable, but they present a number of metabolic and behavioural deficit phenotypes [32]. It has been shown that these phenotypes can be rescued by reintroducing the APPs-α fragment [32]. Mice lacking all three APP homologs (APP, APLP1 and APLP2) are not viable [33]. This suggests that APP, and its related proteins, are physiologically important.

The β and γ-secretase cleavage pathway have received the most attention for its potential pathological status as it results in the secretion of soluble Aβ. However, since low quantities of Aβ are also secreted under normal conditions, it suggests that Aβ may have a 'yet to be discovered' physiological function as well [34-36]. Aβ has several different liberated sizes ranging from 38 to 43 amino acids in length. The most common Aβ fragment is 40 amino acids in length; Aβ1-40 (**Figure 1.1c)** and is estimated to be 90% of the Aβ species produced [13]. The slightly longer and allegedly more toxic 42 amino acid species (Aβ1-42) is a minor product of APP cleavage.

The length of the Aβ species produced is a result of two γ-secretase cleavage sites on the full-length APP that are two amino acids apart. The amyloidogenic pathway is enhanced by certain mutations found either on the *APP* gene or the individual subunits that constitute the γ-secretase enzyme complex. These mutations are associated with the rarer Early onset AD (EOAD) [37] and favour the increased specific production of species Aβ1-42 [16, 38], like the familial 'Swedish' double mutation. This results in a six-fold increase in Aβ1-42 [14, 39] due to increased β-secretase processing [15]. These mutations have been the basis of AD-like transgenic mouse models, where the increased production of Aβ can lead to AD, as is the case for EOAD.

Aβ has a property of being 'sticky' and can spontaneously form aggregates ranging in size from dimers to larger oligomers. These oligomers may multimerize into protofibrils, which can further aggregate into what are known as 'insoluble dense-core Aβ plaques', a hallmark of AD. The mechanics, biochemistry and physics behind amyloid aggregation have been extensively studied [40]. The more toxic Aβ1-42 species is believed to have a greater ability to form aggregates [41], while Aβ1-40 is soluble. The bulk of the plaques and vascular deposits of Aβ seen in the disease

is composed of Aβ1-42 [42, 43]. There are different schools of thought regarding the pathophysiology of AD. The most studied is the 'Amyloid Cascade Hypothesis', which deems the aggregated form of Aβ as the cause of AD. However, there is a recent wave of change in the thinking that suggests that the extracellular dense-core Aβ plaques are not the cause of AD related dementia, but the soluble Aβ oligomers are [44], because there has been no direct correlation between the number of plaques and the severity of dementia in AD [45]. Studies *in vitro* and *in vivo* have demonstrated that oligomers of Aβ have greater neurotoxicity than the insoluble plaques [46-49]. While the mechanism(s) of oligomer formation and toxicity still remain unclear, it is known that the process can occur both extra- and intracellularly (reviewed by Sakono *et al.* 2010 [44]).

1.1.3.2 Risk Factors

1.1.3.2.1 Genetic risk factors

AD is a genetically heterogeneous disorder, with a chronic complex neuropathology that involves multiple factors. Common risk alleles have been either associated with APP directly or with the two different proteins that make up the secretase enzyme complex, Presenilin-1 and 2 (PSEN1, PSEN2). These mutations increase APP metabolism, generating higher proportions of the toxic Aβ1-42 species and are associated with the familial form of the disease [50, 51].

The late onset familial AD termed LOAD has a well-documented association with Apolipoprotein E (*APOE*) e4 allele on chromosome 19. Early onset AD (EOAD), is due to mutations in the *APP* gene on chromosome 21 (10-15% of familial cases), mutations in the presenilin-1 gene (*PSEN1*) mutation on 14q, being the most common (30-70%) form of EOAD and mutations in the *PSEN2*

gene on 1q31 that accounts for <5% of the EOAD cases. Two risk factors associated with sporadic AD have been identified and are the *APOE* genotype and vascular abnormalities [50, 51].

Down syndrome (Aneuploidy): People with trisomy 21 develop neuropathologic hallmarks of AD after 40 years of age. This can be explained due to the presence of the *APP* gene on chromosome 21 resulting in the lifelong over-expression of APP and increased levels of Aβ in the brains of individuals with the additional chromosome [51].

APP mutation: The age of onset is 40-50 years. In 1992, Mullan *et al.* found a double mutation (K670N/M671L) in the *APP* gene in brain samples from a Swedish family that showed an early onset of AD, with an autosomal dominant inheritance pattern. This was termed the 'Swedish mutation'[15]. Another example is the p.Glu693Gly 'Arctic' mutation in *APP* which is associated with enhanced Aβ protofibril formation [52] and marked congophilic angiopathy (i.e. angiopathy in which amyloid deposits form in the walls of the blood vessels of the central nervous system) [53, 54]. Di Fede *et al.* reported a p.Ala673Val mutation in *APP* [55]. This causes disease pathology only in the homozygous state and thus shows autosomal recessive inheritance [53]. This mutation is at the site where BACE1(β secretase) cleaves the APP protein to produce Aβ. The combination of cerebral hemorrhage and presenile dementia is caused by a p.Ala692Gly mutation in the *APP* gene [56].

PSEN1 mutation: The age of onset is usually 40-50 years, but cases with onset as early as 30 years and as late as 60 years have also been reported. Van Broeckhoven *et al.* (1987,1992) presented evidence of EOAD linkage to chromosome 14q [21, 53, 57]. They narrowed down the

candidate region to an 8.9-cM area between locus D14S42 and D14S53. Campion *et al.* (1995) confirmed the location of the responsible gene on chromosome 14q 24.3 [58] followed by the identification of 5 missense mutations in *PSEN1* gene that co-segregate with early onset familial AD3 [59]. These missense mutations leading to the disease were detected by sequence analysis of the coding region and associated intronic regions. A rare 4.6Kb deletion was found spanning exon 9 of the *PSEN1* gene in the Finnish population, which is associated with spastic paraparesis [60]. Mutations in PSEN1 protein, specifically p.Leu113Pro and p.Val89Leu, have been associated with a frontotemporal type of dementia accompanied by personality and behavioural changes. PSEN1 mutations p.Leu392Pro and p.Met139Val were shown to contribute to psychiatric symptoms. Miklossy *et al.* in 2003 reported that the very early onset (30 years) 'Lewy body' pathology was due to mutant p.Met233Val and p.Tyr256Ser PSEN1 [61].

PSEN2 mutation: This has a wider range of age onset than AD1 and AD3 (40-70 years) with a few instances of non-penetrance, where the onset might even be as late as after 80 years. Jayadev *et al.* in 2010 reported cases from the Volga German families carrying the same N141I mutation in *PSEN2* [62]. This premature termination mutation, leading to the loss of function or haploinsufficiency is proposed as the pathogenic mechanism in presenilin 2 associated Alzheimer's disease.

Late onset familial AD: This is the most common form of the disease with an onset usually at 80 years of age. A well-documented association is seen between late onset familial AD and *APOE ε4* allele [63-65]. In 1993, Coder *et al.* found that the risk of AD2 increases from 20% to 90% and the mean age decreases from 80 to 68 years with an increase in the number of variant *APOE ε4*

allele [63-65]. A genome-wide linkage analysis conducted in families with AD for the presence or absence of this allele showed a tight linkage to the *APOE* region (19q13).

APOE codes for Apolipoprotein E, a soluble lipoprotein that is a ligand responsible for packaging and delivery of cholesterol in the brain. Apo-E is produced mainly by astrocytes in the brain [66] and aids in the maintenance of neuronal synapses [67]. It is proposed to play a role in the Aβ production as well as its deposition. Though isoform ApoEε2 is involved in neuroprotection and memory enhancement, the ApoEε4 isoform accelerates the AD pathogenesis. It has a gene dose effect on the risk of developing AD at an earlier age. It is involved not only in the familial AD but the sporadic LOAD as well. It is known to be neurotoxic and leads to NFT formation. It has been shown to modulate brain inflammatory responses and to induce higher oxidative stress in persons with this allele [63-65].

APOE has three major isoforms as a result of single-nucleotide polymorphisms (SNPs), namely, *APOE2*, *APOE3* and *APOE4* [68]. The allelic copy number of *APOE4* determines the risk for developing the sporadic form of AD, and it increases significantly to nearly 12 times depending on the number of *APOE4* copies, compared to the other isoforms [69]. The mechanism for this increased risk is not clear since Apo-E has both neuro-disruptive and neuroprotective properties. Apo-E (sometimes further enhanced by ApoE4) is known to bind and act as a chaperone for Aβ [70], promote Aβ aggregation [71], influence APP metabolism [72] and affect Aβ clearance [73].

Other genetic factors: Other genetic polymorphisms associated with AD include the *NOS3* gene, the *LRP1* gene (low density lipoprotein), and the *VEGF* gene (Vascular endothelial growth factor) [50].

Protective polymorphisms: Jonsson *et al.* (2012) found a coding mutation in the *APP* gene, pAla673Thr substitution. This lies adjacent to the aspartyl protease β-site in APP, i.e. the site where BACE1 cleaves APP to form Aβ. This was shown to protect against AD and cognitive impairment, even in the elderly without AD, providing proof to the hypothesis that a decrease in β cleavage alleviates pathology [74].

1.1.3.2.2 Metabolic factors in AD:

Evidence suggests that mitochondrial DNA polymorphisms may represent another risk factor in AD. In 1999 Blass and Gibson advanced the notion of defective energy metabolism in AD and then in 2000 showed reduced rates of brain metabolism[75, 76]. An increased oxidative utilization has been noted as compared to glucose utilization. In AD patients, the most consistent defect seen in mitochondrial electron transport enzymes is the deficiency of cytochrome c oxidase, which causes abnormal oxidative phosphorylation [77]. The mitochondria contain a molecular switch, referred to as a mitochondrial permeability transition pore, for apoptosis. It activates apoptosis inducing factors and caspases. The opening of this pore can be affected by increased reactive oxygen species (ROS) and/ or toxic free radicals that accumulate due to deficient electron transport [77].

1.1.3.2.3 Environmental factors:

Association studies have identified environmental agents such as diet, trace metals in the brain and viral infections that are as important in the etiology of AD as genetic factors. This was a conclusion drawn from the 'Challenging views of AD' meeting in Cincinnati in 2001 [78].

Dietary Fats: Cohort studies investigated the association between diet and AD and concluded that the total fat consumption and total caloric intake are the most important environmental risk factors, both of which contribute to oxidative stress [79, 80]. Linoleic acid, a polyunsaturated fatty acid, has been associated with cognitive impairment. These are pro-inflammatory and enhance interleukins. Contrastingly, monounsaturated fatty acids reduce risk and including them in the diet can delay the age of onset of AD [79]. A great example of this is fish oil, which is high in omega 3 fatty acids that contain docosahexaenoic acid, an important fatty acid responsible for the development of the brain. Cholesterol is another factor that is governed by diet, especially dietary sugars and saturated fats [79, 80]. Cholesterol esters have been correlated with Aβ production. Statins are prescription medications that reduce the risk of AD by lowering cholesterol and shifting the activity from β and γ to α secretase thereby decreasing the accumulation Aβ [79, 80].

Trace metals: Studies showed elevated levels of trace metals and Aluminium (Al^{+3}) ions in the brains of deceased AD patients compared to healthy individuals, whereas the alkali metal concentration was reduced [79, 80]. Diets high in acids and low in alkali metals are seen to be the contributors. Calcium (Ca^{+2}) and other metals get removed from the body at low pH values and further increase the acidity of the whole body. As pH falls, transition metal ions are released from their oxide forms. They enter the serum and are then transported to the brain [79, 80]. Diets high

in acid ash proteins have been shown to cause excess Ca^{+2} loss and vegetables/fruits high in potassium reverses acid-induced Ca^{+2} loss. These metals and Al^{+3} contribute to oxidative stress and inflammation by catalyzing free radical production and formation of advanced glycation end-products (AGEs), which are proteins or lipids that become glycated as a result of exposure to sugars [79, 80]. These free radicals and AGEs can be a factor in aging and in the development or worsening of many degenerative diseases like diabetes and AD. The stress generated promotes aggregation of physiological concentration of Aβ. Glycoxidation by transition metals has also been shown to accelerate cross linking of Aβ to produce plaques, Al^{+3} in particular causes neurotoxicity and is detected in high concentrations in lesions that resemble either NFTs and/or plaques. It also increases levels of inducible nitric oxide synthetase, leading to ROS production. In addition to this, Al^{+3} activates NF-κB, which turns on inflammatory genes causing neurodegeneration [79, 80].

Viral infections: The latent from of the Herpes Simplex Virus (HSV) resides in the peripheral nervous system (PNS) of most humans. It can cause a rare acute infection of the brain called herpes simplex encephalitis. The encephalitis caused by this virus affects the same regions of the brain that are damaged in AD. Studies show that both the latent viral DNA in the brain and the APOEε4 allele lead to disease state while acting in conjunction with each other and due to their inter-dependence. APOE ε4 is seen as a frequent risk factor of dementia even in other viral infections like HIV and Hepatitis C [79, 80].

1.1.3.2.4 Interactions between genetic and environmental factors:

Twin studies were mostly used to establish a relative contribution of both genes and environment. Recent research suggests the importance of epigenetic mechanisms in defining this relationship between the two. Toxological and epidemiologic studies show that an early life exposure to metals

like lead is associated with latent APP pathway dysregulation [81-83]. An experiment where primates were exposed to lead showed an increased amyloidgenesis and detected the upregulation of proteins like APP and the β site APP cleaving enzyme.

Global changes occurring in AD have been observed in DNA methylation, miRNAs and histone modifications [81-83]. DNA hypomethylation was observed in the entorhinal cortex of AD patients in a post mortem study. Another showed differential regulation of miRNAs- 204, 211 and miR-44691. Age-matched AD cases depict an increase in neuronal global phosphorylation of histone 3. Epigenetic dysregulation of important AD tau and amyloid processing pathway genes leads to a potential mechanism for disease progression.

Environmental toxin lead or a reduced uptake of Vitamin B12 and folate can cause *PSEN1* and *BACE1* to be hypomethylated and their mRNA expression greatly induced [81-84]. In contrast, a low CpG density region of *APOE* promoters is seen to be hypermethylated in cases of LOAD. Unlike the genome, the epigenome of an organism is largely malleable and reactive to the environmental factors. Understanding these environmental interactions can give us a deeper insight into AD etiology and may help in intervention and management of the disease progression.

Epidemiological studies indicate interactions between *APOE ε4* allele and cholesterol levels, leading to an increased risk of AD compared to those without the allele [81-83]. Similarly, APOE ε4 interacts with smoking and alcohol consumption as well to elevate the risk. Thus, environmental factors may cause the phenotype only in the presence of a certain genotype. Since clinical epidemiological studies do not give information about the mechanism, animal models are used to study these interactions [81-83]. Transgenic mice with different mutations (APP, APOE ε4,

APP/PS1) are taken along with the age-matched controls and exposed to various environmental factors under consideration (metals, stress, traumatic brain injury, different diets, exercise, etc.) to give insightful knowledge and mechanistic information about the relationship between genetic factors and environmental risks involved in the disease [81-83].

1.1.4 The canonical amyloid cascade hypothesis and the case for rejecting it

Since the discovery of AD much of the work done to understand the mechanism of pathogenesis was directionless. Amidst this chaos, in 1992, Hardy and Higgins proposed the first hypothesis for AD [12, 85]. Several observations guided them to this hypothesis. Plaques were identified to be comprised of Aβ that was later established as the cleavage product of APP. Certain familial forms of the disease involved mutations in APP and its cleavage enzyme complex. It was also known that people with Down's syndrome often developed early-onset dementia with AD-like symptoms. After the mapping of the *APP* on chromosome 21, it was confirmed that since people with Down's syndrome have trisomy of chromosome 21 their brains were producing an excess of Aβ which could possibly explain AD like symptoms.

The amyloid cascade hypothesis is the most studied and well defined theoretical framework of AD [86]. The hypothesis states that: The deposition of amyloid β protein, the main component of plaques, is the causative agent of AD pathology and that NFTs, cell loss, vascular damage and dementia follow as a direct result of this deposition. Although it is the most studied hypothesis in the last 20 years, it has been heavily criticized and scrutinized [86, 87] and is not universally accepted due to various findings. Evidence for neurotoxicity of Aβ aggregation is not robust [88, 89]. Furthermore, senile plaques can be found in the brains of some Down's Syndrome patients

and the elderly during autopsy, with no apparent neurodegenerative changes [88, 90]. A meta-analysis showed that this clinical model, based on amyloid aggregation with dementia, is apparently unfounded for at least 30% of elderly with detectable amyloid pathology [91].

Moreover, therapeutics based on this hypothesis have been unsuccessful. For example, immunotherapies employing the use of monoclonal anti-amyloid antibodies thus far have failed; although these antibodies showed clearance of amyloid deposits in the brain, they were unable to provide benefits for the cognitive and neurological outcomes of the patients [92]. A study revealed that from 2002-2012, 65% of the clinical trials involved therapeutics with some form of Aβ protein as a pharmacological target. With a 99.6% failure rate, these trials were unable to validate Aβ as a target [93]. These trials also suggested that there was a translational gap between pre-clinical and clinical trials of AD [93].

Although important, Aβ is by itself not necessary to cause the disease, and growing evidence supports the concept that in addition to neurons, the neurovascular unit is affected in AD [94, 95], and it has been shown that AD can be mediated by pathological angiogenesis [88, 96],[97],[98]. Vascular dysfunction now appears to be a crucial pathological hallmark of AD, and the two key precursors to neurodegenerative changes and Aβ deposition in AD are blood brain barrier (BBB) breakdown and Cerebral Blood Flow (CBF) impairment [99-101]. This has given rise to the alternative hypothesis where angiogenesis leads to defective neuro-vasculature, thereby disrupting the BBB and impairing CBF and compromising the clearance of Aβ [99, 102, 103]

1.1.5 AD and vascular dysfunction

1.1.5.1 Initial clinical observations linking AD and vascular disease

Post-mortem analysis has established that 50% to 84% of the brains of persons who die at 80 to 90+ years of age show appreciable cerebrovascular lesions (CVL). Although there is a debate around their impact on AD pathology, it has been suggested that dementia caused by vascular and AD-type pathologies may be independent and have additive or synergistic effects on cognitive impairment [104].

Vascular pathologies that have been seen in the aged human brain include cerebral amyloid angiopathy (CAA), cerebral atherosclerosis, small vessel disease (in most cases caused by hypertensive vasculopathy) and microvascular degeneration or BBB dysfunction, causing white matter lesions, microinfarctions, lacunar infarcts and microbleeds [96]. CAA was shown by Kövari et al. to play a role in the development of microvascular lesions in the aging human brain [105] Cerebrovascular infarcts were shown to be linked to CAA in those with minimal amyloid plaques and the severity of CAA was seen associated with cognition in APOE ε4 negative AD patients [106] Studies in post mortem human brains also found evidence of increased angiogenesis in the hippocampus, midfrontal cortex, substantia nigra pars compacta, and locus coeruleus of AD brains when compared to 'control' brains, suggesting that vascular dysfunction is an inherent part of AD pathology [96, 98]. Buée et al. demonstrated degenerative changes and a global impoverishment of the cortical vascular bed in AD patients [107, 108]. Bouras et al. indicated, through stereological analysis, that the changes in the mean capillary diameter of the hippocampal and entorhinal cortex was related to the clinical dementia rating scores in the AD patients [109].

1.1.5.2 Genetic risk factors linking AD and vascular disease

Epidemiological studies have identified risk factors for AD that are similar to those for cardiovascular disease (CVD) such as hypertension during midlife, diabetes mellitus, smoking, apolipoprotein E (ApoE) ε4 isoforms, hypercholesterolemia, homocysteinemia and, in particular, aging [94]. The familial form of AD is caused most commonly by presenilin 1 (*PSEN1*) or presenilin 2 (*PSEN2*) mutations. It is also seen that the presenilins are expressed in the heart and are critical to cardiac development. The work by Li *et al.* indicated that *PSEN1* and *PSEN2* mutations are associated with dilated cardiomyopathy and heart failure, implicating novel mechanisms of myocardial disease [110]. Amyloid is a known vasculotrope, and increased amyloid aggregation in AD brains interacts with the angiogenic and CAA positive vessels [94]. Apo-E ε3 is responsible for normal lipid metabolism; however, the Apo-E ε4 isoform is strongly associated with late onset AD. Carriers of this isoform show a decreased cerebral blood flow and have also been linked to disorders associated with elevated cholesterol levels or lipid derangements such as hyperlipoproteinemia type III, coronary heart disease, strokes, peripheral artery disease, and diabetes mellitus [111]. These overlapping genetic risk factors might give us a direction for understanding the mechanisms of the disease related pathways.

1.1.5.3 Factors linked to AD and increased angiogenesis: VEGF and amyloid

Overexpression of VEGF receptor-2 (VEGFR2) was observed in newly formed vessels, suggesting that the angiogenic activity of melanotransferrin may depend on the activation of endogenous VEGF [112]. VEGF is the major player in pathological/dysfunctional blood vessel formation. It is shown that VEGF is highly upregulated in AD brains via the inflammatory pathway and also that VEGF co-aggregates with Aβ in AD brains [98]. The role of transglutaminases in AD is highly

debated; however, it is known that the activity of these enzymes might contribute to the formation of protein aggregates in the AD brain [113, 114].

1.2 The blood-brain barrier and AD pathogenesis

The BBB is the anatomical description of the extensive network of capillary blood vessels that permeate the entire brain [115]. It is approximated to be a total length of more than 600 km in humans [116]. These vessels compartmentalize the brain from the peripheral blood with the help of highly specialized endothelial cells that line these vessels. The seal between these cells is conserved by the tight junction proteins (TJP) **(Figure 1.2)**. Compartmentalizing helps create an optimal microenvironment, which restricts ion movement and reduces 'cross-talk' of molecules like neurotransmitters between the brain and peripheral tissues. The BBB also prevents potentially toxic substances from the peripheral immune system and/or pathogens from entering and damaging the CNS.

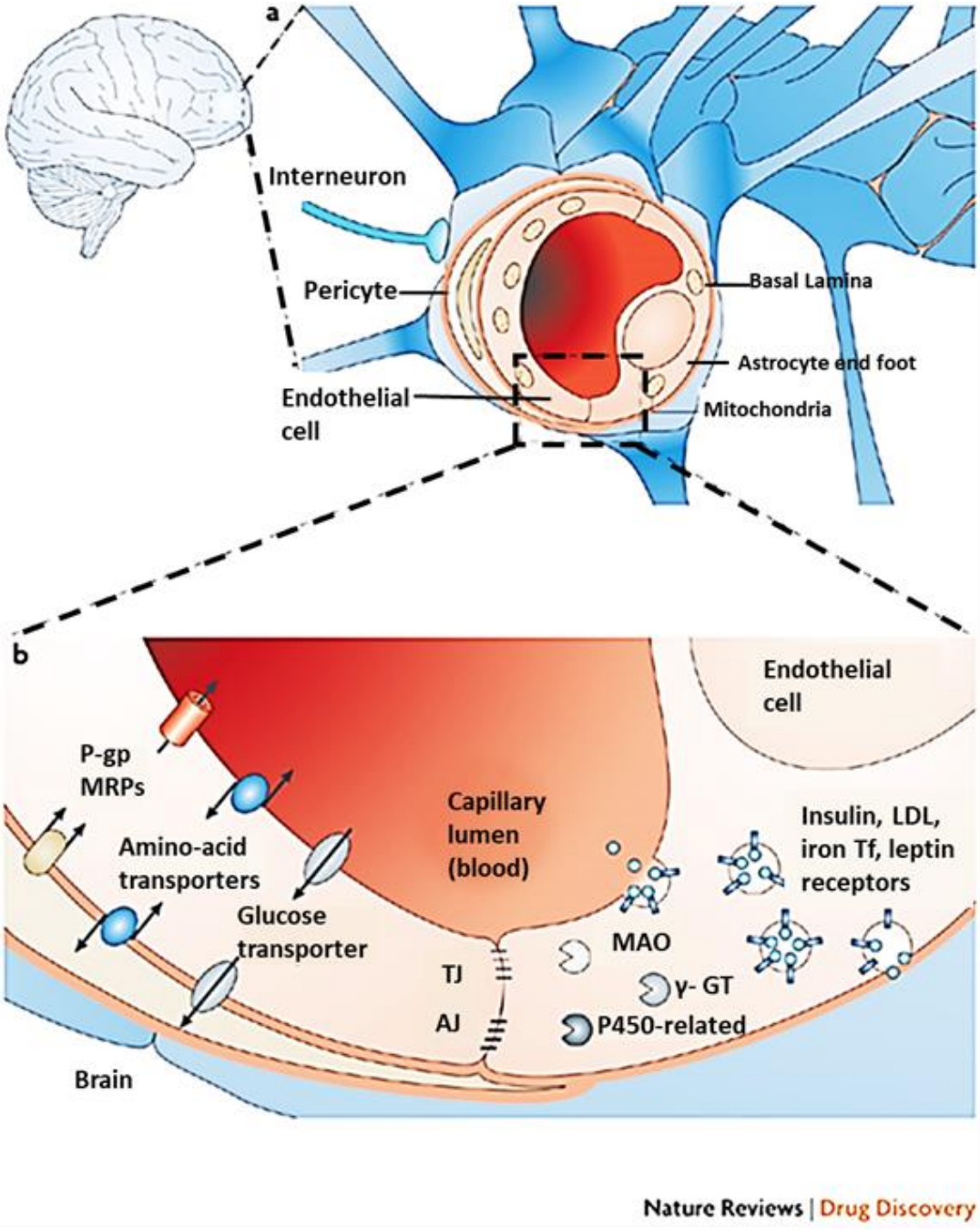

Figure 1.2: The blood-brain barrier.

(a) The BBB is formed by endothelial cells at the level of the cerebral capillaries. These endothelial cells interact with perivascular elements such as basal lamina and closely associated astrocytic end-feet processes, perivascular neurons (represented by an interneuron here) and pericytes to form a functional BBB. (b) Cerebral endothelial cells are unique in that they form complex tight junctions (TJs) produced by the interaction of several transmembrane proteins that effectively seal the paracellular pathway. These complex molecular junctions make the brain practically inaccessible for polar molecules unless they are transferred by transport pathways of the BBB, that regulate the microenvironment of the brain. There are also adherens junctions (AJs), which stabilize cell–cell interactions in the junctional zone. In addition, the presence of intracellular and extracellular enzymes such as monoamine oxidase (MAO), γ-glutamyl transpeptidase (γ-GT), alkaline phosphatase, peptidases, nucleotidases and several cytochrome P450 enzymes, endow this dynamic interface with metabolic activity. Receptor-mediated transcytosis or non-specific adsorptive-mediated transcytosis facilitates the movement of macromolecules such as antibodies, lipoproteins, proteins and peptides to the central compartment. The receptors for insulin, low-density lipoprotein (LDL), iron transferrin (Tf) and leptin are all involved in transcytosis. [Figure and legend are taken from open access review of Cecchelli *et al.*, 2007[117]]

1.2.1 Tight junctions, junctional complexes and the neurovascular unit

The blood brain barrier (BBB) is a specialized physical seal that precludes the transport of various large and/or hydrophilic peripheral blood molecules from entering the brain parenchyma [98, 118]. This restricted exchange barrier protects the brain from indiscriminate exposure to peptides, macromolecules and potentially toxic molecules [98, 118]. The integrity of the BBB is maintained by inter-endothelial complexes called tight junctions (TJs), in the brain capillaries, that is comprised of a variety of plasma membrane spanning proteins (e.g., Occludin), scaffold proteins (e.g., zona occludens protein-1; ZO1) and the actin cytoskeleton [96, 98, 118]. The peripheral membrane protein, ZO1, localizes along blood vessels in the brain parenchyma and along with claudins and occludin ensures the intactness and permeability of the BBB [119, 120]. Junctional complexes are comprised of a variety of plasma membrane spanning proteins, scaffold cytoplasmic proteins and the actin cytoskeleton.

One type of junctional complex is called the adherens junction (AJ). These physically join adjacent endothelial cells together while providing structural support by anchoring to the cytoskeleton. For example, VE-cadherin, an AJ protein, mediates cell-cell adhesion and is linked to the cytoskeleton by various catenins. AJs are critical for the formation of TJs [121]. A second barrier is presented by the basal lamina, composed of type IV collagen, fibronectin and heparin sulfate along with other molecules, which operates as a molecular weight filter [119]. Lastly, there are cells nearby that interact to protect the BBB, known as the Neurovascular Unit (NVU) **(Figure 1.3)**. It is made up of multiple cellular subunits that work in concert to maintain the functioning of the brain: neurons, cerebral endothelial cells, basal lamina, astrocytic foot processes (containing proteases and neurotransmitters) and perivascular macrophages, called pericytes and microglia [119].

Pericytes envelop the endothelium and provide architectural strength to the blood vessel by regulating BBB gene expression and influencing astrocyte function [122]. Astrocyte foot processes surround the pericyte-endothelial cell structure and provide a direct cellular link between them and the neurons [122, 123]. Astrocytes also assist in maintaining the physical and metabolic requirements of the BBB. Microglia are the resident brain macrophages that help in protecting the brain from immune insults. Lastly, the neurons direct the bulk of the metabolic demands in the brain, and these can directly influence cerebral blood flow. A dysfunction in any component of the NVU can have disastrous consequences for brain function.

Since the BBB plays a crucial role in maintaining CNS homeostasis, its dysfunction proves deleterious for the smooth working of the brain. BBB dysfunction includes: (1) BBB disruption, resulting in the discharge of potentially neurotoxic circulating substances into the CNS; (2) transporter dysfunction that consequently creates deficiency of nutrient supply and amplifies toxic substances in the CNS; and (3) altered protein expression and NVU cell secretions that result in inflammatory activation, oxidative stress, and neuronal damage [120]. The three effects have been reported in AD patients, although the scope of this thesis pertains only to BBB disruption.

The compromised integrity of the BBB has been indicated by increased CSF/serum albumin ratios seen in AD patients [120]. Albumin is a macromolecule that is unable to cross an intact BBB [100, 120]. Immuno-histological studies have also revealed the presence of albumin staining around microvessels that show co-localization of amyloid plaques and angiopathy [96, 98, 119]. It is suggested that this staining is a result of an affinity of extravasated albumin for amyloid [120].

Prothrombin is seen at elevated levels particularly around the microvessels in the brains of AD patients [124]. The highest levels of the protein were observed in people scoring higher in the Braak staging, which is a method for classifying the degree of pathology in AD [125, 126]. The increased vascularization of brain endothelial cells damages the BBB by altering the tight junction function. This is consistent with increased transcytotic disruption of the BBB initiated by the release of inflammatory cytokines that act as angiogenic triggers, promoting paracellular leakage [120].

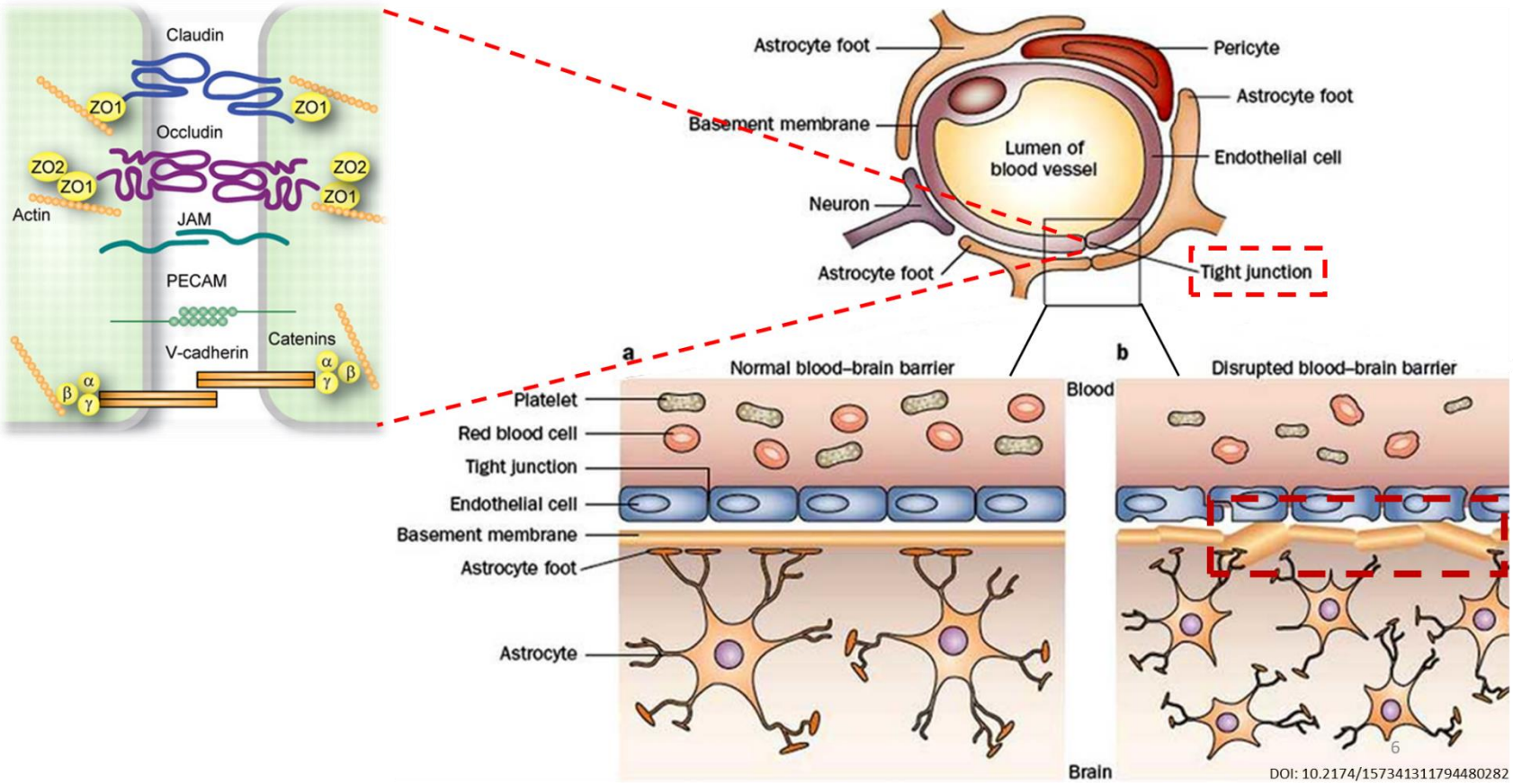

Figure 1.3: Endothelial cell–cell junctions of blood-brain barrier microvessels and the Neurovascular unit

The major components and organization of the junctional complexes as found within the endothelium of the BBB. This figure also illustrates the structure of the neurovascular unit and a normal versus a disrupted blood brain barrier. (modified from Shinde(2011) and Benarroch (2012) [127, 128])

1.2.2 Alzheimer's disease and the BBB pathogenesis: angiogenesis and inflammation

Essentially, a physical seal is present between the vasculature in the brain and the central nervous system that restricts fluid and unwanted molecules from being transported into the brain from the systemic circulation [98, 129]. Dysfunction of the blood brain barrier was originally described in animal models of AD [130] and was later established as a prominent, but an unexplained clinical feature of AD in patients [129]. Though it remains unknown what the BBB dysfunction stems from, it is, however, thought that Aβ may be directly involved in this process [118, 119]. Leakiness of the BBB has been demonstrated in a number of AD transgenic animal models that have overexpression of APP, including the Tg2576 mouse, which manifests as a form of early-onset AD [118, 130]. Studies show that BBB integrity is compromised in this mouse model as early as 4 months of age, much earlier than the onset of other disease pathology, such as the consolidated amyloid plaques [100, 130]. Hence, the mechanism leading to the BBB disruption is an additional potential target for AD therapy.

1.2.3 Cerebral Blood Flow Impairment: A road to hypervascularity in mouse models and humans

Vascular dysfunction is a crucial pathological hallmark of AD [96, 131]. The two key precursors to neurodegenerative changes and Aβ deposition in AD are BBB breakdown [96, 131] and cerebral blood flow (CBF) impairment [132]. Various studies employing non-invasive imaging techniques (e.g., Arterial spin labeling MRI) have shown that AD is associated with a global, as well as a regional CBF impairment, also known as cerebral hypoperfusion [133]. While AD patients exhibit a global decrease (average 40%) in blood flow compared to healthy controls, the CBF reduction is seen only in specific brain regions (such as hippocampus) that are usually implicated in the

disease state [94, 133]. Whether diminished blood flow in AD is a cause or consequence of the disease remains a matter of debate.

Hypoperfusion is associated with both structural and functional changes in the brain and hence plays a pivotal role in influencing the permeability of the BBB [133]. Severe reductions in CBF have been seen in the elderly at a high risk for cognitive decline and AD [133]. Individuals who are carriers of the major AD risk allele, *APOE ε4*, have a more impacted regional deterioration of CBF than non-carriers of the allele [134, 135]. AD-related vascular pathology impairs cerebral autoregulation and causes cerebrovascular insufficiency [115]. This impaired CBF and compromised BBB result in the accumulation of potentially neurotoxic molecules (*e.g.*, increased Aβ concentration) in the brain along with the entry of unwanted blood products via peripheral circulation [136, 137].

Data obtained from structural MRI scans show atrophy in the different regions of the brain and an overall change in cortical thickness is observed due to hypoperfusion in AD patients [133]. The thickness of the cortex is an important predictive measure of the evolution of AD for subjects with mild cognitive impairment [133]. Carriers of the *APOE ε4* allele, a demographic reported to have glucose hypo-metabolism, demonstrate hastened cortical thinning in areas most vulnerable to aging such as medial prefrontal and peri-central cortices as well as in areas associated with AD and amyloid-aggregation, *e.g.*, occipito-temporal, basal temporal cortices and hippocampus [133].

Aging is a leading risk factor for the development of late-onset AD. Aberrations in vascular ultrastructure, vascular reactivity, resting cerebral blood flow (rCBF) and oxygen metabolism are

all associated with age and act as a catalyst for cerebrovascular diseases and subsequent cognitive deficits [138]. To cope with the decrease in blood flow, the brain has evolved a compensatory mechanism, whereby it increases the formation of blood vessels resulting in hypervascularity, a phenomenon which is seen not only in mouse models [138-141] but also in post mortem brain samples of AD patients [141].

1.2.4 Involvement of angiogenesis and not apoptosis

The ‘‘Vascular Hypothesis’’ as stated currently states that vascular damage is a consequence of diminished blood perfusion of the brain, leading to hypoperfusion/ hypoxia, which in turn causes BBB dysfunction [142]. A subsequent amalgamation of accumulated Aβ, neuro-inflammation and the eventual disintegration of the neurovascular unit are seen, culminating in vascular death [98, 118, 143]. In a state of hypoperfusion, hypoxia-inducible factors initiate angiogenesis, a process where the formation of blood vessels occurs through the upregulation of pro-angiogenic factors [118].

The main player in this blood vessel formation is VEGF, which induces differentiation and proliferation of endothelial cells from their progenitors, the hemangioblast and the angioblast [144]. The differentiation and proliferation of these progenitors form an inefficiently differentiated primitive vascular plexus by a process called vasculogenesis [145]. The vascular plexus undergoes remodelling that is triggered by Angiopoietin-1 (Ang-1) into a hierarchically structured mature vascular system established through endothelial cell sprouting, trimming of cells, endothelial cell differentiation and pericyte recruitment. These are the events that take place during physiological angiogenesis [146].

In contrast to these events, in AD it is observed that a downstream cell signalling molecule to VEGF, angiopoietin-2 (Ang-2), destabilizes the vessel wall of mature vessels [131, 147-149]. The quiescent endothelial cells become sensitive to VEGF and other angiogenic factors proliferate indiscriminately and then migrate to form new vessels that are not able to mature and eventually lead to the establishment of a leaky network of blood vessels [131]. This phenomenon is termed 'pathological angiogenesis', which occurs during the development of tumours. In accordance with the current version of the 'Vascular Hypothesis', BBB disruption is due to vascular cell death caused by apoptosis and angiogenesis. Angiogenesis in this scenario would only be required to ensure tissue regeneration and is likely be limited to replacing the damaged tissues as well as ensuring oxygenation of brain tissues [96, 98].

However, the role of apoptosis in BBB dysfunction is highly debated. Recent studies have shown that endothelial cell proliferation during pathological angiogenesis results in hyper-vascularity [96]. As a compensatory mechanism to the decreased blood flow caused by the leaky blood vessel network, vascular remodelling and structural changes take place in the physical re-arrangement of the tight junction proteins, resulting in compromised BBB integrity [96, 150].

The work of Biron *et al.* characterized the relationship between amyloidogenesis and BBB integrity through changes in TJ morphology in the Tg2576 AD mouse. They reported that the Tg2576 AD mice exhibit no apparent vascular apoptosis but have significant TJ disruption, which was noted to be directly linked to pathological angiogenesis, resulting in a significant increase in vascular density in AD brain [96]. Hence, it can be said that these data support the model that TJ

disruption results from increased vascular permeability that takes place during extreme neovascularization in AD.

1.2.5 Angiogenesis: inflammation and vascular activation

Increasing evidence suggests that vascular perturbation appears as a common feature in the hallmark AD pathology: amyloid plaques and neurofibrillary tangles. Over the years, the emphasis has been given to the accumulation of Aβ in AD, which, as a result of its impaired clearance from the brain, is thought to be responsible for the onset of cognitive decline [88, 137, 151, 152]. Paradoxical to the amyloid cascade hypothesis, aggregated Aβ can be extensively present in the human brain in the absence of AD symptoms [89, 90, 153]. Although Aβ plays a crucial role in AD, it is neither necessary nor by itself sufficient to cause disease pathology [100].

The alternate idea is that the production of Aβ, which is called amyloidogenesis, promotes extensive pathological angiogenesis, leading to the redistribution of TJs, which then causes disruption of BBB integrity, thereby increasing vascular permeability, subsequent hypervascularization and eventual AD pathology. This alternate 'Vascular hypothesis' stems from a body of data that now establishes hypervascularization as a mechanistic explanation for amyloid-associated TJ pathology [96]. It provides new possibilities for therapeutic intervention that target the restoration of the BBB by modulating angiogenesis, thereby possibly preventing AD onset and potentially repairing damage in the AD brain.

A second study by Biron *et al.* demonstrated that immunization with Aβ peptides neutralized the amyloid trigger that causes pathological angiogenesis and thereby reverses hypervascularity in

Tg2576 AD mice [154]. The Aβ plaques were seen to be dissolved, while solubilized Aβ was removed from the brain parenchyma along perivascular drainage routes. This is thought to result in a decrease in the hypervascularity [154]. The study by Biron *et al.* supports a vascular angiogenesis model for AD pathophysiology and provides the first evidence that modulating angiogenesis repairs damage in the AD brain.

Pathological angiogenesis and hypervascularization in an AD brain occur in response to impaired cerebral perfusion and inflammatory response to vascular injury [155]. We have already discussed the impaired perfusion in section 2.2. In this section, we will look at the inflammatory activation of angiogenesis. Morphological and biochemical evidence includes regionally increased capillary density, unresolved vascular sprouting, glomeruloid vascular structure formation, and upregulated expression of angiogenic factors: VEGF, transforming growth factor β (TGF β) and tumour necrosis factor α (TNF α) [155].

In AD, inflammatory pathways, when stimulated, cause the release of angiogenic cytokines such as thrombin and VEGF, contributing to pathological angiogenesis [155]. It is hypothesized that a thrombogenic region develops in the endothelial cells of the vessel wall, leading to intravascular accumulation of thrombin. This thrombin activates vascular endothelial cells to secrete APP via a receptor mediated protein kinase C (PKC) dependent pathway. Progressive deposition of amyloid precursor protein leads to accumulation of the Aβ plaques, which generates more reactive oxygen species and induces further endothelial damage in a cycle of neurotoxic insult. This establishes a cycle of neurotoxicity and death, instituted by the discharge of thrombin following Aβ-induced neuroinflammatory responses [155].

Other studies further support the interaction of Aβ with thrombin and fibrin throughout the clotting cascade to increase neurovascular damage and neuroinflammation [156-158]. Astrocytes cultured *in vitro* and stimulated with Aβ [147, 148] showed a release of neuroinflammatory cytokines that resulted in the increased expression of VEGF. Other pro-inflammatory cytokines such as interleukin-1β are increased during AD and known to induce VEGF and growth of new blood vessels [150, 159]. Additional evidence implicates Aβ as a vasculotrope, modulating blood vessel density and vascular remodelling through angiogenic mechanisms. Brain microvessels have been shown to be closely associated with Aβ plaques with the aid of ultrastructural studies. It was observed that AD brain capillaries contained pre-amyloid deposits [155].

Aβ stimulates angiogenesis in a highly conserved manner, which is speculated to be mediated through γ-secretase activity and Notch signalling [155, 160]. *In vitro* studies of human umbilical vein endothelial cells (hUVEC) exposed directly to Aβ1-40 and Aβ1-42 show an angiogenic effect on the hUVEC, which exhibited an increase in the number of tip cells and branching [155].

The involvement of Aβ-related angiogenesis has been extended *in vivo* as well, which can be observed with the chick embryo chorioallantoic membrane assay [160]. Aβ1-40 and Aβ1-42 stimulated embryos illustrated an escalated vascular growth [160]. *In vivo* studies, using various APP mutant AD mouse models that have an overproduction of Aβ, show modifications in brain vasculature compared to wild type animals [96, 118].

APP23 mice exhibit significant blood flow alterations correlated with structural modifications of blood vessels [149]. A study using three-dimensional architectural analysis revealed significant changes in the vasculature [150] to be accelerated only in amyloid-positive vessels [159]. Interestingly, brain homogenates taken from Aβ-overexpressing AD model mice demonstrated an increase in the formation of new vessels in an *in vivo* angiogenesis assay [150]. This increase in vessels was blocked on exposure to a VEGF antagonist [150]. The vascular changes observed in these mice may be thought to be due to unrelated, 'off-target' effects of the APP mutation. However, given that the vascular changes observed in transgenic mice correlate well with vascular disturbances reported in human AD brains, it is safe to say that angiogenesis might play a crucial role in the establishment of AD pathology.

Post-mortem studies of human brains also show evidence of increased angiogenesis in the hippocampus, mid-frontal cortex, substantia nigra pars compacta, and locus coeruleus of AD brains as compared to healthy individuals [99, 141]. Elevated serum levels of pro-angiogenic proteins was seen in a cohort study of AD patients which were seen associated with the cognitive status of the healthy and the AD patients [161]. Further analysis in mouse models found no correlation between the number of microglia (activation of apoptosis) and angiogenesis or microglia with vessel density, suggesting that it may be the presence of Aβ that is initiating angiogenesis and not activation of apoptosis that subsequently causes BBB dysfunction [162, 163].

There are additional proteins at the BBB, which act to regulate brain Aβ levels and the disruption of which take the brain towards upregulated angiogenesis. The receptor for advanced glycation products (RAGE), a multi-ligand receptor, regulates the entry of peripheral Aβ to the brain [163-

165]. Its expression is upregulated by binding with ligands, including Aβ and pro-inflammatory cytokine-like mediators [163]. This facilitates the entry of Aβ into the cerebral neurons, microglia, and vasculature [165]. *In-vitro* studies have also implicated RAGE in the vascular pathogenesis of AD by suppressing the CBF, leading to hypoperfusion [163, 166].

1.2.6 Haemostatic mechanisms in relation to angiogenesis in AD

Maintenance of the fluidity of blood and limiting its loss upon blood vessel endothelium injury is a crucial physiological process known as haemostasis [167]. Haemostasis is possible due to the existence of a delicate balance between pro-coagulation and anti-coagulation, along with numerous pathways and feedback loops [167, 168]. Haemostasis has three distinct phases: primary haemostasis is involved in adhering platelets to a site of injury, forming a 'haemostatic or platelet plug' [167]; Secondary haemostasis involves the activation of the coagulation cascade, culminating in a fibrin clot; the last stage is 'fibrinolysis', or the dissolution of the clot [167].

Accompanied by vascular dysfunction, an altered haemostatic scenario is increasingly implicated in AD. Most research, with a few exceptions, supports an association of a pro-coagulation mechanism in AD. Proteins like transglutaminases are core components of the coagulation system that could be used as therapeutics to resolve the altered hemostasis in AD.

1.3 Alzheimer's disease mouse models

Several unknowns have made it difficult to model AD accurately. The knowledge of the physiological functions of Aβ and APP are still not known. The exact involvement of the

neuropathological mechanism(s) of Aβ and NFTs in AD is also unclear. Furthermore, the cause of the sporadic form of AD has yet to be clarified. However, according to the amyloid cascade hypothesis, altered Aβ metabolism leads to several downstream effects including the formation of NFTs, inflammation and oxidative stress resulting in neuronal dysfunction and death seen in AD. The bulk of the support for the hypothesis is based on studies using various AD mouse models, incorporating the genetics of the familial form of AD. To date, there are well over 106 different strains of AD mouse models currently available to researchers [169]. A short list of the most popular mice is summarized in **Table 1.1**.

Table 1.1: Neuropathological characteristics of some common AD transgenic mouse models.
+++, extensive phenotype; +, detectable; −, not detected; nr, not reported.

Model [Ref]	Transgene	Promoter	Age of plaque onset (mo)	Neuritic plaques	Diffuse plaques	CAA	Intraneuronal Aβ accumulation	CNS specific expression	Neuro-degeneration	N-terminal truncated Aβ
PDAPP [170]	APP minigene V717F (Indiana)	PDGF	6–8	+++	+++	+	Nr	+++	-	Nr
APP-London [171]	Human APP695 cDNA V642I (London)	Mouse Thy1	> 12	+++	+++	+	Nr	+++	-	Nr
Tg2576 [172]	APP695 cDNA KM670/671NL (Swedish)	Hamster PrP	9–11	+++	+	+	+	+	-	+
APP23 [173]	APP751 cDNA with Swedish mutations	Murine Thy1	6	+++	+	+	Nr	+++	-	Nr
Tg-CRND8 [174]	human APP695 cDNA with Swedish/Indiana mutations	Hamster PrP	3	+++	+	+	Nr	+	-	Nr
APPDutch [175]	human APP751 cDNA with E693Q (Dutch) mutation	Mouse Thy1	22–25	-	+	+++	+	+++	-	Nr

Tg-SweDI [176]	Human APP cDNA with Swedish/ Dutch/D694N (Iowa) mutations	Mouse Thy1	3	-	+++	+++	Nr	+++	-	nr
Tg-ArcSwe [177]	Human APP695 cDNA with Swedish/E693G (Arctic) mutations	Murine Thy1	6	+++	+	+	+++	+++	-	nr
3xTg-AD [178]	Human APP695 cDNA with Swedish + PS1 (M146V) + tau (P301L)	Mouse Thy1	6	+++	+++	+	+++	+++	-	nr
5xFAD [179]	Human APP695 cDNA with Swedish/London/I 716V (Florida) mutations + PS1 (M146L and L286V)	Mouse Thy1	2	+++	+	Nr	+++	+++	+	nr

Nearly all the available AD mouse models are based on the genetics of familial form of AD (reviewed by Philipson *et al.* 2010 [180]), even though this form of AD represents <5% of all AD cases. Therefore, technically the bulk of these mice are models of the predementia phase of familial AD rather than the more prevalent sporadic form. The mutations in APP, PS1 and PS2 isolated from families with familial AD affect the processing and metabolism of APP. A variety of transgenic mice have been created that over-express the mutant variants of APP, PS1 and or PS2 genes in an attempt to recapitulate the pathologies of AD. The resulting AD mouse models perform this task with varying levels of success. No mice that over-express mutant variants of APP, PS1 or PS2 have been known to develop NFTs. Furthermore, to date, there is no mouse expressing a single gene that displays all known AD pathologies.

One example of a familial AD mutation that has gained popularity as a model is the double Swedish mutation found on APP **(Figure 1.1c)**, which was originally identified in 1992 from a Swedish family [181]. The mutation is located on two consecutive amino acids (KM670/671NL) just outside the N-terminus of the Aβ domain on APP. Earlier it was thought that the Swedish mutation increases the production of total Aβ by nearly six to eight times *in vitro* [14] by favouring processing by β-secretase [15] however, recent studies now show that it is the ratio of Aβ 42/42 that increases in familial AD which could be due to increase of Aβ42 or a decrease of Aβ40 levels both *in vitro* and *in vivo* [182]. Subsequently, the Swedish mutation was used to identify the β-secretase enzyme, BACE1 [183]. Several transgenic mice have been created that incorporate the Swedish mutation. In the knock-in mouse model $APP^{NLh/NLh}$ (**Table 1.1**), the Aβ domain of the endogenous mouse APP was humanized and incorporated with the Swedish mutation [184]. This created a mouse that expresses mouse APP (under its natural promoter) with the Swedish mutation

generating humanized Aβ. However, after 22 months of age, the $APP^{NLh/NLh}$ mice failed to develop Aβ plaque pathology [185]. The APP23 mouse (**Table 1.1**) over-expresses the Swedish mutation in the APP751 isoform under the control of a mouse specific neuron promoter Thy-1 [173]. This mouse develops Aβ plaques by six months of age and is known to develop cognitive defects [186] and CAA associated blood-brain barrier leakage [187].

Finally, the most popular AD mouse model and the model that we have used for this thesis, Tg2576 was created by Hsiao et al. in 1996 [172] (**Table 1.1**). Tg2576 mice also incorporate the Swedish mutation (K670N/M671L) on the APP695 isoform under the control of the hamster prion promoter [172, 188]. The Tg2576 mouse develops many of the common Aβ related pathologies seen in AD, including accumulation of Aβ (1-40 and 1-42), Aβ plaques beginning by nine months of age [172], CAA [172, 189], cognitive defects [172], cerebrovascular defects [130, 190-192], astrogliosis [193], microglosis [194], oxidative stress [195] and dystrophic neuritis [193]. However, this mouse does not develop tau pathologies or neuronal loss and is, therefore, a useful but incomplete model of AD. This model has been well characterized and studied for its cognitive decline shown by the age of 9 months which progresses as the mouse ages [196]. It has previously been established that this model shows vascular pathology and subsequent breakdown in the BBB prior to the establishment of the hallmark Aβ[96].

1.4 Therapeutic modalities in treating pathogenic angiogenesis in AD

Angiogenesis, as stated by the studies mentioned in this chapter, can be viewed as that stage in AD pathology where all the different pathways (hypoperfusion, BBB dysfunction, inflammation) merge, leading to the AD pathology. Observations showing increased cerebrovascular

permeability prior to the appearance of the hallmarks of AD suggest a novel paradigm for integrating vascular remodelling (angiogenesis) with the pathophysiology of the disease. Targeting this integral step in the pathophysiology of AD and developing a novel therapeutic intervention using anti-angiogenic drugs may help alleviate the global societal burden of AD.

1.4.1 Antiangiogenics: small molecule tyrosine kinase inhibitors

Anti-angiogenics, including small molecule tyrosine kinase inhibitors, have been tested and approved as anti-cancer therapeutic agents and have been shown to maintain normal physiological vasculature [197-199]. Sunitinib, sold under the trade name of Sutent® by Pfizer, is a broad-spectrum tyrosine kinase inhibitor. This is known to inhibit the phosphorylation of multiple receptor tyrosine kinases and is a potent inhibitor of VEGF as well as platelet derived growth factor (PDGF-β). Currently, it has been approved for clinical use for managing gastrointestinal stromal tumours, renal cell cancer and pancreatic cancer. Sunitinib was shown to decrease the amyloid burden and reverse cognitive decline in AD model mice, suggesting that if angiogenesis is the target then increase in the accumulation of Aβ can be reduced and this will reduce the cognitive decline associated with AD [198].

1.4.2 Biologics as VEGFR inhibitors

We now know that VEGF is the prime and central component of pathological blood vessel formation. There are biologics that specifically target the VEGF ligand or its receptor. This specific targeted therapy could prove more efficient and less deleterious, due to avoidance of unwanted 'off target' effects. Bevacizumab (Avastin) is an anti-VEGF-A antibody used to treat glioblastoma

and lung carcinomas [200]. Another example is Ramucirumab, a monoclonal antibody against VEGFR2 used for gastric cancer and metastatic colorectal cancer.

These are examples of some of the therapeutic routes that could target angiogenesis; however, understanding the molecular mechanism behind angiogenesis causing eventual AD pathology is of utmost importance in order to search for safe and effective novel therapeutics for AD and other vascular diseases.

1.4.3 Haematopoietic stem cells: a powerful tool in understanding AD pathology

Cell-based therapies have been very popular in the recent past as a tool to treat many diseases like leukemia, Hodgkin's disease and autoimmune diseases among others [201-203]. Haematopoietic stem cells (HSCs) have also found a place in addressing various pathologies seen associated with AD in animal models of AD. HSC-derived microglia have been shown to enhance the clearance of Aβ in AD mouse models [204]. HSC-derived monocytes have also been shown to induce inflammation to clear Aβ in animal models of AD [205]. Neuronal loss associated with AD is shown to be countered by HSC therapy as well as increasing the synaptic plasticity to enhance hippocampal dependent cognition in mouse models of AD [206, 207]. This suggests that HSC therapy could prove beneficial in patients with the probable diagnosis of AD.

Although HSC transplants may prove beneficial to treat aspects of AD, they can also be exploited to understand AD pathology by the transfer of HSCs from a donor, the Tg2576 AD mouse model, that overproduces Aβ into a recipient that does not express endogenous Aβ. This idea is explored

further in Chapter 5 and can help us understand the role of circulating HSC-derived Aβ molecules in establishing AD pathology.

1.5 Concluding Remarks

As the Western world ages, the tables are turning: it does not take a village anymore to raise a child, but it takes the entire village to care for the aging. AD represents an ailment that is placing a significant burden on all aspects of society. This burden primarily falls on family, caregivers and has been estimated to cost billions of dollars in lost productivity and healthcare costs. Currently, there is a lack of understanding regarding the cause(s) of the disease that translates into a lack of viable treatments or cures. Over the years, limited progress has been made with regard to the clinical translation of the popular amyloid hypothesis for treating AD, and hence new thinking towards AD pathogenesis is surely needed. Vascular risk factors and neurovascular dysfunction associated with hypotension, hypertension, cholesterol levels, type II diabetes mellitus, smoking, oxidative stress and iron overload have been found to play integral roles in the pathogenesis of AD. Observations showing increased cerebrovascular permeability prior to the appearance of the hallmarks of AD give rise to a novel paradigm for integrating vascular remodelling (angiogenesis) with the pathophysiology of the disease. Taking this into account, research focused on understanding the molecular mechanisms behind the angiogenesis leading to AD pathology may contribute in the development of novel therapeutic interventions targeting this pathological blood vessel formation to help alleviate the global societal burden of AD.

1.6 Project rationale and general approach

AD is strongly associated with vascular risk factors. In addition, there is an increasing amount of evidence for the disruption of the cerebro-vasculature that accompanies AD disease pathology. Furthermore, disruptions in the BBB can directly lead to interruptions in cerebral blood flow, which can directly impact brain function. Interruptions in blood flow suggest that an altered haemostatic system may be involved in the development of AD.

The exact pathogenic mechanism of the endothelial dysfunction observed in AD patients and various AD mouse models are not known. It is usually assumed that Aβ accumulation is responsible for the observed cerebrovascular abnormalities in AD. The focus of this thesis is to investigate the effect of anti-angiogenic drugs on reversing the cerebrovascular dysfunction seen in the Tg2576 mouse model of AD and the effect of such treatment on other pathologies like amyloid load, increased BBB permeability and cognitive decline associated with the disease. I also wanted to delve into understanding the molecular mechanism by which Aβ causes pathogenic angiogenesis that leads to the eventual breakdown of the BBB. My last objective was to look at whether soluble Aβ generated by the transfer of the bone marrow from a Tg2576 donor mouse was able to establish AD pathology in a recipient APP-KO mouse which lacks the *APP* gene. This thesis had several hypotheses that were tested:

1. Antiangiogenic drugs revert AD pathology, maintain amyloid load, reverse BBB disruption and inhibit cognitive decline,
2. Amyloidgenesis initiates dysregulated neo-angiogenesis via Ang-2 dependent Tie-2 receptor activation, and
3. AD pathology can be established in APP-KO mice with bone marrow transplant from amyloid overproducing, Tg2576 mice, suggesting the role of soluble Aβ in AD pathogenesis.

Taken together, my findings suggest that disruption in the vascular system during AD may have profound effects on the progression of neurodegeneration. Characterizing this pathology and its mechanism could help to define an early therapeutic intervention point to slow the progression of AD.

Chapter 2 Material and Methods

2.1 Mice and cells

The Tg2576 AD model mouse expresses the Swedish mutant of the amyloid precursor protein (K670N/M671L) [172, 188] under control of the hamster prion protein promoter (Taconic). Mice were maintained on mixed C57Bl6/SJL background by mating heterozygous Tg2576 males to C57Bl6/SJL F1 females. Wild-type littermates were used as controls.

The genotyping protocol was performed as described by [188] by PCR. Briefly, two parallel PCR reactions were performed to distinguish heterozygote from wild-type. The PrP-APP fusion DNA (corresponding to the heterozygote) was amplified using primers 1502 (hamster PrP promoter, 5'-GTGGATAACCCCTCCCCCAGCCTAGACCA-3') and 1503 (human APP, 5'-CTGACCACTCGACCAGGTTCTGGGT-3'). The primer combination 1502 and 1501 (mouse PrP, 5'-AAGCGGCCAAAGCCTGGAGGGTGGAACA-3') was used as a positive control for the reaction.

Aged Tg2576 and wild-type mice of both sexes were used at 10 months of age. The Jefferies group maintains its own colony of Tg2576 and wildtype littermates at UBC.

APP-KO (Jackson Labs) mice that are generated on a C57BL/6 background were used for the bone marrow reconstitution experiment to assess the role of soluble Aβ in the establishment of AD pathology. These were created by using a targeting vector containing neomycin resistance and herpes simplex virus thymidine kinase genes to disrupt a region of the App gene encoding the promoter and exon 1. The construct was electroporated into 129S7/SvEvBrd-derived AB2.1

embryonic stem (ES) cells. Correctly targeted ES cells were injected into C57BL/6J blastocysts. The resulting chimeric animals were backcrossed to C57BL/6J mice.

Mouse numbers used in the respective Alzheimer's mouse experiments are noted in the figure legends. Mice were fed standard lab chow and water *ad libitum* and kept under a 12-hour light/dark cycle. All protocols and procedures involving the care and use of animals in these studies were reviewed and approved by the UBC Animal Care Committee.

Human brain endothelial cells, HBEC-5i (ATCC® CRL-3245™) were cultured on 0.1% gelatin coated tissue culture plates in DMEM-F12 media (Gibco; cat. # 10565-018) supplemented by 10% heat-inactivated fetal bovine serum (FBS) (Gibco; cat. # A31607-01) and 40µg/ml endothelial growth supplement (Sigma-Aldrich; cat. # E2759). Cells were grown until they reached 70% confluency and then used for experiments. Bone marrow cells were isolated from the femur and tibia of Tg2576 mice and their wildtype litter mates (B6/SJL). The cells were obtained by a method adapted from Dobson *et al.* [208].

2.2 Pharmacological treatments

Sunitinib (LC laboratories, MA), DC-101 (Bio X cell, NH) and Axitinib (LC laboratories, MA) were administered to the Tg2576 mice and their WT littermates. Control groups containing both Tg2576 and WT animals were given the vehicle (PBS+DMSO) alone. Sunitinib at a dose of 80mg/kg or Axitinib at a dose of 10 mg/kg (both dissolved in 100% DMSO at 30mg/ml solubility and 40mg/ml solubility respectively and diluted to a desired concentration in PBS) or the vehicle were administered to the mice via oral gavage. The treatment schedule was three times a week for

a duration of one month. DC-101 was intraperitoneally injected at a dose of 0.8mg/mouse twice a week for a month. After one month of treatment, the animals were tested for cognitive performance to evaluate the different aspects of memory and learning using a battery of tests: open field test, y-maze, fear conditioning and radial arm water maze, before euthanizing the mice to analyse the brain tissue.

2.3 Open Field Test

A plexiglass chamber measuring 50 cm (length) x 50 cm (width) x 38 cm (height) with dark coloured walls and a light source focused in the centre was used. Animals across all groups were placed one at a time in the arena. The floor of the chamber was demarcated into central and peripheral regions. The field was also calibrated in the computer software, so the camera can create physical distance data from pixel-based information. The system was connected to a black and white analog tracking camera with an RTV24 Digitizer that was placed overhead of the open field. The path travelled, and time spent in either region of the field was tracked and recorded for a total of 5 minutes using this computer tracking system (ANY-maze, Stoelting). The test exploits the innate behaviour of 'thigmotaxis' where the mice tend to stay towards the shaded edges of an open field and keep away from the brighter centre. This implies that mice that have intact cognition and awareness of the potential danger in the environment will spend less time in the centre of the field. This test assesses an animal's anxiety, locomotion and exploration of a novel environment.

2.4 Spontaneous alternation (Y-maze)

The test for novelty exploration using spatial and working memory was conducted using a symmetrical Y-maze with a grey steel bottom plate and grey Perspex® walls (Stoelting Co, Wood

Dale, IL). Each arm of the Y-maze was 35 cm long, 5 cm wide, and 10 cm high, and the wall at the end of each arm was identified by a different colour: white, blue or red. The spatial acquisition phase comprised a one-day trial with the mice tracked while moving freely through the three arms of the Y maze during an 8-minute session. The movements were tracked by a computer tracking system (ANY-maze, Stoelting). The performance was gauged by the percentage of alternations that was calculated as the total number of alternations × 100/ (total number of arm entries − 2). Alternation was defined as successive entries into the three arms on overlapping triplet sets. A high percentage of alternation was indicative of sustained cognition, as the animals must remember which arm was entered last to avoid re-entering it.

2.5 Contextual Fear Conditioning

The apparatus consisted of a transparent chamber inside an enclosure with an opening in the ceiling to allow video recordings. The chamber consisted of a steel grid floor connected to a shock generator scrambler. The test encompassed two sessions: conditioning and a context test. On the conditioning day, the mice were individually placed in the chamber and allowed to explore freely for 5 minutes during which, at the 180th second, they received a foot shock of 0.50–0.80 mA for 3 seconds through the bars of the floor. 24 hours after conditioning, the mice were individually placed back in the chamber for 4 minutes, this time with no noxious stimuli. The mice were monitored for movement and freezing behaviour was recorded using computer software (Limelight, ActiMetrics, Wilmette, IL, USA). Exclusion criteria were set for freezing events less than 2 seconds. This test was used to determine associative working memory. We explored the animal's ability to associate an environment with a noxious event that it experienced there. When the animal is returned to the same environment, it generally will demonstrate a freezing response

if it remembers and associates that environment with the shock. Freezing is a species-specific response to fear, which is defined as “the absence of movement except for respiration.” This may last for seconds to minutes depending on the strength of the aversive stimulus and whether the subject is able to recall the shock.

2.6 Radial arm water maze (RAWM)

The RAWM contains eight swim paths (arms) extending out of an open central area, with an escape platform located at the end of any of four alternate arms called the ‘goal arms’. The start position and the goal arms were fixed throughout the duration of the study. The mice were individually placed at the ‘start position’ of the maze and given 60 seconds to locate one of the 4 escape platforms. With each trial, the platform that was used to escape was removed and not placed back into the maze until the end of that test day. The test was repeated until only one platform was left. Once the animal found the last platform it marked the end of the test for that day. In between each trial, the animal was removed and placed back in its heated home cage for 90 seconds to avoid hypothermia. These trials were conducted daily for a total of 5 days. The latency to reach the platform for each trial and the arm entries were recorded manually. Performance of memory and learning was gauged each day based on the average time taken to find the escape platforms and the total number of errors, i.e., Reference memory errors + Working memory errors. Reference memory error is defined as the entry into an arm which never had an escape platform and working memory error is said to be the subsequent entry into an arm where the platform had been removed in the previous trial.

2.7 Tissue preparation

After the behaviour studies, the animals were terminally anesthetised with ketamine/xylazine (100 mg/kg; 10 mg/kg) and perfused with PBS for 5 minutes at a 5 ml/minute flow rate. Brains were removed, and one hemisphere was fixed with 4% paraformaldehyde (PFA) for histology and stored at 4˚C and the other hemisphere was flash frozen for biochemical studies and stored at -80 ˚C until it was ready to be analyzed.

The PFA fixed hemispheres were embedded in a 4% agarose block and microtome sectioned to be used for immunofluorescence, whereas the flash frozen mouse brain hemispheres were homogenized mechanically using a douncer. The cytosolic fraction was used to detect soluble proteins. The pellet left behind after the initial centrifugation was resuspended in 2% sodium dodecyl sulfate (SDS) solution in dH_2O. The supernatant from this treatment contained the membrane-bound proteins. The portion of the pellet that was not dissolved in 2% SDS contained the plaque-associated Aβ that was solubilized by 70% sulfuric acid treatment, lyophilized and resuspended in 1X PBS solution. 1X Halt protease and phosphatase inhibitor cocktail (ThermoFisher Scientific; 78440) was added to prevent protein degradation.

2.8 Immunoblotting analysis and co-immunoprecipitation

For western blot analysis, the fractional homogenate samples were prepared with Dithiothreitol (DTT) in the sample buffer (100 mM Tris-Cl (pH 6.8), 4% (w/v) SDS, 0.2% (w/v) bromophenol blue, 20% (v/v) glycerol and 200 mM DTT). Homogenates were electrophoresed and immunoblotted with indicated antibodies. For co-immunoprecipitation, homogenates were first pre-cleaned by incubating with a bead slurry and centrifuged at 14,000xg for 4 minutes at 4^{o}C.

Beads were discarded, and supernatant kept for co-immunoprecipitation. Protein A or protein G beads were washed twice with wash buffer (10 mM Tris HCl pH 7.4, 150 mM NaCl, 1% Nonidet P-40, 1 mM EDTA, 1X Halt protease and phosphatase inhibitor cocktail and 20 mM N-Ethylmaleimide), centrifuged at 3,000xg for 2 minutes at 4^{o}C and incubated with the indicated antibody for 4 hours at 4^{o}C on a rotating shaker. Beads were then washed twice and incubated with pre-cleaned homogenates overnight at 4^{o}C. Beads were washed, and the complex was eluted by using 2 x 50 µl SDS loading buffer without DTT and heating at 50^{o}C for 10 minutes. A second elution was carried out by 2x SDS buffer in the presence of DTT. The proteins in the eluate were resolved on the acrylamide gel according to standard practices. Immunoblotting was performed on nitrocellulose membranes using primary antibodies against the various proteins. The signal intensities were imaged by using the Odyssey infrared image system (LICOR), and relative levels of immunoreactivity were analyzed by the Image Studio Lite software.

2.9 Antibodies, peptides and chemicals

Antibodies used for western blots, immunofluorescence and immunoprecipitation: anti-CD105/Endoglin (R&D systems; AF1097), anti-amyloid beta 6E-10 (BioLegend; 39320), anti-amyloid 1-42 (abcam; cat # 39377), anti-ZO1 (ThermoFisher Scientific; cat. # 61-7300), anti GAPDH antibody (abcam; ab181602), anti-actin (Santa Cruz; sc1615), anti-occludin (abcam; ab31721), anti-CD31 (abcam; ab28364), anti-albumin (abcam; ab19194), anti-phosphoTie2 (R&D systems; AF 3909), anti-Tie2/TEK (Millipore; cat. # 05-584), anti-amyloid (1-16) 6E10 (Biolegend; cat. # 803002), anti-VEGFR2 (abcam; ab11939), anti-pVEGFR2-phospho Y1214 (abcam; ab131241) anti-FAK (abcam; ab40794), anti-phospho FAK (abcam; ab81298), anti-

VEGF-A165 (abcam; ab69479), anti-Ang-1 (abcam; ab8451), anti-Ang-2 (abcam; ab8452), Notch antibody (abcam; ab8925) and p-Erk-1 antibody (abcam; ab24157).

Peptides used for treating of HBEC-5i cells and used as positive controls for immunoblotting and immunoprecipitation: Aβ1-42 peptide (NovoPrep synthetic peptide; cat. # A-42-T-1), Aβ1-16 peptide (AnaSpec; AS-24225), human Ang-2 peptide (abcam; ab99482), human VEGFA peptide (abcam; ab46160).

Antibodies for FACS: FITC anti-mouse CD45.2 Antibody (Biolegend; cat. # 109805), PE/Cy7 anti-mouse CD45.1 Antibody (Biolegend; cat. # 110729).

Chemicals used: NP-40 (abcam; ab142227), 100X Halt protease and phosphatase inhibitor cocktail (ThermoFisher Scientific; cat. # 78440).

2.10 Immunofluorescence and Confocal imaging

The brain hemispheres that were fixed with 4% PFA overnight were transferred into PBS+0.01% sodium azide and stored at 4 °C. The brains were embedded in 4% agarose, fixed onto the microtome stage and sectioned at a thickness of 50μm. Mouse hippocampus (CA1 and DG) and cortex (entorhinal and prefrontal cortex), regions involved in learning and memory that are affected in AD, were examined. The brain sections were blocked with buffer (3% skimmed milk in PBS; 0.1% Tween-20) for 1 hour at room temperature followed by overnight incubation at 4°C with primary antibodies against the various proteins of interest: CD105 (R&D Systems; AF1097), Aβ (BioLegend 39320) and tight junction protein, Occludin (abcam; ab31721), CD-31 (abcam;

ab28364), and albumin (abcam; ab19194). For co-localization experiments, multiple antibodies were used on the sections simultaneously. The fluorophore conjugated secondary antibody incubation was done at room temperature for 1 hour. DAPI was used for nuclear counterstaining. Sections were then washed using PBS with 0.1% Tween-20 before being cover slipped with Fluoromount-G. Slides were allowed to air-dry overnight in the dark.

The image acquisition was done using the Olympus FV-10i confocal microscope with the high-resolution Olympus 60 X/1.4 oil-immersion objective lens. For 3D image data set acquisition, the excitation beam was first focused at the maximum signal intensity focal position within the brain tissue sample and the appropriate exposure times were selected to avoid pixel saturation. A series of 2D images (Z stack) were taken at a step size of 1µm. The beginning and end of the 3D stack were set based on the signal level degradation. The Volocity software (PerkinElmer) was then used to process the series of images that were taken and generate a 3D reconstruction of the tissue.

Volume estimation was performed on the 3D image data sets recorded from four or more cortical or hippocampal areas of brain tissue samples. In this procedure, a noise removal filter (either Gaussian or kernel size of 3X3) was used to remove the noise associated with the images. To define the boundary between the objects (for instance, blood capillaries or amyloid) and the background, the lower threshold level in the histogram was set to exclude all possible background voxel values. The sum of all the voxels above this threshold level was determined to be the volume. The total fluorescence volume (TFV) was detected in the field of interest and was integrated above the background by the software. The ratio of the TFV and the total volume of the field was used as a numerical representation of the expression of the protein of interest in a unit volume of the

voxel. Co-localization of proteins was established by selecting the background as an area of interest [209]. The thresholds for different channels/target proteins were set using this region of interest (ROI). Clicking a point outside the ROI gave the scatter plot for the entire image [209]. The Thresholded Pearson's Correlation coefficient (PCC) was calculated by the software [209]. The closer the value of PCC is to 1, the stronger the statistical correlation is between the two targets.

2.11 Semi-quantitative analysis of TJ morphology

Brain sections were processed for immunofluorescence by staining for co-localized CD-31 and occludin proteins. In the hippocampus and cortex, individual vessels stained with anti-CD31 were scored as either normal (1) or abnormal (0) for occludin expression. Normal occludin expression was defined by observation of strong, continuous, intense and linear staining. In contrast, abnormal occludin expression was judged as weak, punctate and/or discontinuous staining. To minimize the recording of incomplete or undulating vessels as abnormal due to observed ‘‘gaps’’ in occludin staining, evidence of vessel continuity was sought in the images with the help of CD31 staining. The percentage of TJ disruption in a given region of the brain was defined as the percentage of blood vessels that display abnormal TJ morphology. The image acquisition and analysis were done as described above.

2.12 Blood Brain Barrier Permeability Assay

Drug- and vehicle-treated mice (n=3) were weighed and intraperitoneally (i.p.) injected with 50µg Evans blue dye (in PBS; Sigma-Aldrich #E2129) per gram weight of the mouse[101]. Three hours after injection, the mice were terminally anesthetized with ketamine (100 mg/kg i.p.; Narketan,

Vetoquinol) and xylazine (10 mg/kg i.p.; Rompun, Bayer) and transcardially perfused with PBS for 5 minutes at 5 ml/minute flow rate [101]. After removing the cerebellum and olfactory bulbs, the brains were weighed. The Evans blue dye was extracted through the following process; 1 mL of 50% trichloroacetic acid was added to the brain, and the samples were Dounce homogenized (pulling the plunger up and down 10 times). The homogenates were centrifuged at 13,000 rpm for 10 minutes and the supernatant diluted 1:4 with 100% ethanol. The supernatant with ethanol was read with an ELISA plate reader (Spectra Max 190; Molecular Devices, Sunnyvale, CA) at 620 nm to determine the optical density of the Evans Blue. The readings were divided by the weight of the brain, and the data statistically analyzed with unpaired t-tests. Evans Blue is a dye that has a high affinity for serum albumin [101]. An intact BBB is impermeable to serum albumin and thus the injected Evans Blue remains bound to the serum albumin and does not stain the neuronal tissue. When the BBB has been compromised, albumin-bound Evans Blue enters the CNS and stains it blue, allowing for visual qualitative confirmation in addition to the fluorescent quantitative immunohistological assay.

2.13 Phospho-kinase and Angiogenesis Proteome Arrays

Total brain tissue homogenates were prepared as described above. Homogenates were incubated on nitrocellulose membranes containing different antibodies printed in duplicates provided with Proteome Profiler Human Phospho-Kinase Array Kit (R&D Systems; ARY003B) and Proteome Profiler Mouse Angiogenesis Array Kit (R&D Systems; ARY015). The Proteome Profiler Human Phospho-Kinase Array Kit (R&D Systems; ARY003B) can also be used for mouse samples and has previously been tested by[210, 211] [127, 128]. The phospho-kinase analysis and angiogenesis analysis were performed according to the manufacturer's instructions. Phospho-kinase levels and

levels of proteins involved in angiogenesis in Tg2576 mice versus the WT littermates were depicted as fold change.

2.14 Cell culture

Human brain endothelial cells were grown in 10 cm tissue culture plates. The cells were treated with either PBS, Aβ1-42 peptide (10μM), Aβ1-16 peptide (10μM), Ang-2 peptide (200ng/ml) or VEGFA-165 (100ng/ml) peptide for 24 hrs in a starving medium. After the treatment, the medium was removed, and cells were washed with PBS and then lysed with RIPA buffer that contained protease and phosphatase inhibitors. These cells were then used to analyze different proteins of interest.

2.15 Bone marrow reconstitution

The tibia and femur of the age-matched (12-months of age) donor mice (Tg2576 and B6/SJL) were cleaned, the proximal ends of the bone were cut off and placed in a 0.5ml microfuge tube. The bottom of the 0.5ml tube was cut and this set up was placed inside a 2ml centrifuge tube. The tubes were centrifuged at 2000rpm for 5 seconds. The marrow pellet was then resuspended in culture medium and treated with RBC lysis buffer. The cells were then centrifuged and resuspended in PBS, cells were counted with the Bio-Rad TC20 automated cell counter. Dilutions were made such that all samples were at a concentration of $2X10^6$ cells/100μl PBS.

The APP-KO recipient mice were X-irradiated at 900Rads. $2X10^6$ donor bone marrow cells were injected via the tail vein into each recipient mouse. The mice were assessed for a successful bone marrow reconstitution after 2 months of the injections. This was done by FACS analysis of the

lymphocyte CD45 type. The donors used were positive for CD45.1 whereas the recipients were CD45.2 positive. After reconstitution, the recipients were checked to see the percentage of lymphocytes that were CD45.1 positive. 90% or more reconstitution was considered as successful reconstitution.

2.16 FACS analysis of lymphocytes

Blood draws were performed on the mice and collected in EDTA-coated tubes. Lymphocytes were isolated after RBC lysis and incubated with antibodies against CD45.2 and CD45.1 in FACS buffer. The samples were analysed for CD 45 type.

2.17 Bar graph generation and fold change calculation

Bar graphs were generated in GraphPad Prism software (GraphPad Prism Software, San Diego, CA).

Fold change of phospho-kinase levels and angiogenesis protein levels in Tg2576 mice was calculated by normalizing the mean pixel density with the WT (B6/SJL) mice.

2.18 Statistical Analysis

The data are presented as the mean ± standard deviation. The statistical analyses were done with the help of the GraphPad Prism software using unpaired students t test when comparing two groups and a 2-way ANOVA test for multiple comparisons with a Bonferroni's test to correct for the multiple comparisons. The sample size for each experiment is indicated in the figure legend.

Chapter 3
Effect of Anti-angiogenic drugs on the impaired cognition and other AD pathologies associated with the AD mouse model Tg2576

3.1 Introduction

Growing evidence opposing the popular amyloid cascade hypothesis, as stated in Chapter 1, has encouraged researchers to steer away from a reductionist approach and instead view the AD holistically, linking the complexities and various pathways involved in the pathologies that occur. This approach may help to discover novel therapeutic targets and hence help in developing new treatments.

The amassing of the Aβ peptide in the brain is fundamental to the amyloid cascade hypothesis, in spite of the evidence that Aβ aggregates can be extensively found in the human brain in the absence of AD symptoms [137, 151, 152]. Despite this paradox, for over two decades most research has focused on investigating mechanisms that lead to the accumulation of Aβ. Recent studies increasingly point to impaired clearance of brain Aβ as a more relevant factor in AD pathogenesis.

To have a better understanding of what causes AD, it is imperative to identify the initial triggers of the neurodegenerative cascade. The two crucial vascular precursors to the neurodegenerative changes and Aβ deposition occurring in AD are the breakdown of the BBB [101, 212] and impaired CBF (hypoperfusion) [213]. In addition, the inflammatory changes observed in AD brains can drive the upregulation of angiogenic mediators such as vascular endothelial growth

factor (VEGF), resulting in pathological angiogenesis through which Aβ may further be generated [99].

The influence of these factors will be discussed in greater detail later in the thesis, and collectively they provide a strong case that AD is a disease of vascular origin. We hypothesize that an aberrant cerebral vasculature is the focal point of disease pathology **(**Figure 3.1**),** which can be triggered by various factors: inflammation, hypoperfusion and vasculotropic Aβ, leading to dysregulated angiogenesis. We propose that this hyper-vascular state is a cause, rather than a result, of the rearrangement of tight junctions and disruption of the BBB, leading to eventual damage to the CNS and loss of cognition.

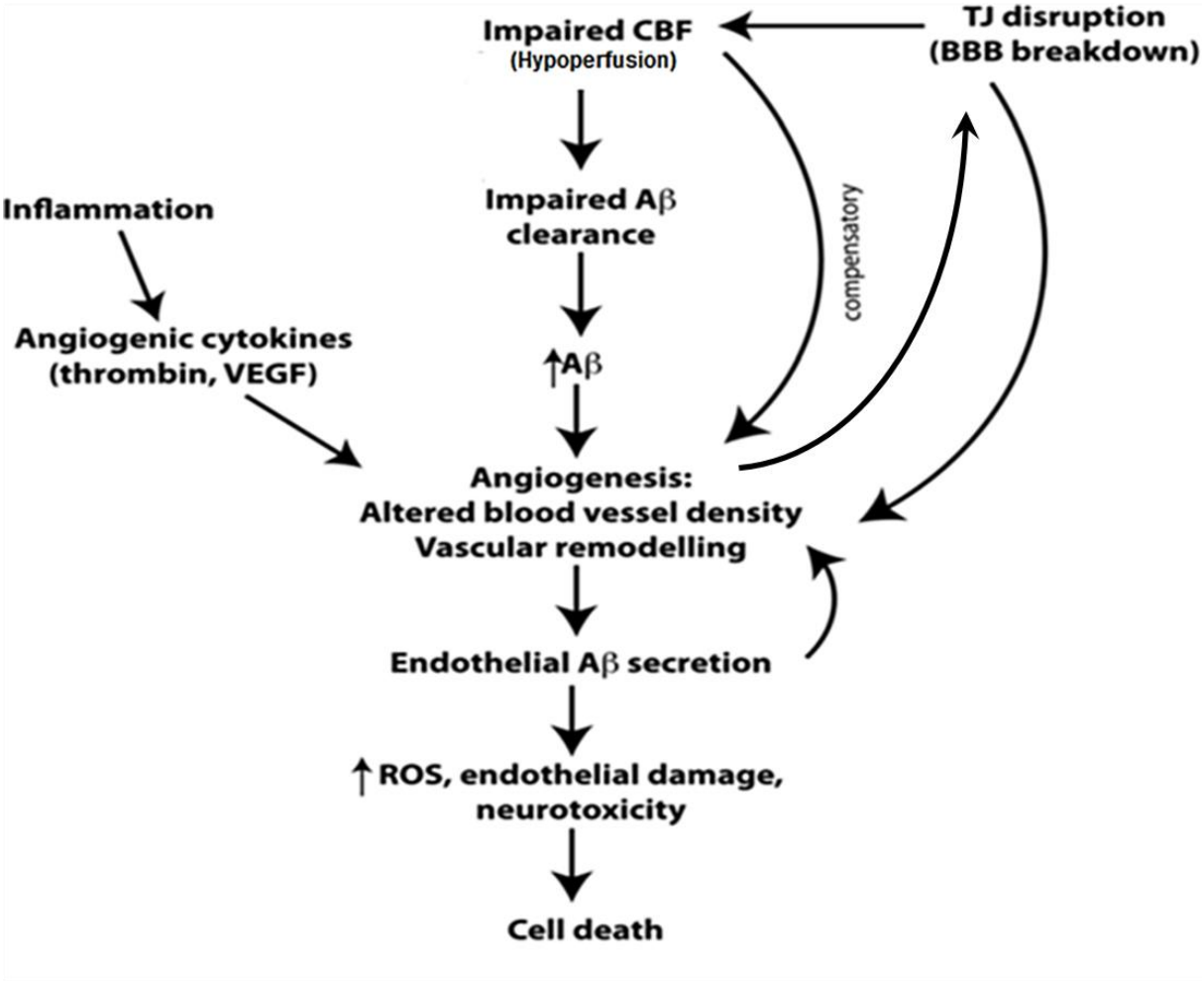

Figure 3.1: Schematic showing the proposed mechanism of pathogenesis of AD

Impaired cerebral blood flow negatively affects Aβ clearance. An increase in the amount of Aβ, a vasculotrope, triggers angiogenesis. Other factors like inflammation also increase angiogenesis. This increases vessel density and causes vascular remodelling, resulting in the dysregulation of the cerebral vasculature. The dysregulated vasculature leads to the disruption of tight junction proteins and hence breakdown of the BBB, causing harmful blood metabolites and pathogens to gain unhindered access to the CNS. This, in turn, causes neurotoxicity and other damage, leading to the decline in brain function and specific memory issues seen in AD patients.

This thesis focuses on amyloidgenesis causing vascular pathology that leads to BBB disruption and impaired cognition, and the use of drugs that target angiogenesis to see if they can reverse the AD pathogenesis associated with the familial mouse model of AD, Tg2576. It has been shown that the neurovascular unit is affected in patients suffering from AD [94, 95], and it is speculated that AD is mediated by pathological angiogenesis [88, 96-98].

For the purpose of this thesis, the effect of angiogenesis inhibitors on cognition and other AD pathologies was investigated. Angiogenesis inhibitors interfere in several ways with various steps in blood vessel growth. They may either be monoclonal antibodies that specifically recognize and bind to VEGF and make it unavailable for binding to and activating, the VEGFR, which is one of the key initiators of the pathway. The other class of angiogenesis inhibitors, i.e., small molecules, work by binding either to VEGF and/or its receptor as well as to other receptors on the surface of endothelial cells or to other proteins in the downstream signaling pathways and blocking their activities. For this chapter, we tested the effects of a small molecule tyrosine kinase inhibitor, Sunitinib, as well as a biologic, DC-101, on the AD mouse model, Tg2576.

3.1.1 Small molecule tyrosine kinase inhibitors:

A tyrosine kinase inhibitor (TKI) is a pharmaceutical drug that inhibits tyrosine kinases. Tyrosine kinases are enzymes that are responsible for the activation of many proteins by signal transduction cascades. TKIs inhibit the phosphorylation of proteins and hence curb their activity. TKIs are typically used as anticancer drugs where the uncontrolled growth of blood vessels is seen.

3.1.1.1 Sunitinib

Sunitinib (marketed as **Sutent** by Pfizer, and previously known as **SU11248**) is an oral small-molecule, multi-target receptor tyrosine kinase (RTK) inhibitor (structure shown in Figure 3.2). In 2006, it was approved by the FDA for the treatment of renal cell carcinoma (RCC) and imatinib-resistant gastrointestinal stromal tumor (GIST). Sunitinib was the first cancer drug simultaneously approved for two different indications. It has been shown to maintain normal vasculature [197-199]. Sunitinib is known to inhibit the phosphorylation of multiple receptor tyrosine kinases and is a potent inhibitor of VEGF as well as platelet derived growth factor (PDGF-β) (Figure 3.3.)

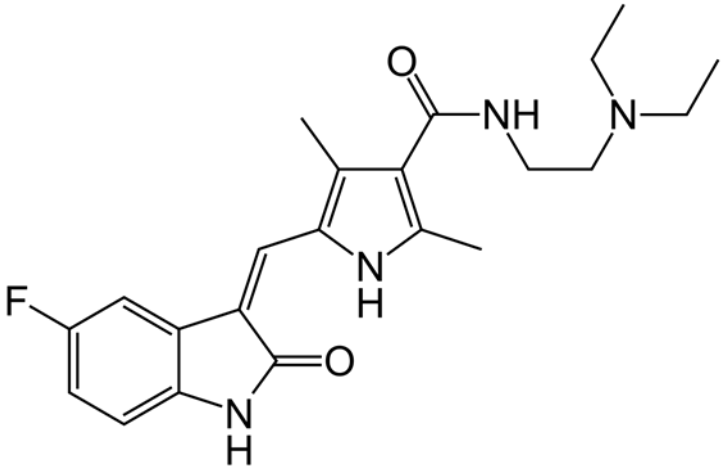

Figure 3.2: 2D Structure of Sunitinib

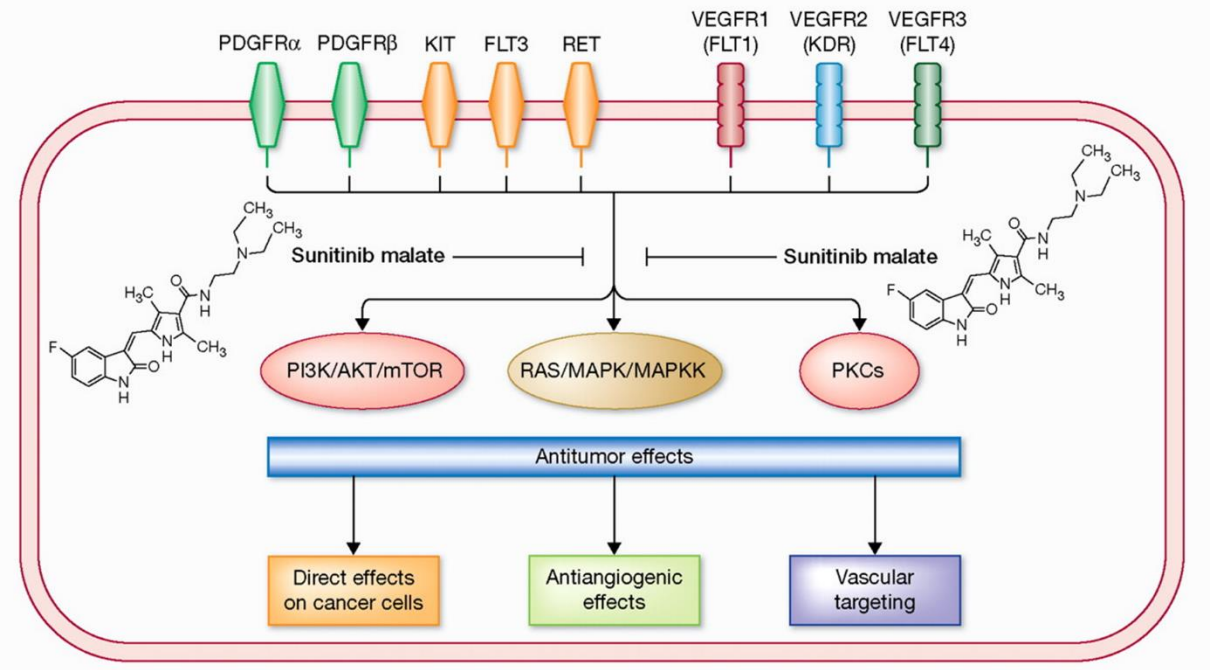

Figure 3.3: Sunitinib: mechanism of action

The inhibition of signalling pathways involved in proliferation and survival impart anti-tumor properties to Sunitinib [Figure taken from Guadalupe Aparicio-Gallego, 2011 [214]].

Sunitinib is a first-generation anti-angiogenic drug that is currently approved to treat gastrointestinal stromal tumours, renal cell cancer and pancreatic cancer. Sunitinib is used in patients suffering from gastrointestinal stromal tumor whose condition has become worse while taking imatinib mesylate or who are not able to take imatinib in the first place. Sunitinib is used in pancreatic cancer patients with progressive neuroendocrine tumors that cannot be removed by surgery, are locally advanced, or have metastasized. The drug is also used in cases where renal cell

carcinoma has reached an advanced state and as an adjuvant therapy in adults who have had nephrectomy and a high chance of tumor recurrence.

In a previous study, Sunitinib was shown to decrease the amyloid burden and reverse cognitive decline in an AD mouse model, suggesting that if we target angiogenesis, we can revert the increased accumulation of Aβ and the cognitive decline associated with AD [198].

3.1.1.2 Biologics

We now know that VEGF is the prime mediator and central component of pathological blood vessel formation [215, 216]. There are biologics that specifically target the ligand or its receptor. This specific targeted therapy can prove more efficient and less deleterious due to avoidance of unwanted 'off target' effects. A potential therapeutic target is VEGFR-2 of the VEGF receptor family. Ramucirumab is a humanized monoclonal VEGFR-2 antibody used for treating gastric cancer and metastatic colorectal cancer. DC-101 is a monoclonal antibody which is a mouse equivalent of Ramucirumab i.e. it targets mouse VEGFR-2 and inhibits the binding of the receptor with its ligand. In one study it was shown that DC-101 induced apoptosis of tumor vessel endothelium in colorectal cancer metastases [217]. Another study described how the use of DC-101 reduced tumor microvascular density and blood flow [218]. It has been demonstrated in a skin carcinoma model that after treatment with DC-101 the morphology in tumour vasculature moved towards a normal state where the blood vessels in the tumours treated with DC-101 exhibited a continuous basement membrane, normal pericyte coverage and regular intracellular junctions

[219]. This provides a conceptual foundation for the potential of DC-101 and Ramucirumab, as a therapeutic for AD [220].

In this chapter, we discuss the effect of the drugs, Sunitinib and DC-101, on angiogenesis to show how the abatement of pathogenic and dysregulated vessel formation might affect pathogenesis in AD. It is, however, understanding the molecular mechanism behind AD pathology that is of utmost importance (further studied in Chapter 4) in looking for safe and effective novel therapeutics for AD and other vascular diseases.

3.2 Results for Sunitinib

3.2.1.1 Sunitinib modulates cognition to improve certain aspects and prevents others from declining in aged transgenic AD mice -Tg2576 mice

To assess the caution and awareness shown by mice in a novel open arena, an open field test was performed on the transgenic AD model mice, Tg2576, and their wildtype (WT) littermates treated with either Sunitinib or vehicle alone (PBS+DMSO) thrice weekly for one month at 10 months of age.; both male and female mice were used for the study.

Figure 3.4a. shows the time spent in the centre of the field, the number of entries made into the central region and total distance travelled by the mice. Inherent to their nature, it was observed that the pre-treatment-WT littermate mice (B6/SJL) spent significantly less time in the centre of the field as compared to the pre-treatment-Tg2576 mice at 10 months of age. Similarly, the vehicle-treated WT mice spent significantly lesser time in the centre compared to the vehicle-

treated Tg2576 mice that explored the entire field indiscriminately. Sunitinib-treated WT mice also spent the majority of the time confined to the peripheral region of the field and very rarely explored the centre of the open field. After treatment with Sunitinib, Tg2576 mice spent less time in the centre with no significant difference when compared to the Sunitinib-treated WT mice. A significant difference was also seen between the Sunitinib-treated Tg2576 mice and both, the vehicle-treated and the pre-treatment Tg2576 mice. Similar outcomes were observed with the total number of entries made in the centre of the field and the total distance travelled by the mice.

Spatial and working memory assessment was done using a spontaneous alternation test (Y-maze) **(Figure 3.4b)**. Pre-treatment WT mice showed an alternation of 67.25±5.5% (mean ± standard deviation) and vehicle-treated WT mice showed an alternation of 43.27±3.6% between arms; no significant change was seen when WT animals were treated with the drug. Contrastingly, pre-treatment Tg2576 mice exhibited a poor performance on the test with an alternation of 52.82±4.7%. The vehicle-treated Tg2576 mice significant lower percentage of alternation (29.1±9.7%) compared to the vehicle-treated WT mice. The Sunitinib-treated Tg2576 mice, with 49.3±12.1% alternation, show significantly higher alternation compared to the vehicle-treated Tg2576 mice, however, was not significantly different compared to the pre-treatment Tg2576 mice.

In contextual fear conditioning for the associative memory assessment, mice remained stationary after being placed in an environment where they had previously received an electric shock **(Figure 3.4c)**. Both pre-treatment and vehicle -treated WT animals (B6/SJL) exhibited higher associative memory of 15.9±3.2% and 11.5±2.5% respectively than the pre-treatment and vehicle-treated

Tg2576 mice showing freezing percentages of 3.2±1.6 and 1.04±1.1% respectively. Sunitinib-treated WT mice had a significantly higher % alternation (25.4±19.4) as compared to vehicle-treated WT as well as Sunitinib-treated Tg2576 mice. Associative cognition of the Sunitinib-treated Tg2576 animals (10.9±5.8%) was significantly greater than in the vehicle-treated Tg2576 animals however it was not significantly higher than the pre-treatment Tg2576 mice.

Evaluation of reference memory (long-term) and working memory (short-term) was done by testing mice with the Radial Arm Water Maze (RAWM). **Figure 3.4d** shows the total latency time whereas **Figure 3.4e** shows the number of errors made by the mice when locating the submerged escape platform.

Comparison in the number of errors and the latency time were made between the first test day and the fifth test day within each group. Significant differences in the performance on the first test day versus the fifth test day were seen for the pre-treatment WT mice, vehicle-treated WT mice and the Sunitinib-treated WT mice. No significant difference was seen in the pre-treatment Tg2576 mice and the vehicle-treated Tg2576 mice on the first day compared to the fifth day. Interestingly, Sunitinib-treated Tg2576 mice showed a significant difference in the latency time and the number of errors when performance was compared between the first test day and the fifth test day.

The latency time and the number of errors made on the fifth test day were compared between the different groups. A significant decrease in the latency time and the number of errors between pre-treatment WT mice and pre-treatment Tg2576 mice, as well as between vehicle-treated WT and vehicle-treated Tg2576 mice was seen. A significant difference in the performance on the fifth day

was also seen between the pre-treatment and Sunitinib-treated Tg2576 mice, as well as between the vehicle-treated and Sunitinib-treated Tg2576 mice.

No significant difference was observed in the latency time and the number of errors in the performance on the fifth day between the Sunitinib-treated WT and the Sunitinib-treated Tg2576 mice. It can thus be said that over the course of 5 days, pre-treatment, vehicle-treated and Sunitinib-treated WT mice, as well as the Sunitinib-treated Tg2576 mice, showed cognitive learning in terms of reference memory and working memory aspects.

a.

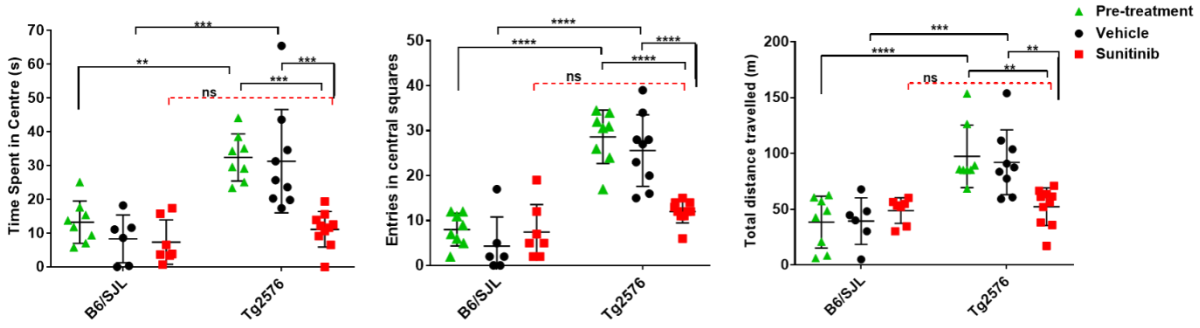
Time Spent in Centre (s)
Entries in central squares
Total distance travelled (m)
B6/SJL
Tg2576
Pre-treatment
Vehicle
Sunitinib
ns

b.

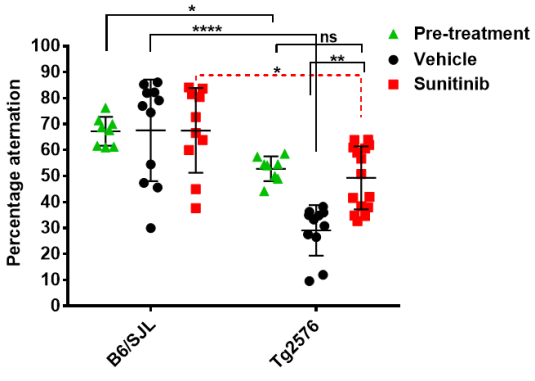
Percentage alternation
B6/SJL
Tg2576
Pre-treatment
Vehicle
Sunitinib
ns

c.

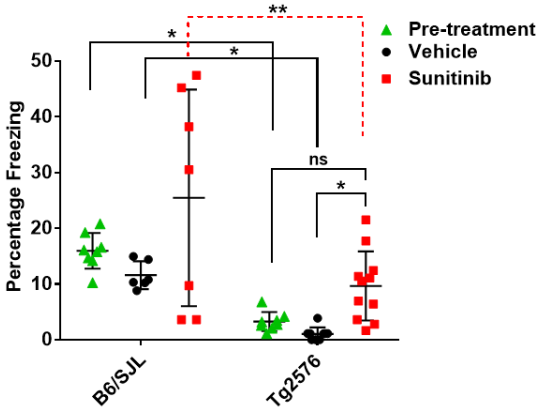
Percentage Freezing
B6/SJL
Tg2576
Pre-treatment
Vehicle
Sunitinib
ns

d.

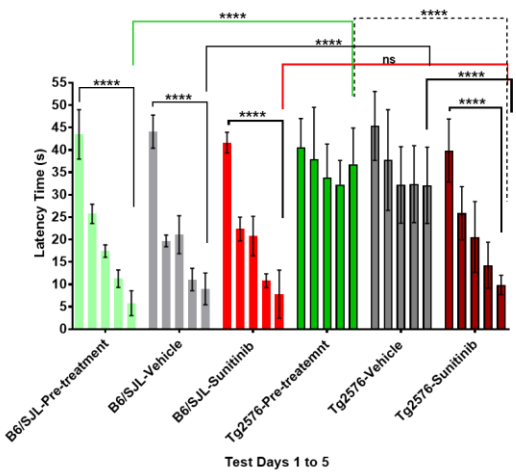
Latency Time (s)
B6/SJL-Pre-treatment
B6/SJL-Vehicle
B6/SJL-Sunitinib
Tg2576-Pre-treatemnt
Tg2576-Vehicle
Tg2576-Sunitinib
Test Days 1 to 5
ns

e.

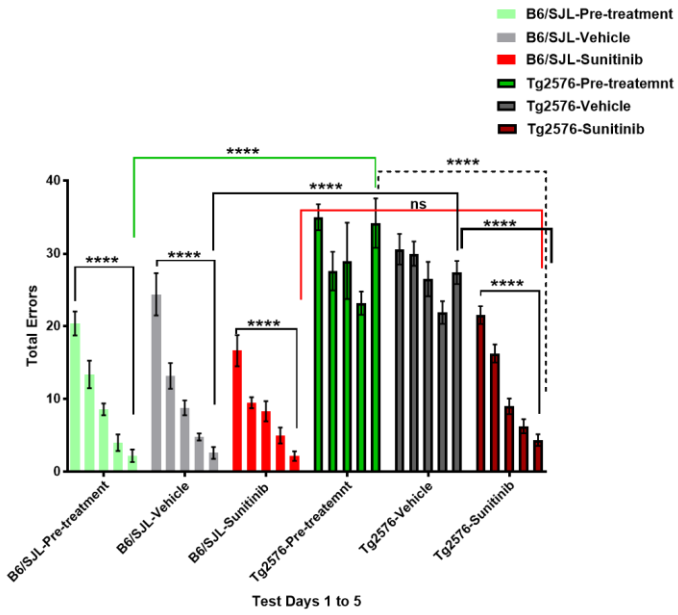
B6/SJL-Pre-treatment
B6/SJL-Vehicle
B6/SJL-Sunitinib
Tg2576-Pre-treatemnt
Tg2576-Vehicle
Tg2576-Sunitinib
Total Errors
Test Days 1 to 5
ns

Figure 3.4: Treatment with the anti-angiogenic drug, Sunitinib, reduces cognitive impairment in aged Tg2576 mice.

10-month-old Tg2576 and WT littermate mice were treated with the anti-angiogenic tyrosine kinase inhibitor, Sunitinib, for 1 month at a dose of 80mg/kg, 3 days/week. Pre-treatment 10-month old mice and Post-treatment 11-month old mice were assessed for their cognitive status, using tests for the analysis of different memory aspects. The data were pooled from 3 different trials and is represented as mean±standard deviation. Statistical analysis was carried out using a 2-way ANOVA with correction for multiple comparisons using the Bonferroni's test **(* p<0.03; ** p<0.002; *** p<0.0002; **** p<0.0001).**
For open field test, fear conditioning and RAWM tests: pre-treatment-WT, n=8; WT-vehicle, n =6; WT-Sunitinib, n=7; pre-treatment-Tg2576, n=8; Tg2576-vehicle, n = 9; Tg2576-Sunitinib, n=11.
For Y-maze: pre-treatment-WT, n=8; WT-vehicle, n =11; WT-Sunitinib, n=10; pre-treatment-Tg2576, n=8; Tg2576-vehicle, n = 11; Tg2576-Sunitinib, n=15).

a) Open Field Test. WT mice (B6/SJL) spent less in the center of the field, with no significant difference seen pre-treatment as well as when treated with Sunitinib. Vehicle-treated Tg2576 mice spent more time exploring the center but this was not seen when the Tg2576 mice were treated with Sunitinib. A significant difference was seen between the pre-treatment WT and Tg2576. A significant difference was also seen between pre-treatment Tg2576 and Sunitinib-treated Tg2576 mice. There was no significant difference noted between the Sunitinib-treated WT and Sunitinib-treated Tg2576 mice. However, a significant difference was observed between vehicle-treated and Sunitinib-treated Tg2576 mice. Similar results were observed in the number of entries in the central squares and the total distance travelled by the different group of mice.

b) Spontaneous alternation (Y-maze). Cognitively aware mice show a high percentage of alternation, as was seen in the pre-treatment, vehicle-treated and Sunitinib-treated WT mice. There was a significant difference between the pre-treatment WT and Tg2576 mice as well as between the vehicle-treated WT and Tg2576 mice. A significant increase in the percentage alternation was seen in the Sunitinib-treated Tg2576 mice compared to the vehicle-treated Tg2576 mice, however, there was no significant difference seen between the Sunitinib-treated and pre-treatment Tg2576 mice. Sunitinib-treated Tg2576 mice did not reach the level of performance as the Sunitinib-treated WT mice as a significant difference was seen between the two groups.

c) Contextual Fear conditioning. WT mice, both pre-treatment and vehicle-treated, showed high freezing percentages indicative of good associative memory. Sunitinib-treated WT mice showed a significant increase in freezing percentage compared to the vehicle-treated WT mice but not when compared to pre-treatment. Pre-treatment and vehicle-treated Tg2576 mice displayed a significantly lower freezing percentage compared to pre-treatment and vehicle-treated WT mice respectively. A significant increase was seen in the Sunitinib-treated Tg2576 mice when compared to vehicle-treated Tg2576 mice, however, this increase was not significant when compared to pre-treatment Tg2576 mice. A significant difference still remained between the Sunitinib-treated WT and the Sunitinib-treated Tg2576 mice.

d, e) Radial arm water maze. (d) the time it takes for the mice to locate the escape platforms i.e. *Latency time*, and **(e)** the *number of errors* (working and reference memory errors) made by the mice when locating the escape platforms. Pre-treatment, vehicle- and Sunitinib-treated WT mice showed a significant decrease in the latency time and the number of errors made when comparing test day 1 and test day 5. A similar improvement over the course of the trial was seen in the Sunitinib-treated Tg2576 mice. No significant difference between test day 1 and test day 5 were seen in the pre-treatment and the vehicle-treated Tg2576 mice.

A significant difference was seen in the latency time and number of errors made on test day 5 between the pre-treatment WT and Tg2576 mice as well as the vehicle-treated WT and Tg2576 mice. A significant difference was also observed between the pre-treatment and Sunitinib-treated Tg2576 mice as well as between the vehicle-treated and Sunitinib-treated Tg2576 mice. No significant difference was observed when comparing latency time and number of errors made by the pre-treatment and vehicle-treated Tg2576 mice as well as the Sunitinib-treated WT and Tg2576 mice on test day 5.

3.2.1.2 Sunitinib treatment reduces cerebral vascular pathology, cerebral Aβ load and tight junction disruption in Tg2576 mice

To assess the effect of the drug on AD pathology, the brains of treated mice were analysed by semi-quantitative western blotting to look for protein expression of the neoangiogenic marker CD105, as well as of Aβ, amyloid precursor protein (APP) and the tight junction protein, ZO1. CD105 and APP proteins levels were analyzed using the cytosolic fraction where as the membrane bound SDS fraction was used for ZO1 and formic acid fraction was used for Aβ. One-month Sunitinib treatment of 10-month old Tg2576 mice resulted in a significant decrease in the expression of CD105 as compared to the vehicle-treated Tg2576 mice **(Figure 3.5a)**. Higher expression of ZO1 in Tg2576 mice treated with the drug compared to the vehicle-treated Tg2576 mice **(Figure 3.5a)** indicated the presence of tight junctions in treated animals. Significantly lower Aβ expression was observed in Tg2576 mice treated with Sunitinib in comparison to vehicle-treated Tg2576 **(Figure 3.5b)**. A reduction in overall APP protein expression was also observed in Sunitinib-treated Tg2576 mice in comparison to vehicle-treated Tg2576 mice **(Figure 3.5c)**.

Immunohistological analysis of these proteins in the cortex and hippocampus of the mouse brains confirmed the western blotting data. **Figure 3.5d** shows representative micrographs. It can be noted in the histograms that there is amyloid staining in the vehicle-treated Tg2576 mice and that amyloid is significantly less abundant in the Sunitinib-treated Tg2576 group.

Expression of CD105, the sprouting vessel marker, was higher in the vehicle-treated Tg2576 group, which indicates a state of hypervascularity, as compared to the WT animals. This hyper-vascular state was not apparent when Tg2576 mice were treated with Sunitinib. Lower expression

of the tight junction protein, occludin, indicative of BBB impairment, can be seen in the vehicle-treated Tg2576 as compared to B6/SJL or Sunitinib-treated Tg2576 mice (**Figure 3.5d).**

a.

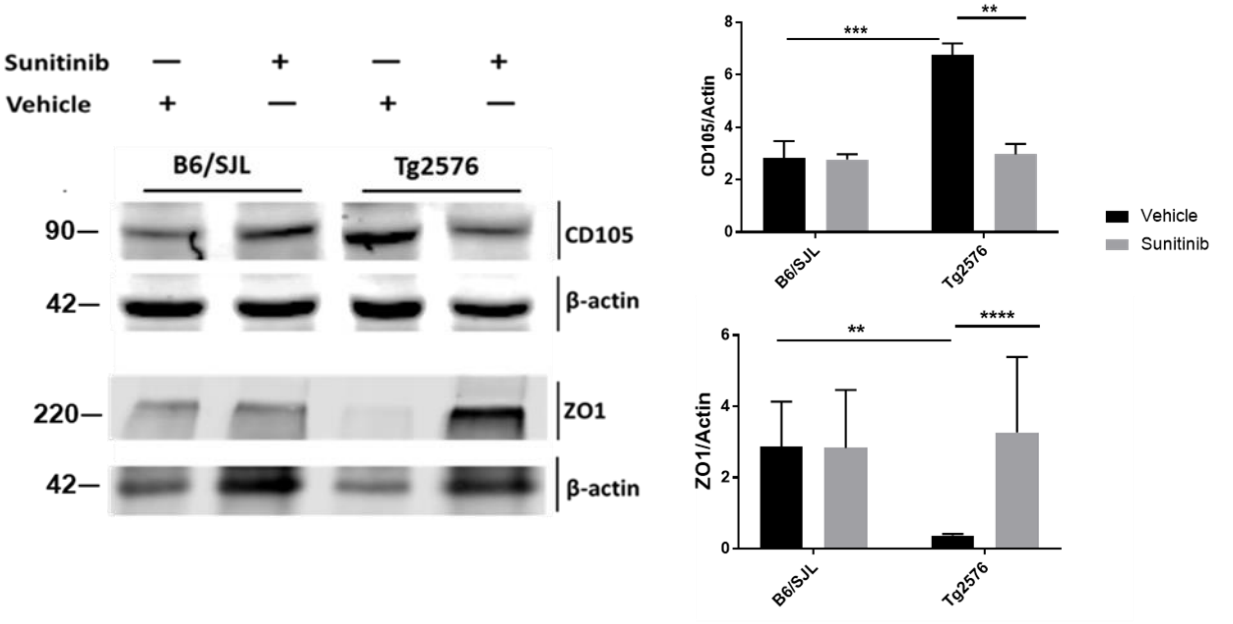

b.

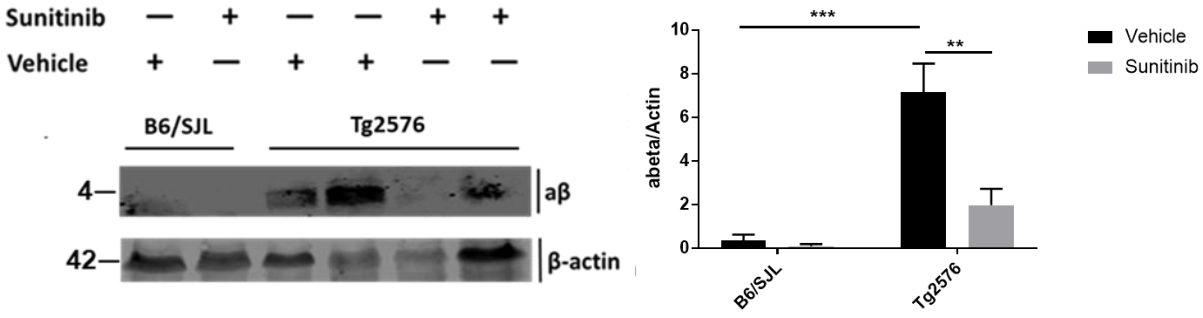

c.

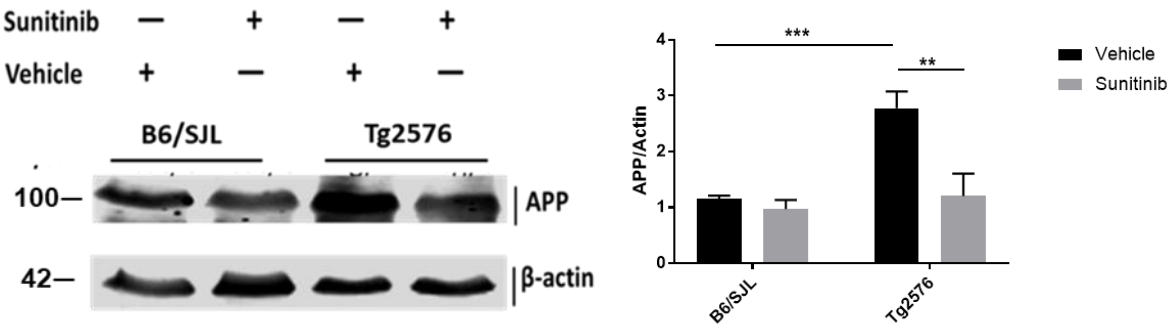
Sunitinib — + — +
Vehicle + — + —
B6/SJL
Tg2576
100—
APP
42—
β-actin
APP/Actin
***
**
Vehicle
Sunitinib
B6/SJL
Tg2576

d.

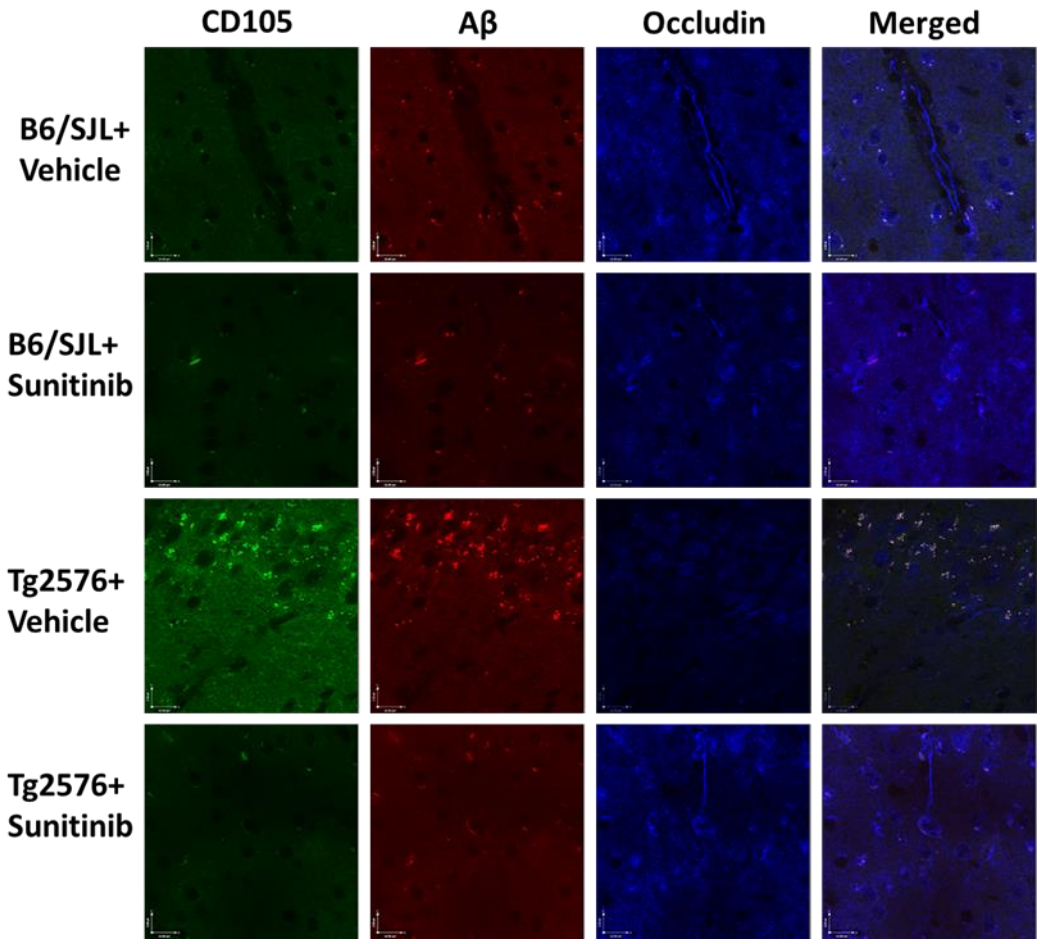
CD105
Aβ
Occludin
Merged
B6/SJL+ Vehicle
B6/SJL+ Sunitinib
Tg2576+ Vehicle
Tg2576+ Sunitinib

Figure 3.5: Treatment with Sunitinib reduces expression of Aβ, angiogenic marker, CD105 and tight junction proteins, ZO1 and occludin in aged Tg2576 mice.

Brains from perfused mice were used for molecular analysis. Homogenates were used for western blotting and fixed brain sections for histological analysis. Representative data from three separate experiments are shown for mice from the different groups with WT n= 6 and Tg2576 n= 6. The histograms show mean± standard deviation. Statistical analysis is done using unpaired Student's t test **(* *p*<0.03; ** *p*<0.002; *** *p*<0.0002; **** *p*<0.0001).**

Semiquantitative western blot analysis (a-c): a) Expression of **CD105** and **ZO1.** Brain expression of CD105, an angiogenesis marker, was significantly lowered after Sunitinib treatment of Tg2576 mice, resembling the WT brain levels. The expression of tight junction protein, ZO1, was significantly lower in vehicle-treated Tg2576 mice compared to the WT mice and Tg2576 mice treated with Sunitinib. **b)** The presence of **Aβ** and **c)** the presence of **APP** were significantly less after Sunitinib treatment in comparison to vehicle-treatment in the Tg2576 mouse brain so that levels in the brains of Sunitinib-treated animals resembled those in WT animals. *note: Aβ1-42 (#39377; abcam) used here, specific for both human and mouse APP.

Immunofluorescence analysis (**d**)**:** brain sections of mice from different groups were stained for the combination of markers CD105, Aβ and tight junction protein occludin. The micrograph panels shown are representative of the cortical and hippocampal regions of the brains from mice belonging to the different treatment groups. Heavy amyloid staining in the Tg2576 mouse brain compared to the WT mice. More sprouting vessels (CD105) and Aβ plaques and less occludin expression were seen in vehicle-treated Tg2576 compared to the WTs or Sunitinib-treated Tg2576 mice.

3.2.1.3 Sunitinib treatment reduces the loss of tight junction structure and BBB integrity in aged Tg2576 mice.

The physical seal of the BBB is maintained mainly by an intact continuous arrangement of the tight junction proteins (TJP), ZO1, claudin and occludin, along with other components of the neurovascular unit. Their alteration can lead to disruption of the tight junctions between the endothelial cells and increased permeability of the barrier, resulting in unhindered movement of damage-promoting blood products into the brain, advancing AD pathology.

The percentage the TJP disruption was analysed in Sunitinib-treated Tg2576 and control mice **(Figure 3.6e)**. WT mice showed a normal continuous expression pattern of TJPs (as indicated with the white arrows in the micrographs) and thus a low percentage of disruption, irrespective of Sunitinib or vehicle treatment. In the vehicle-treated Tg2576 mice, however, there was a significant increase in the disruption of the TJPs. Tg2576 mice treated with Sunitinib showed a TJP expression pattern similar to that in the WT mice.

To prove that this intact arrangement of the TJP influenced the permeability of the BBB in the animals, we conducted an Evans Blue assay. Evans Blue dye binds to serum albumin, a protein to which the normal BBB is impermeable. A disrupted BBB allows albumin to move across and enter the central nervous system (CNS), which is indicated by the presence of the dye in the brain.

Brains (cortex and hippocampus) were assessed for the extent to which the dye had crossed into the CNS.

Figure 3.7**a.** illustrates absorbance attributed to Evans blue staining in terms of optical density/unit mass of brain. A higher absorbance was noted in vehicle-treated Tg2576 mice compared to WT littermates. Lower uptake of Evans Blue into the CNS was seen after Sunitinib treatment of Tg2576 mice than in vehicle-treated Tg2576 mice. Representative micrographs of the cortical and hippocampal regions of the brain in

Figure 3.7**b** show the presence of albumin detected with the help of fluorochrome labeled antibody and the auto-fluorescing Evans blue in the CNS. Minimal amounts of albumin were seen in the WT brains, indicating an intact BBB, whereas the substantial Evans Blue staining seen in the vehicle-treated Tg2576 mice implies a disrupted and highly permeable BBB. The brains of the Sunitinib-treated Tg2576 mice show that much less albumin crosses into the CNS in comparison to the vehicle-treated mice, demonstrating a functional BBB after Sunitinib treatment.

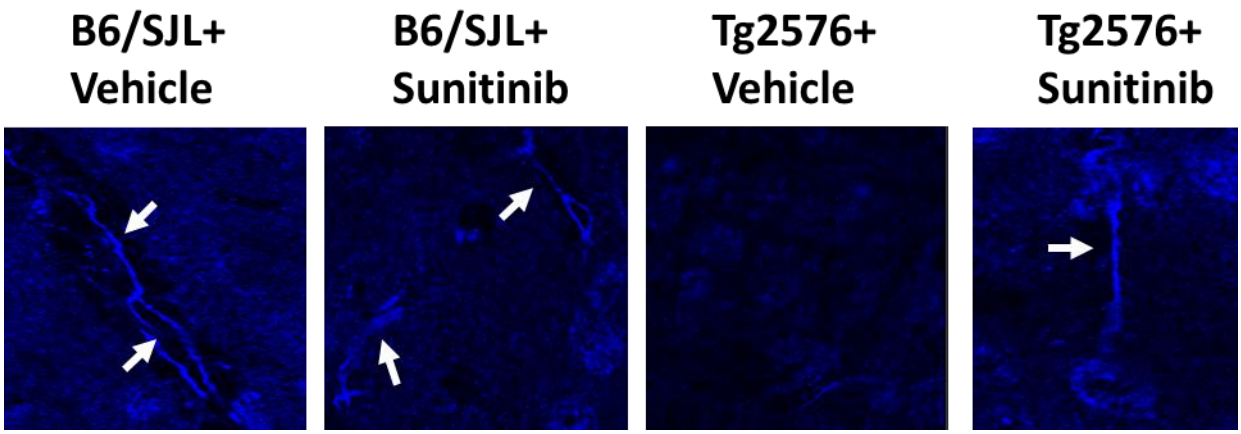

Figure 3.6: Treatment of aged Tg2576 mice with the anti-angiogenic drug, Sunitinib, reduces the loss of tight junctions in cerebral vessels.

The brain sections of mice from different groups were stained for the tight junction protein, occludin. The micrograph panels shown are representative of the cortical and hippocampal regions of the brains from mice belonging to the different treatment groups with WT n= 6 and Tg2576 n= 6. Disrupted occludin expression was noted in the vehicle-treated in Tg2576 as compared to WT mice (B6/SJL). In contrast, occludin expression in the Sunitinib-treated Tg2576 mice was similar to WT. Normal expression patterns of occludin are indicated with the white arrows in the micrographs.

a.

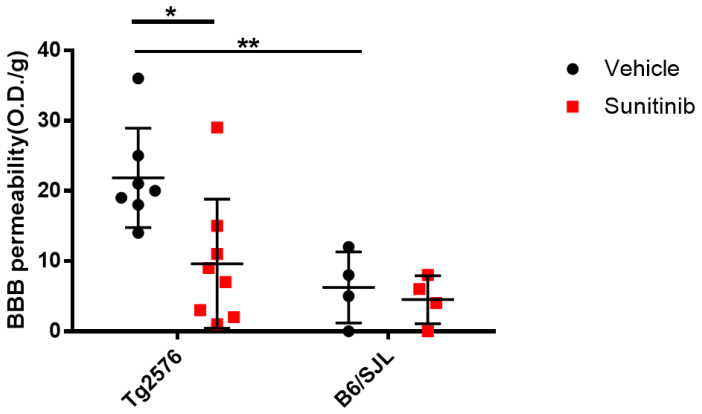
*
**
BBB permeability(O.D./g)
40
30
20
10
0
Tg2576
B6/SJL
Vehicle
Sunitinib

b.

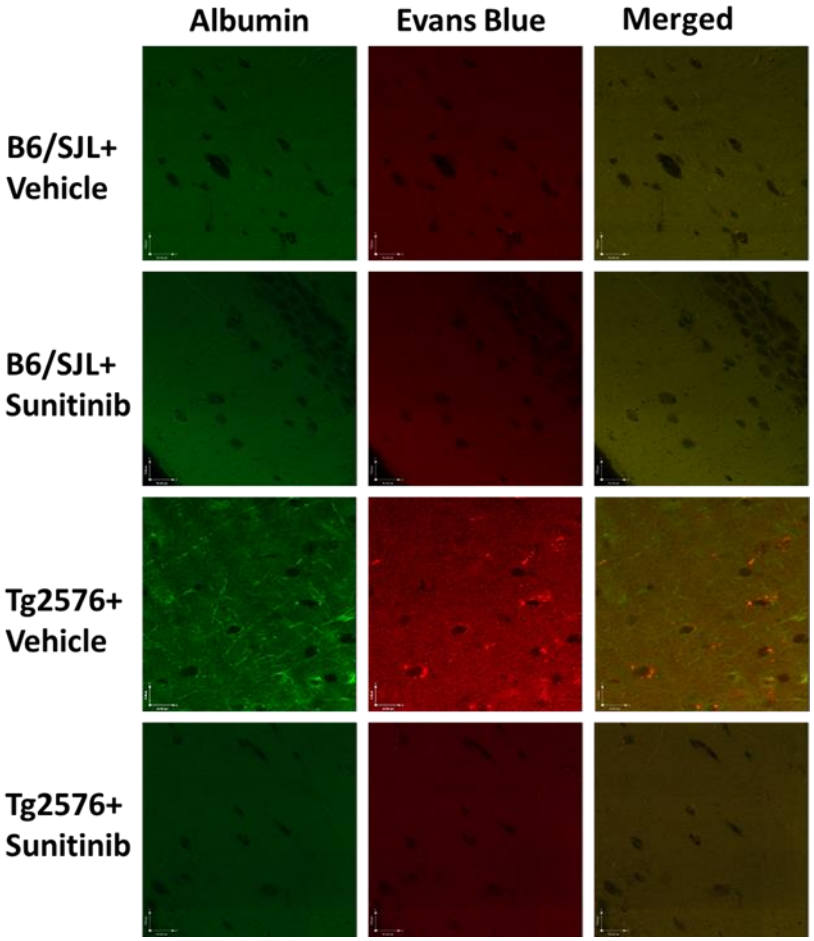
Albumin
Evans Blue
Merged
B6/SJL+
Vehicle
B6/SJL+
Sunitinib
Tg2576+
Vehicle
Tg2576+
Sunitinib

Figure 3.7: Functional BBB in aged Tg2576 mice after Sunitinib treatment

a) Evans Blue dye was i.p. injected into mice from the treatment trial. Brains were harvested and homogenized with 50% trichloroacetic acid followed by dilution with ethanol. The absorbance was read with an ELISA plate reader (Spectra Max 190; Molecular Devices, Sunnyvale, CA) at 620 nm. The readings were divided by the weight of the brain. This experiment was repeated twice. Data represents mean± standard deviation. Statistical analysis was done using unpaired Student's t test **(* p<0.03; ** p<0.002; *** p<0.0002; **** p<0.0001)**.

The absorbance of the dye in different groups. Greater uptake of Evans Blue in the CNS was seen in the brain homogenates of the vehicle-treated Tg2576 mice, higher BBB permeability or leakiness compared to the WT mice (B6/SJL) or Sunitinib-treated Tg2576 animals.

b) Representative 2D micrographs of coronal brain sections from WT and Tg2576 mice treated with vehicle or Sunitinib, where green indicates albumin that has leaked into the brain and red indicates Evans blue dye. Sunitinib treatment of aged Tg2576 resulted in less albumin and Evans blue in the brain, indicative of a functional BBB, in comparison to vehicle-treatedTg2576 mice.

3.3 Results for DC-101

3.3.1.1 DC-101 modulates cognition to improve certain aspects and prevents others from declining in aged transgenic AD mice -Tg2576 mice

To assess the caution and awareness shown by mice in a novel open arena, an open field test was performed on the transgenic AD model mice, Tg2576 and their wildtype (WT) littermates which were treated with either DC-101 or vehicle alone (PBS+DMSO) thrice weekly for one month at disease onset. Both male and female mice at 10 months of age were used. No differences were seen between male and female mice in the behavioural testing or in their responses to the treatments, so data for both sexes were pooled in all analyses.

Inherent to their nature, it was observed that the WT littermate (B6/SJL) mice pre-treatment, as well as vehicle-treated spent majority of the time confined to the peripheral region of the field and very rarely, explored the centre of the open field. This did not change in the WT mice treated with DC-101 **(Figure 3.8a)**. On the other hand, the pre-treatment and vehicle-treated Tg2576 mice explored the entire field indiscriminately, with significantly more distance travelled compared to all the other groups and spent significantly more time and a higher number of entries into the centre of the field to as compared to the WT littermates. After treatment with DC-101, the Tg2576 mice explored the field to a lower extent and spent significantly less time in the centre as compared to the pre-treatment and vehicle-treated Tg2576 mice.

Spatial and working memory assessment was done using a spontaneous alternation test (Y-maze). WT mice pre-treatment and vehicle-treated showed an alternation of 65.25±5.5% and 70.1±13.6% respectively (mean± standard deviation) between arms with no significant change seen after

treatment with DC-101 (71.2.6±12.1%). In contrast, Tg2576 mice pre-treatment and vehicle-treated showed poor performance on the test with a statistically significant lower percentage alternation of 52.82±4.7% and 40.4±5.3% respectively. The DC-101-treated Tg2576 mice were significantly different compared to vehicle-treated Tg2576 mice and DC101-treated WT however DC101-treated Tg2576 mice were indistinguishable from pre-treatment Tg2576 mice **(Figure 3.8b)**.

In contextual fear conditioning for the associative memory assessment, mice were seen to "freeze" (remain stationary) after being placed in an environment where they had previously received an electric shock. Pre-treatment, vehicle-treated and DC-101 treated WT (B6/SJL) animals exhibited good associative memory with freezing percentages of 15.96±3.2%, 20.5±7.5% and 29.06±12.7% respectively **(Figure 3.8c)**. Contrastingly, pre-treatment and vehicle-treated Tg2576 mice showed poor freezing percentages of 3.2±1.6% and 0.98±1.3% respectively. (Figure 3.8: Anti-angiogenic drug, DC-101, partially prevents the cognitive decline associated with aged AD mouse model Tg2576). DC-101-treated Tg2576 mice showed a freezing percentage to 9.6± 6.2%. This was significantly different from vehicle-treated Tg2576 mice and DC-101-treated WT mice, however, were not significantly different from pre-treatment Tg2576 mice.

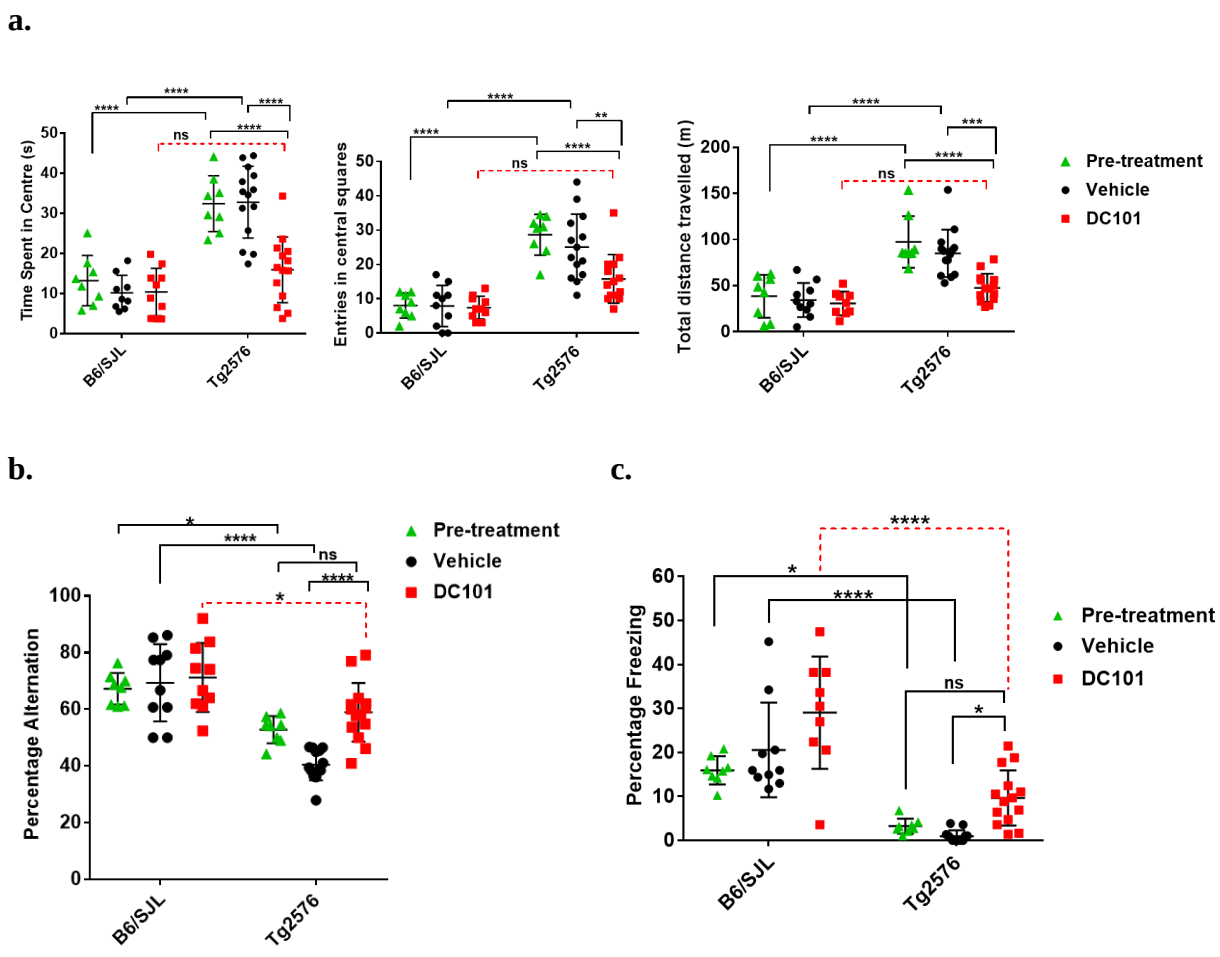

Figure 3.8: Anti-angiogenic drug, DC-101, partially prevents the cognitive decline associated with aged AD mouse model Tg2576

10-month-old Tg2576 and WT littermate mice were treated with DC-101, a monoclonal antibody that targets VEGFR-2, for 1 month at a dose of 0.8mg/mouse, 3 days/week. After treatment, the mice were assessed for their cognitive status, using tests for the analysis of different memory aspects **(* p<0.03; ** p<0.002; *** p<0.0002; **** p<0.0001).** The above data represents the mean± standard deviation from 3 different trials. Statistical analysis was done using 2-wat ANOVA

(Pre-treatment WT and Tg2576, n= 8; WT-vehicle and WT-DC101, n =10; Tg2576-vehicle and Tg2576-DC101, n = 14)

a) Open Field Test: Pre-treatment and vehicle-treated WT mice (B6/SJL) spend less in the center of the field, with no significant difference seen when treated with DC-101. Pre-treatment and vehicle-treated Tg2576 mice spend significantly more time exploring the center compared to the WT mice and DC-101-treated Tg2576 mice. A similar result was seen in the total distance travelled by the mice and the number of entries made in the center of the field.

b) Spontaneous alternation (Y-maze): Cognitively aware mice show a high percentage of alternation, as was seen in the pre-treatment and vehicle-treated WT mice with no significant change observed after treatment with DC-101. Pre-treatment and vehicle-treated Tg2576 mice exhibited poor performance on the test, with a significantly lower percentage of alternation compared to the WT mice. DC-101-treated Tg2576 mice showed a significant difference compared to the vehicle-treated Tg2576 mice but no significant difference compared to the pre-treatment Tg2576 mice.

c) Contextual Fear conditioning: WT mice, pre-treatment, vehicle-treated and DC-101-treated, showed high freezing percentages indicative of good associative memory. Pre-treatment and vehicle-treated Tg2576 mice displayed a significantly lower freezing percentage. DC-101-treated Tg2576 animals showed a significant difference compared to vehicle-treated Tg2576 mice but no significant difference compared to the pre-treatment Tg2576 mice.

3.3.1.2 DC-101 reduces expression of cerebral Aβ, angiogenic marker, CD105 and tight junction proteins in aged Tg2576 mice

To assess the effect of the antibody, DC-101, on AD pathology, the brains of treated mice were analysed by semi-quantitative western blotting to look for protein expression of the neoangiogenic marker CD105, as well as of Aβ and the tight junction protein, ZO1. CD105 protein level was analyzed using the cytosolic fraction where as the membrane bound SDS fraction was used for ZO1 and formic acid fraction was used for Aβ. One-month treatment of Tg2576 mice with DC-101 resulted in a decrease in Aβ and CD105 expression levels **(Figure 3.9a)** and increase in the expression in ZO-1 compared to those treated with the vehicle alone **(Figure 3.9b)**.

Immunofluorescence analysis of these proteins in both, the cortex and hippocampus of the mouse brains confirmed the western blotting data. Figure 3.9**c** shows representative micrographs of the cortex and hippocampus. Higher amyloid and CD105 staining were observed in the vehicle-treated Tg2576 mice but not in Tg2576 mice that had been treated with DC-101. Reduced occludin expression was observed in the vehicle-treated Tg2576 mice, but after treatment with DC-101 occludin expression was similar to the expression seen in the WT animals.

a.

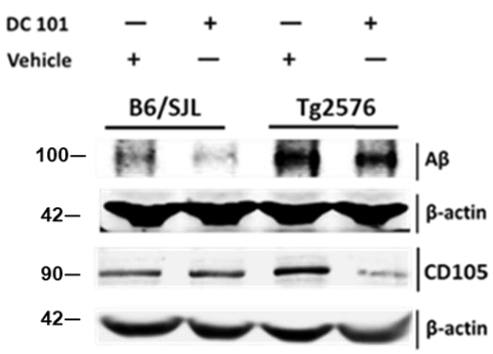
DC 101 — + — +
Vehicle + — + —
B6/SJL
Tg2576
100—
Aβ
42—
β-actin
90—
CD105
42—
β-actin

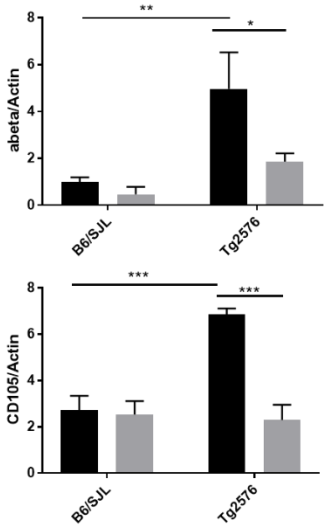
abeta/Actin
**
*
0
2
4
6
8
B6/SJL
Tg2576
CD105/Actin
***
***
0
2
4
6
8
B6/SJL
Tg2576

b.

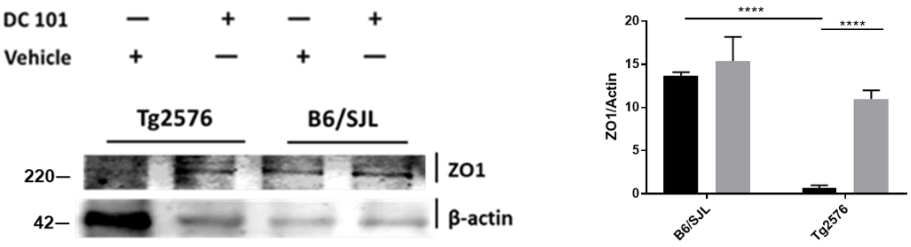
DC 101 — + — +
Vehicle + — + —
Tg2576
B6/SJL
220—
42—
ZO1
β-actin
ZO1/Actin
20
15
10
5
0
****
****
B6/SJL
Tg2576

c.

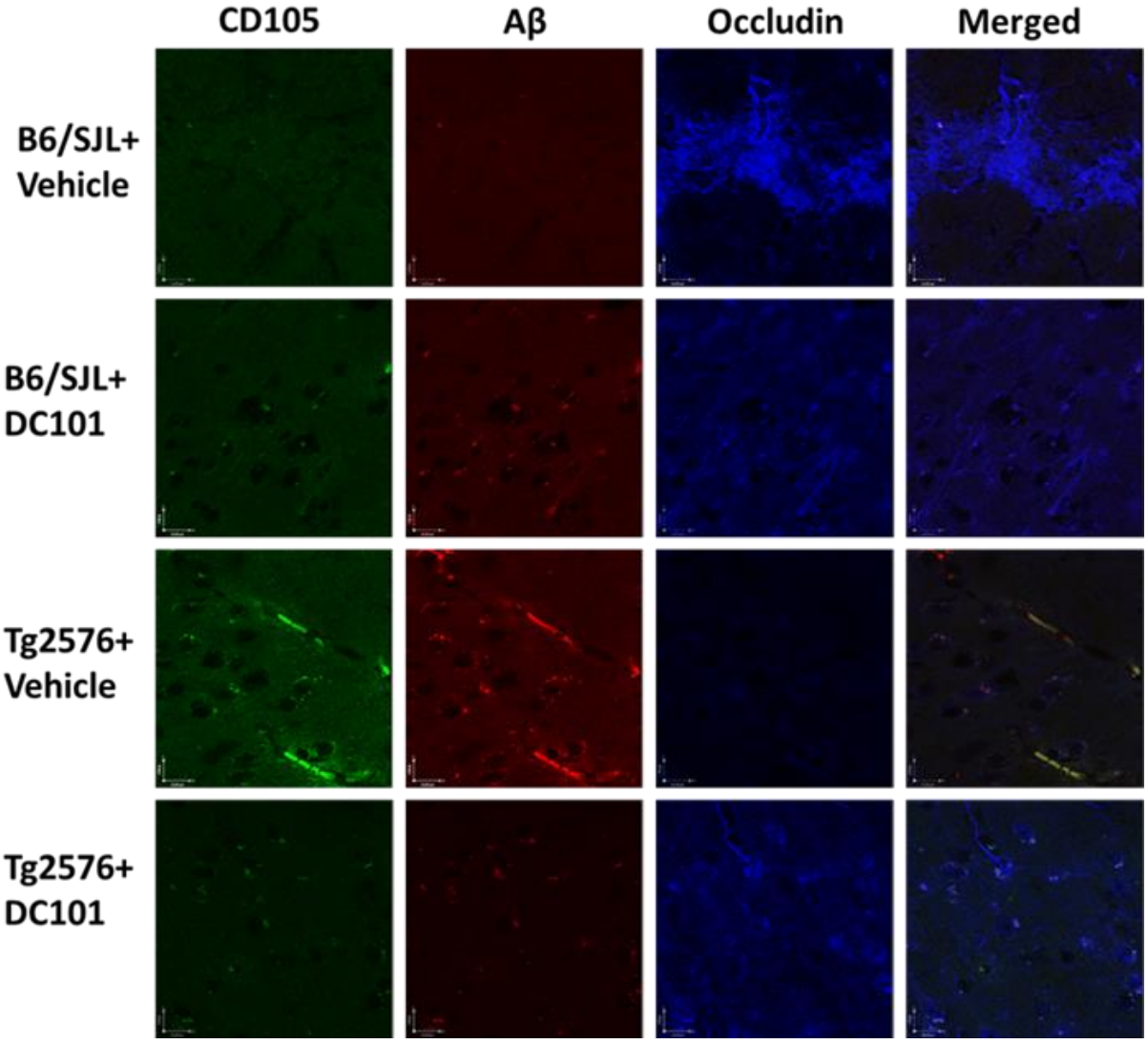

Figure 3.9: DC101 treatment of aged Tg2576 mice shows lower expression of Aβ, angiogenic vessel marker, CD105 and higher expression of tight junction proteins

Brains from perfused mice were used for molecular analysis. Homogenates were used for western blotting analysis and fixed brain sections were used for immunofluorescence analysis. The graphs show data as the mean ± standard deviation and are pooled from three separate experiments with total WT n= 12 and Tg2576 n=12. Statistical analysis was done using unpaired students t test.

Semiquantitative western blot analysis (a-b): a) The presence of Aβ and CD105 in the Tg2576 mouse brain was significantly lowered by DC-101 treatment so that levels in the brain resembled the WT levels **b)** The expression of tight junction protein, ZO1, was significantly lower in vehicle-treated Tg2576 mice than DC-101-treated Tg2576 mice or WT mice.

Immunofluorescence analysis (c): brain sections of mice from different groups stained for the combination of markers; CD105, Aβ and tight junction protein occludin. The micrograph panels shown are representative of the cortical and hippocampal regions of the brains from the mice belonging to the different treatment groups. **d)** Heavy amyloid staining and more Aβ plaques are seen in the vehicle-treated Tg2576 mouse brain compared to DC-101-treated Tg2576 or WT mice. More sprouting vessels (CD105) are seen in vehicle-treated Tg2576 compared to DC-101-treated Tg2576 or WTs. Substantially diminished occludin expression was noted in the vehicle-treated Tg2576 compared to WT mice (B6/SJL),

3.3.1.3 DC-101 treatment reduces the loss of tight junction structure and BBB integrity in aged Tg2576 mice.

A normal occludin expression pattern, indicated by white arrows in **Figure 3.10,** is strong and continuous. It was observed that the WT mice showed a normal expression pattern of TJPs and thus a low percentage of BBB disruption, irrespective of DC-101 or vehicle treatment. In the vehicle-treated Tg2576 mice, however, there was a disruption of the TJPs that was not seen in Tg2576 mice treated with DC-101.

To show that this intact arrangement of the TJP influences the impermeability of the BBB in the DC-101-treated Tg2576 animals, we i.p injected Evans Blue dye in the mice. Evans Blue dye binds to serum albumin, a protein to which the normal BBB is impermeable. A disrupted BBB will allow albumin to move across and enter the central nervous system (CNS), which is indicated by the presence of the dye in the brain. **Figure 3.11** shows that when Evans Blue dye is injected into mice that have an intact BBB, the dye is unable to cross into and stain the brain. Representative micrographs of the cortical and hippocampal regions of the brain in Figure 3.11 show minimal amounts of albumin in the WT brains, indicating an intact BBB. In contrast, substantial presence of both Evans blue and albumin is apparent in the brains of vehicle-treated Tg2576 mice, implying a disrupted and permeable barrier. The brains of the DC-101-treated Tg2576 mice appear similar to those of the WT mice, indicating a functional BBB.

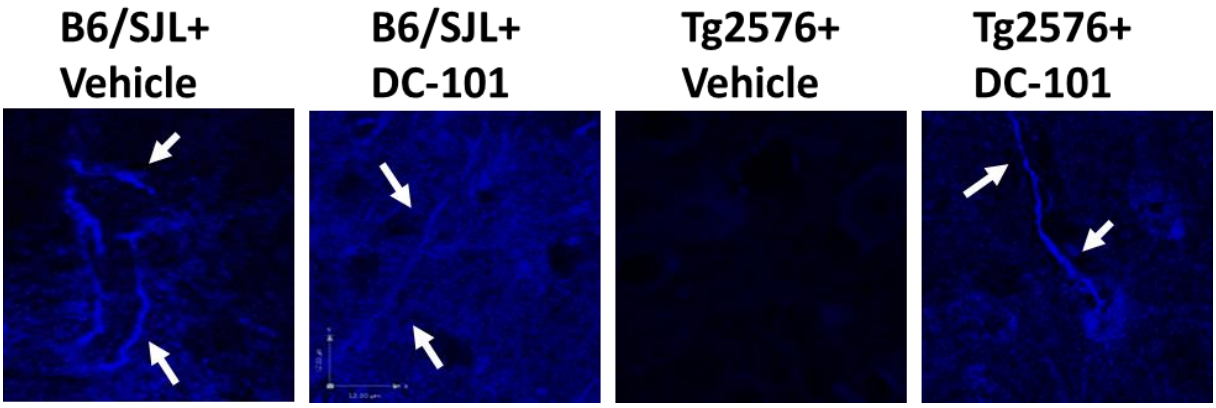

Figure 3.10: Treatment of aged Tg2576 mice with the anti-angiogenic antibody, DC-101 reduces the loss of tight junctions in cerebral vessels.

The brain sections of mice from different groups were stained for the tight junction protein, occludin. The micrograph panels shown are representative, of the cortical and hippocampal regions of the brains from the mice belonging to the different treatment groups with WT n= 5 and Tg2576 n= 6. Abnormal occludin expression was noted in the brains of vehicle-treated Tg2576 mice as compared to the WT (B6/SJL) or DC-101-treated Tg2576 mice. Normal expression pattern of occludin is indicated with the white arrows in the micrographs.

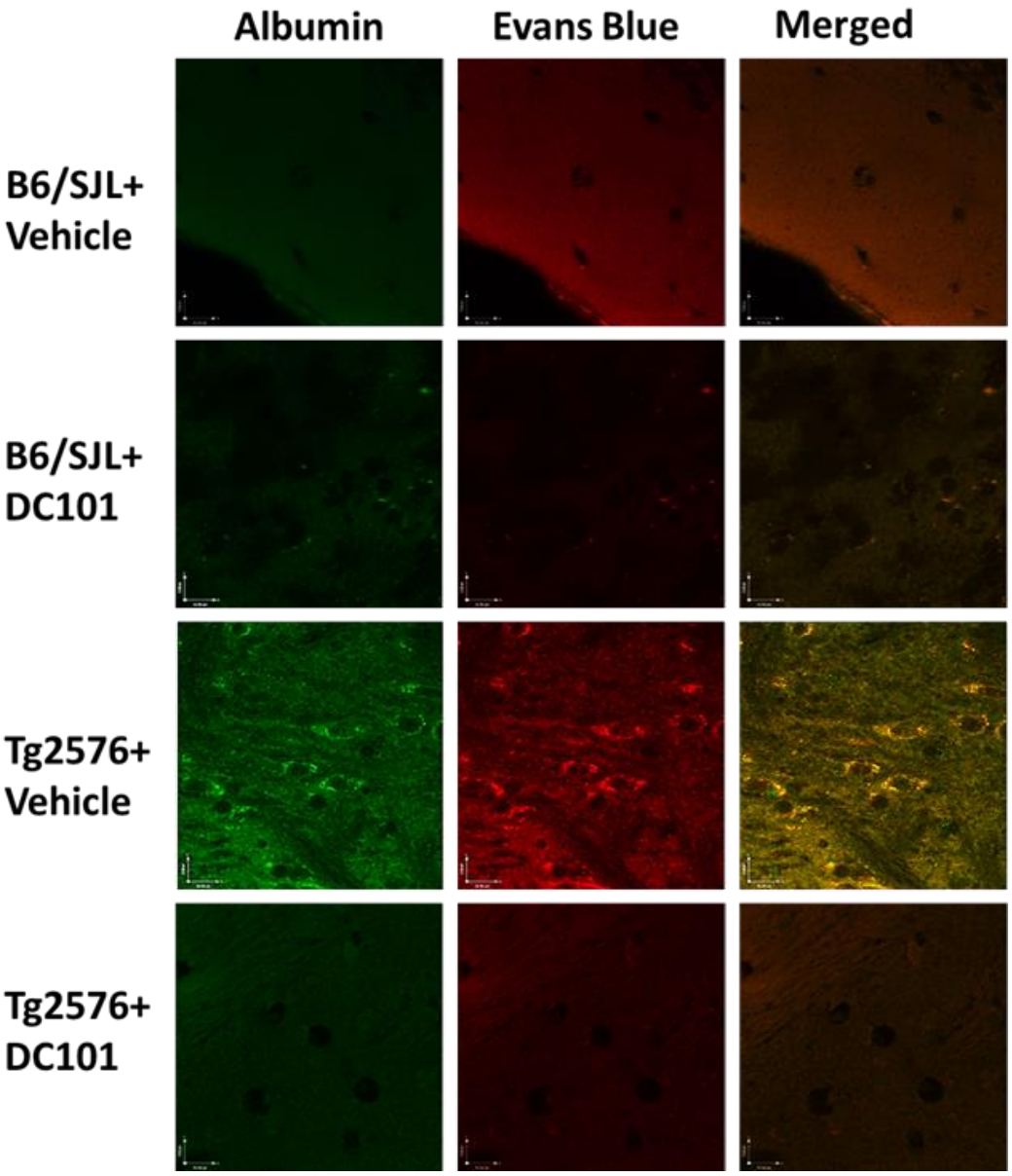

Figure 3.11: Functional BBB in aged Tg2576 mice after DC-101 treatment

Representative micrographs of coronal brain sections from mice (WT or Tg2576) treated with vehicle or DC-101, where green indicates immunostaining of albumin that has leaked into the brain and red indicates the Evans blue dye. Vehicle-treated and DC101-treated WT mice and DC101-treated Tg2576 mice show lower Evans blue dye and immune-stained albumin compared to vehicle-treated Tg2576 mice.

3.4 Discussion

AD mouse model Tg2576 mice pre-treatment at 10 months of age showed a significant cognitive decline compared to age-matched WT littermates, particularly in the case of spatial awareness, associative memory, working memory and reference memory. A similar result was observed when compared 11-months-old vehicle-treated Tg2576 mice to vehicle-treated WT mice after one month of treatment. Modulation of cognition was assessed in aged Tg2576 mice and their age-matched WT littermates after a one-month treatment with either small molecule TKI, Sunitinib or with a VEGFR2 antibody, DC101.

Sunitinib treatment showed no change in the spatial memory, the reference memory or the working memory aspects of cognition in WT mice however an increase in the associative memory was seen in Sunitinib-treated WT mice compared to pre-treatment and vehicle-treated WT mice.

The effect of the drug, after one-month treatment, on Tg2576 mice was intricate. Sunitinib-treated Tg2576 mice showed significantly higher scores of performances compared to the vehicle-treated Tg2576 mice in the various memory tests: open field, Y-maze, fear conditioning and radial arm water maze. However, in certain memory aspects, like associative memory assessed by fear conditioning test or spatial awareness assessed by Y-maze, the Tg2576 mice showed no significant difference compared to the pre-treatment Tg2576 mice. Similarly, DC-101 treatment showed no effect on WT animals when compared to the pre-treatment and vehicle-treated WT animals. In Tg2576 mice DC-101 treatment showed improvement in anxiety levels, locomotion and awareness of a novel environment compared to pre-treatment and vehicle-treated Tg2576 mice however no significant difference was observed between DC101-treated and pre-treatment Tg2576 mice with respect to associative and spatial memory aspects.

The conclusion drawn from these results is that one-month treatment with Sunitinib can improve memory aspects like reference memory, working memory and awareness of a novel environment to promote thigmotaxis and can also prevent the further decline of spatial and associative memory in aged Tg2576 mice. One-month treatment with DC-101 also improves the awareness in a novel environment while preventing further decline of spatial and associative memory in Tg2576 mice.

The molecular and immunohistochemical analysis of AD pathology after one-month of treatment with Sunitinib and DC-101 show that there was a lower expression of Aβ and CD-105 and a higher expression of ZO1 and occludin in vehicle-treated and Sunitinib/DC-101-treated WT mice, as well as Sunitinib/DC-101, treated Tg2576 mice compared to the vehicle-treated Tg2576 mice. It was also observed that the with the one-month Sunitinib and DC-101 treatments there was a higher functionality of the BBB as compared to the vehicle-treated Tg2576 mice. Thus, Sunitinib and DC-101 have the ability to modulate cerebral pathology, cognitive decline and other pathological indications seen in the Tg2576 mouse model of AD and show great potential as therapeutics of AD.

11-month old vehicle-treated Tg2576 mice showed a higher presence of amyloid in the brain compared to their age-matched WT littermates. This was expected as it has been documented in previous studies that in this mouse model Aβ accumulation is initiated between 6-9 months [221] and plaques are developed by the age of 9 months [172, 222]. Vascular pathology was seen higher in Tg2576 mice compared to WT littermates which include increased microvessel density, as indicated by the higher expression of the neo-angiogenic marker, CD105 and higher BBB

permeability as indicated by the higher presence of the Evans blue and immunostained albumin in the CNS. This result was expected as it was shown previously that vascular pathology and BBB disruption were initiated as early as 4 months of age in the Tg2576 mouse model and increase significantly as the mice age compared to age-matched WT littermates [96]. The data presented in this chapter and from other studies suggest that vascular changes are a crucial component of AD pathogenesis.

The data from this chapter demonstrate that vascular pathology is a crucial component of the pathogenesis of AD and its modulation with anti-angiogenic molecules can help to prevent or treat aspects of disease pathology. Since vascular changes were observed in aged Tg2576 animals as opposed to the WT littermates that displayed a normal vasculature, it can be implied that the production of Aβ has a role to play in the initiation of neo-angiogenesis leading to vascular pathology. Secondly, since vascular pathology precedes Aβ accumulation and plaque formation [96] it can be concluded that vascular pathology directly or indirectly facilitates in this Aβ accumulation and plaque formation. We need to study the vascular aspect of AD pathology in depth to further understand the molecular mechanism and the role that vascular pathology plays in establishing overall AD pathology.

Chapter 4 VEGFR2-specific small molecule tyrosine kinase inhibitor, Axitinib, prevents cognitive decline and development of AD pathology of Tg2576 mice.

4.1 Introduction

Alzheimer's disease (AD) is a progressive neurological dementia that affects thinking, orientation and memory, causing impairment in cognition, social behaviour and motivation in over 48 million people worldwide [1],[2]. One current model seeking to explain pathogenesis in AD is termed the 'amyloid cascade hypothesis', and it has influenced the study of AD pathogenesis for over two decades. The hypothesis is that the accumulation of amyloid beta (Aβ) in the brain, caused by impaired clearing, is the primary cause for cognitive decline [12, 85]. However, the hypothesis is not universally accepted due to various findings: evidence for aggregated Aβ being the most important factor in AD is not robust [88, 89], senile plaques cannot be the cause of neuronal sickness since they are the very product of sick neurons [88], and, senile plaques can be found in the brains of Down's syndrome patients and the elderly during autopsy without clinical evidence of neurodegenerative changes [88, 90]. A meta-analysis showed that this clinical model, based on Aβ aggregation with dementia, is unfounded for at least 30% of elderly with detectable Aβ pathology [91].

Moreover, therapeutics based on this hypothesis have been unsuccessful. For example, immunotherapies employing the use of monoclonal anti-Aβ antibodies thus far have failed: although these antibodies showed clearance of Aβ deposits in the brain, they did not provide

benefits for the cognitive and neurological outcomes of the patients [92]. From 2002-2012, 65% of clinical trials for Alzheimer's disease involved therapeutics with some form of Aβ protein as a pharmacological target. With a 99.6% failure rate, these trials were unable to validate Aβ as a target [93]. These trials also suggested that there was a translational gap between pre-clinical and clinical trials of AD [93].

Growing evidence supports the concept that, in addition to neurons, the neurovascular unit is affected in AD [94, 95] and that AD may be mediated by pathological angiogenesis [6],[96],[97],[98]. Vascular dysfunction now appears to be a crucial pathological hallmark of AD, and two key precursors to neurodegenerative changes and Aβ deposition in AD are BBB breakdown and CBF impairment [99-101]. These observations have led to an alternative hypothesis where angiogenesis caused by amyloidgenesis may lead to defective neuro-vasculature, thereby disrupting the BBB, impairing CBF, compromising the clearance of Aβ, which being vasculotropic, promotes more vascular pathology and hence the vicious cycle of abnormalities goes on [99, 102, 103].

CBF plays a pivotal role in influencing the permeability of the BBB, and severe reductions in CBF have been seen in elderly individuals at high risk for cognitive decline and AD. Impaired CBF and compromised BBB result in the accumulation of potentially neurotoxic blood products from peripheral circulation in the brain [115]. Furthermore, physical breakdown of the BBB during angiogenesis results in disrupted tight junctions (TJs) or adherens junctions, reduction of pericytes and capillary basement membrane degradation [94, 213].

Consistent with emerging literature relating to the pathology of the BBB in AD, we proposed a new testable paradigm for integrating vascular remodelling with the pathophysiology observed in AD in which counteracting the hypervascularity caused by neoangiogenesis might help restore the physiological state of the brain. One of the major factors modulating angiogenesis in the brain is the vascular endothelial growth factor receptor 2 (VEGFR2) [223],[224],[225]. Axitinib is a tyrosine kinase (TK) inhibitor of VEGFR 1 through 3. It is a second-generation TK inhibitor that has 50-450 times more inhibition potency than first generation inhibitors like Sunitinib (Sutent; Pfizer), which is a multi-targeted TK inhibitor. Axitinib (Inlyta; Pfizer), which is approved for use in renal cell cancer in the USA and Canada, Europe, the UK and Australia [226, 227], has been shown to block angiogenesis, tumour growth and metastasis. In this study, we explore the ability of Axitinib to alleviate the pathogenic cerebrovascular activation, disrupted BBB and impaired cognitive function that is associated with the Swedish-familial AD mouse model, Tg2576[172]. Finally, we demonstrate mechanistically how amyloidgenesis activates angiogenic mechanisms to cause the disruption of the BBB.

4.2 Results

4.2.1 Axitinib treatment maintains the cognitive status of the Tg2576 AD mice

To assess the caution and awareness shown by mice in a novel open arena, an open field test was performed on the transgenic Tg2576 AD model mice and their wildtype (WT) littermates which were treated with either Axitinib or vehicle alone (PBS+DMSO) thrice weekly for one month at disease onset. Both male and female mice at 10 months of age were used. No differences were seen between male and female mice in the behavioural testing or in their responses to the treatments, so the data from males and females were combined. Data from 3 different mouse trials

and were pooled for statistical analysis (WT vehicle-treated and WT Axitinib-treated, n =15 each; Tg2576 vehicle-treated and Tg2576 Axitinib-treated, n = 20 each)

Figure 4.1**a** shows the time spent in the centre of the field,

Figure 4.1**b** shows representative track plots of the mice from the different groups in the open field test. Inherent to their nature, it was observed that the pre-treatment and vehicle-treated-WT mice (B6/SJL) spent a majority of the time confined to the peripheral region of the field and rarely explored the centre of the open field. The results were similar in the Axitinib-treated WT mice. On the other hand, the pre-treatment and the vehicle-treated Tg2576 mice explored the entire field indiscriminately, with more distance travelled compared to all the other groups and significantly more time in the centre of the field compared to their respective WT littermates. Interestingly, after treatment with Axitinib, the Tg2576 mice explored the field to a lesser extent, preferred to move along the wall instead of into the open central area, and spent significantly less time in the centre as compared to the pre-treatment and vehicle treated Tg2576 mice, implying that the Axitinib-treated Tg2576 were more aware of their surroundings and cautious in an open field than vehicle-treated Tg2576 animals.

Spatial and working memory assessment was done using a spontaneous alternation test (Y-maze). Pre-treatment and vehicle-treated WT mice showed an alternation of 67±5.5% (mean± standard deviation) and 70±13.8% respectively, with no significant change seen when treated with the drug **(**

Figure 4.1**c)**. In contrast, pre-treatment and vehicle-treated Tg2576 mice showed poor performance on the test compared to their respective WT littermates, with a significantly lower percentage of alternation 52.8±4.7% and 41.2±8.3% respectively. Axitinib-treated Tg2576 mice showed significantly more alteration than pre-treatment and vehicle-treated Tg2576 mice, a performance that was indistinguishable from WT mice.

In contextual fear conditioning for the associative memory assessment, normal mice are expected to "freeze" (remain stationary) after being placed in an environment where they had previously received an electric shock. Pre-treatment, vehicle-treated and Axitinib-treated WT animals (B6/SJL) exhibited good associative memory scores by showing freezing percentages of 15.9±3.2%, 18.51±9.1% and 17.74±14.4% respectively **(**

Figure 4.1**d)**. The vehicle-treated Tg2576 mice showed much lower freezing scores (2.3±1.5%), while the scores of Axitinib-treated Tg2576 animals were similar to those of WT control animals (14.4±7.3%). There was a significant difference between the Axitinib-treated Tg2576 mice and the pre-treatment and the vehicle-treated Tg2576 mice.

Evaluation of reference memory (long-term) and working memory (short-term) was done by testing mice with the Radial Arm Water Maze (RAWM). **Figure 4.1e** shows the total latency time whereas **Figure 4.1f** shows the number of errors made by the mice when locating the submerged escape platform.

Comparison of the number of errors and the latency time were made between the first test day and the fifth test day within each group. Significant differences in the performance on the first test day versus the fifth test day were seen in the pre-treatment WT mice, vehicle-treated WT mice and the Axitinib-treated WT mice. No significant difference was seen in the pre-treatment Tg2576 mice and the vehicle-treated Tg2576 mice on the first day compared to the fifth day. Interestingly, Axitinib-treated Tg2576 mice showed a significant difference in the latency time and the number of errors when performance was compared between the first test day and the fifth test day.

The latency time and the number of errors made on the fifth test day were compared between the different groups. A significant decrease in the latency time and the number of errors between pre-treatment WT mice and pre-treatment Tg2576 mice, as well as between vehicle-treated WT and vehicle-treated Tg2576 mice was seen. A significant difference was also seen between the pre-treatment and Axitinib-treated Tg2576 mice, as well as between the vehicle-treated and Axitinib-treated Tg2576 mice.

No significant difference was observed in the latency time and the number of errors between the fifth day performance of the Axitinib-treated WT and the Axitinib-treated Tg2576 mice. It can thus be said that over the course of 5 days, pre-treatment, vehicle-treated and Axitinib-treated WT mice, as well as the Axitinib-treated Tg2576 mice, showed cognitive learning in terms of reference memory and working memory aspects.

a.

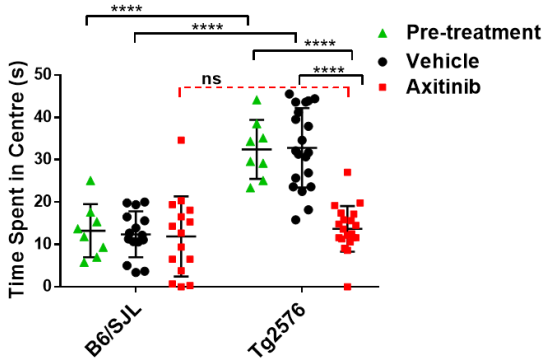
Time Spent in Centre (s)
Pre-treatment
Vehicle
Axitinib
****
****
****
****
ns
B6/SJL
Tg2576

b.

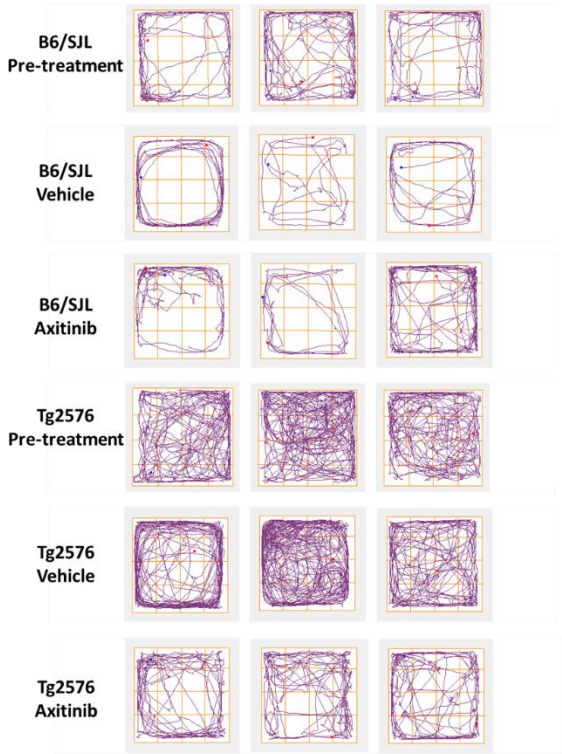
B6/SJL
Pre-treatment
B6/SJL
Vehicle
B6/SJL
Axitinib
Tg2576
Pre-treatment
Tg2576
Vehicle
Tg2576
Axitinib

c.

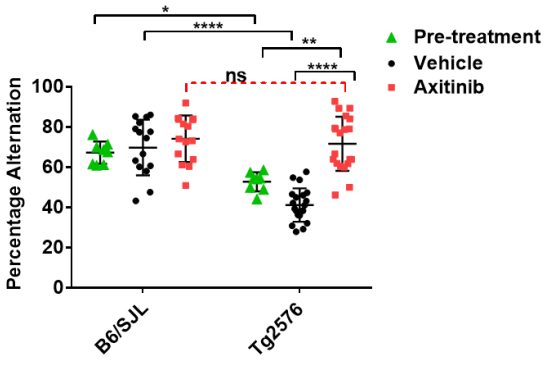
Percentage Alternation
Pre-treatment
Vehicle
Axitinib
*
****
**
****
ns
B6/SJL
Tg2576

d.

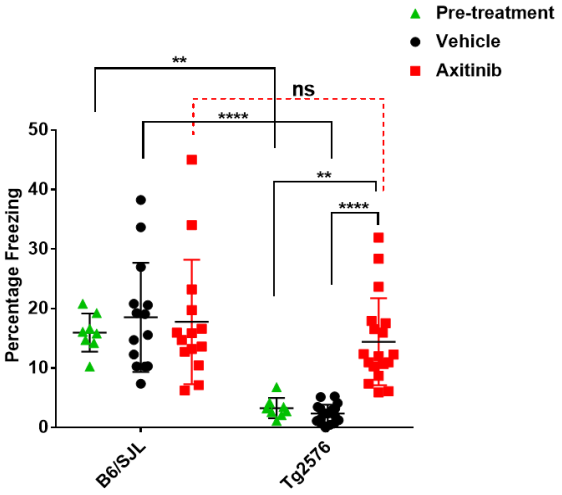
Percentage Freezing
Pre-treatment
Vehicle
Axitinib
**
ns
****
**
****
B6/SJL
Tg2576

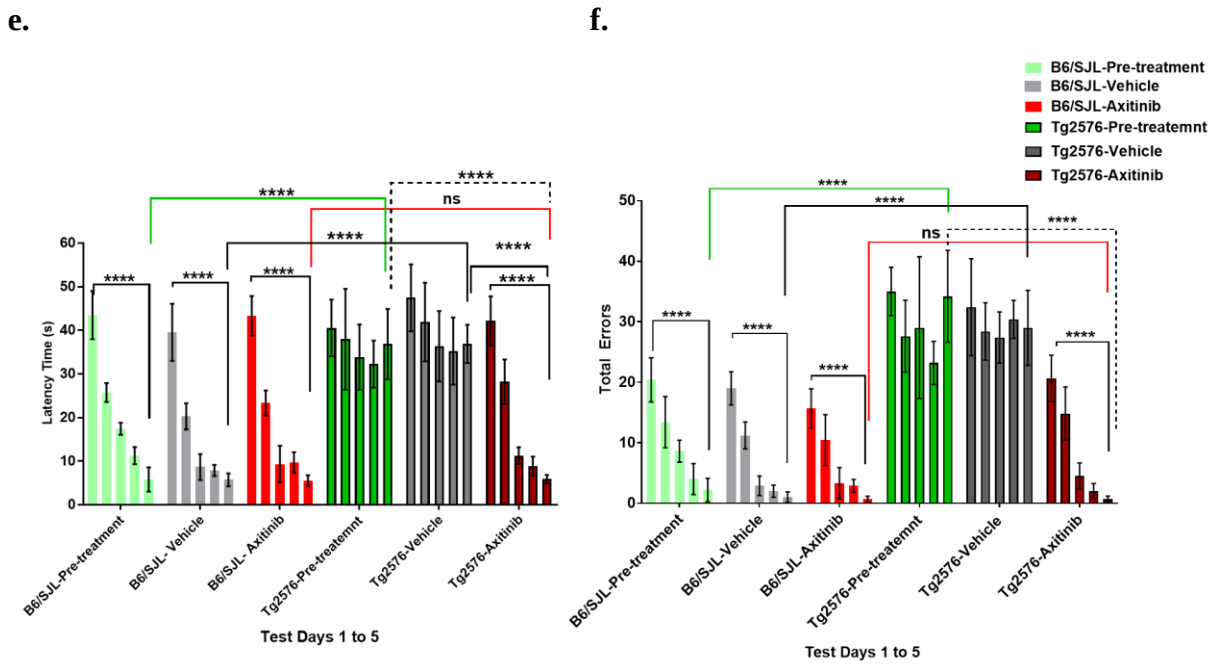

Figure 4.1: Treatment with the anti-angiogenic drug, Axitinib, reduces cognitive impairment in aged Tg2576 mice.
10-month-old Tg2576 and WT littermate mice were treated with the anti-angiogenic tyrosine kinase inhibitor, Axitinib, for 1 month at a dose of 10mg/kg, 3 days/week. Pre-treatment 10-month old mice and Post-treatment 11-month old mice were assessed for their cognitive status, using tests for the analysis of different memory aspects. The data were pooled from 3 different trials and is represented as the mean± standard deviation. Statistical analysis was carried out using a 2-way ANOVA with correction for multiple comparisons using the Bonferroni's test **(* p<0.03; ** p<0.002; *** p<0.0002; **** p<0.0001).**

a) Open Field Test. WT mice (B6/SJL) spent less time in the center of the field, with no significant difference seen pre-treatment as well as when treated with Axitinib. Vehicle-treated Tg2576 mice spent significantly more time exploring the center than Axitinib-treated Tg2576 mice or WT mice. A significant difference was seen between the pre-treatment WT and Tg2576. A significant difference was also seen between pre-treatment Tg2576 and Axitinib-treated Tg2576 mice. There was no significant difference noted between the WT mice and Axitinib-treated Tg2576 mice.

b) Representative track plots from the open field test. Cognitively aware WT and Axitinib-treated Tg2576 mice spend less time exploring the open center of the test arena and more time exploring the edges than cognitively-impaired pre-treatment and vehicle-treated Tg2576 mice.

c) Spontaneous alternation (Y-maze) Test. Cognitively aware mice show a high percentage of alternation, as was seen in the pre-treatment WT mice, with no significant difference observed with the vehicle and Axitinib treatment. Pre-treatment and vehicle-treated Tg2576 mice exhibited poor performance on the test, with a significantly lower percentage of alternation compared to the

pre-treatment and vehicle-treated WT mice respectively. Axitinib-treated Tg2576 mice showed a significantly higher rate of alternation compared to the pre-treatment and vehicle-treated Tg2576 mice. No significant difference was observed between the WT mice and the Axitinib-treated Tg2576 mice.

d) Contextual Fear conditioning Test. Pre-treatment, vehicle-treated and Axitinib-treated WT mice exhibited good associative memory by showing high freezing percentages. The pre-treatment and vehicle-treated Tg2576 mice displayed a significantly lower freezing percentage compared to the pre-treatment and vehicle-treated WT mice respectively. Axitinib-treated Tg2576 animals performed similarly to the WT mice. Axitinib-treated Tg2576 mice showed significantly higher performance compared to pre-treatment and vehicle-Tg2576 mice.

e, f) Radial arm water maze. Radial arm water maze. (e) the time it takes for the mice to locate the escape platforms i.e. *Latency time*, and **(f)** the *number of errors* (working and reference memory errors) made by the mice when locating the escape platforms. Pre-treatment, vehicle- and Axitinib-treated WT mice showed a significant decrease in the latency time and a number of errors made when comparing test day 1 and test day 5. A similar improvement over the course of the trial was seen in the Axitinib-treated Tg2576 mice. No significant difference between test day 1 and test day 5 were seen in the pre-treatment and the vehicle-treated Tg2576 mice.

A significant difference was seen in the latency time and number of errors made on test day 5 between the pre-treatment WT and Tg2576 mice as well as the vehicle-treated WT and vehicle-treated Tg2576 mice. A significant difference was also observed between the pre-treatment and Axitinib-treated Tg2576 mice as well as between the vehicle-treated and Sunitinib-treated Tg2576 mice. No significant difference was observed when comparing latency time and number of errors made by the pre-treatment and vehicle-treated Tg2576 mice as well as the Sunitinib-treated WT and Tg2576 mice on test day 5.

4.2.2 Axitinib treatment reduces cerebral vascular pathology, cerebral Aβ load and tight junction disruption in Tg2576 mice

To assess the effect of the drug on AD pathology, the brains of treated mice were analysed by semi-quantitative western blotting to look for expression of the neoangiogenic marker CD105, as well as Aβ, amyloid precursor protein (APP) and the tight junction protein, ZO1. CD105 and APP proteins levels were analyzed using the cytosolic fraction where as the membrane bound SDS fraction was used for ZO1 and formic acid fraction was used for Aβ.

One-month treatment of the Tg2576 mice with Axitinib resulted in a significant decrease in the expression of CD105 compared to the vehicle-treated Tg2576 mice **(Figure 4.2a)**. Interestingly, in Axitinib-treated Tg2576 animals, there was also a significant decrease in Aβ expression by more than one-half in comparison to the vehicle-treated Tg2576 mice **(Figure 4.2c)**. In contrast, the expression of ZO-1 was greater in Axitinib-treated Tg2576 mice compared to the vehicle-treated Tg2576 mice **(Figure 4.2b)**.

Immunofluorescence analysis of these proteins in both the cortex and hippocampus of the mouse brains confirmed the western blotting data. **Figure 4.3** shows representative micrographs of the cortex and hippocampus. As shown in the micrographs and histograms, amyloid staining is much heavier in the brains of vehicle-treated Tg2576 mice than in the brains of Axitinib-treated Tg2576 animals. Staining of the mature vessel marker, CD31, is similar in all the different groups; however, CD105, the sprouting vessel marker, is greater in the vehicle-treated Tg2576 group as compared to the Axitinib-treated Tg2576 or WT mice, which indicates a state of hypervascularity

in the vehicle-treated Tg2576 animals. Low expression of Occludin was seen in the vehicle-treated Tg2576 as compared to the Axitinib-treated Tg2576 mice and WT (B6/SJL) animals **(Figure 4.4)**.

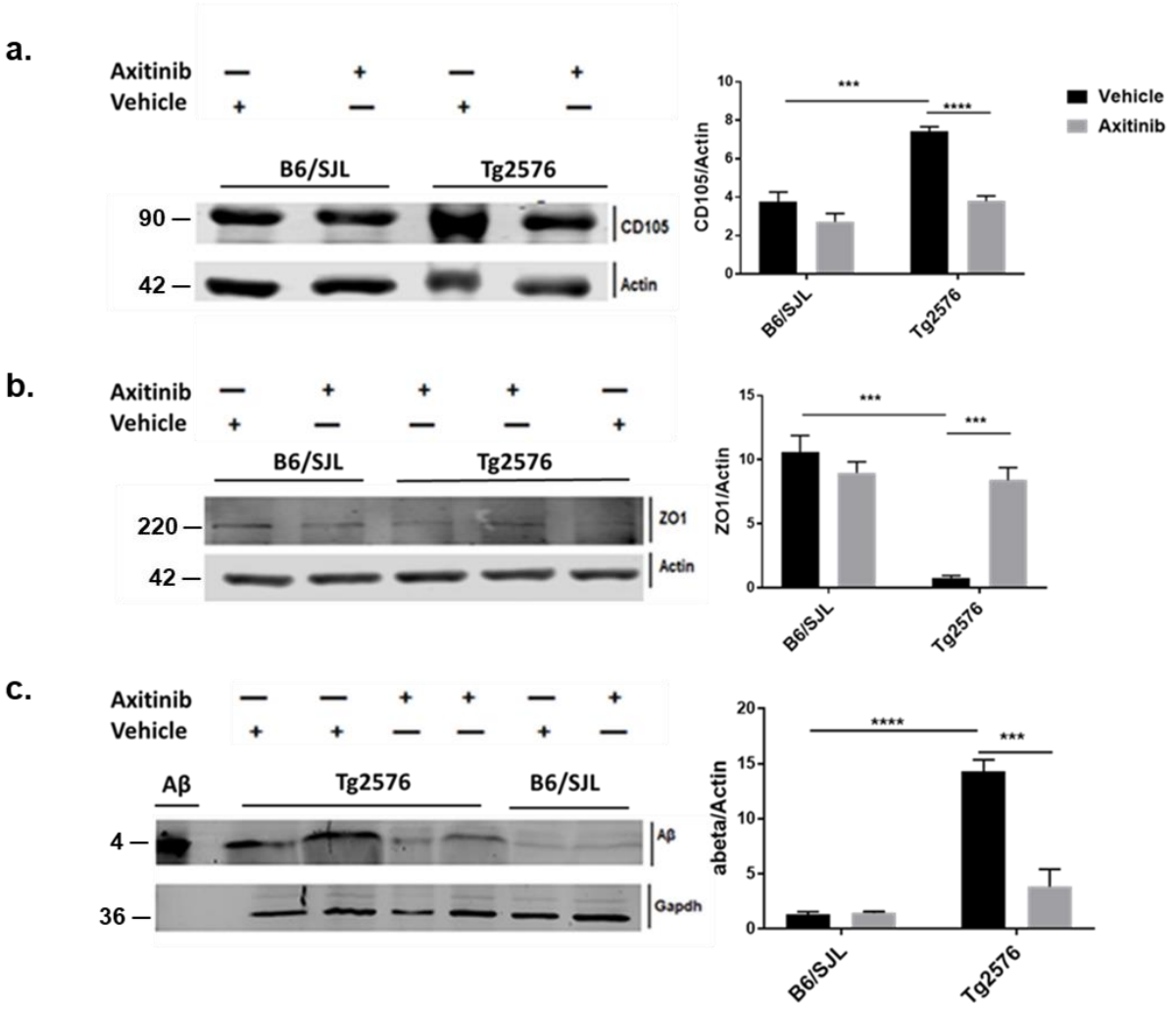

Figure 4.2: Treatment of Tg2576 mice with the anti-angiogenic drug, Axitinib, reduces expression of Aβ, angiogenic marker, CD105 and tight junction proteins, ZO1 and occludin in aged Tg2576 mice.

Brains from perfused mice were used for molecular analysis. Homogenates were used for western blotting analysis. The data are representative of means of individual animals with error bars representing the standard deviation from three separate experiments with WT n= 6 and Tg2576 n= 6 per treatment group. **(* p<0.03; ** p<0.002; *** p<0.0002; **** p<0.0001).**
Semiquantitative western blot analysis (a-c): a) Expression of the angiogenesis marker, CD105, was significantly higher in brains of vehicle-treated Tg2576 mice than in the brains of Axitinib-treated Tg2576 or WT animals. **b)** The expression of tight junction protein, ZO1, was significantly lower in vehicle-treated Tg2576 mice compared to the WT mice or Axitinib-treated Tg2576 mice. **c)** The presence of amyloid in the Tg2576 mouse brain was much higher in vehicle-treated than in Axitinib-treated animals, in which levels resembled those seen in WT brains. Representative blots are shown for mice from the different groups.

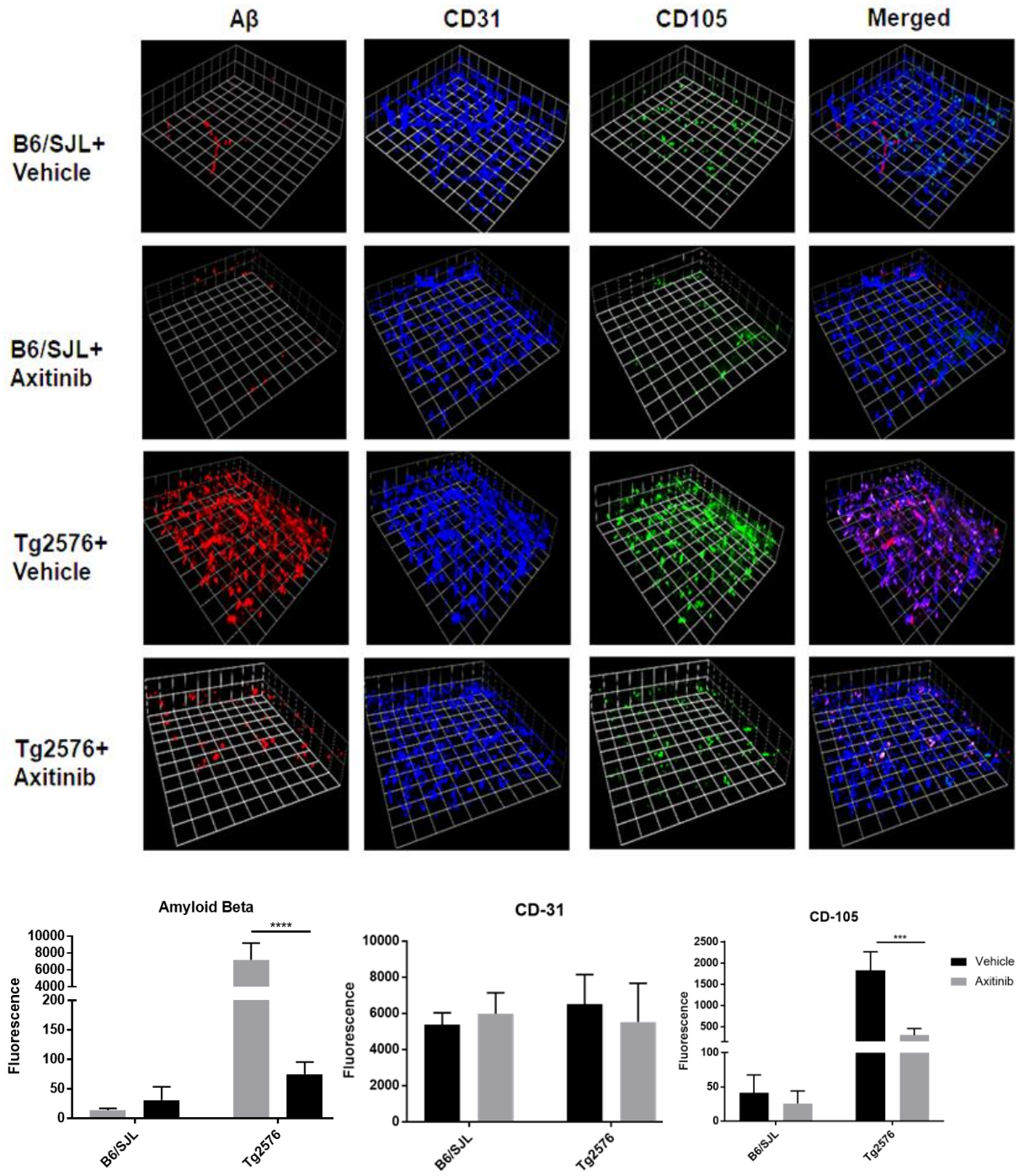

Figure 4.3: Immunofluorescence analysis shows Axitinib treatment reduces amyloid load, angiogenic cerebral vascularity in aged Tg2576 mice

The micrographs here show the voxels of the field of view of the imaged sections represented by the grid. The data were pooled from 3 different trials and represented as the mean± standard

deviation. Statistical analysis was carried out using unpaired Student's t test with WT n= 6 and Tg2576 n= 6 per treatment group. **(* p<0.03; ** p<0.002; *** p<0.0002; **** p<0.0001).**

Brain sections of mice from different groups were stained for the combination of markers CD105, Aβ and CD31. The micrograph panels are representative of the cortical and hippocampal regions of the brains from the mice belonging to the different treatment groups. Heavy amyloid Aβ staining and more Aβ plaques were seen in the vehicle-treated Tg2576 mouse brain compared to the brain of Axitinib-treated Tg2576 or WT mice. There was no difference in the overall expression of the mature vessel marker (CD31) between the groups, but the expression of the sprouting vessel marker (CD105) was much greater in vehicle-treated Tg2576 mice compared to Axitinib-treated Tg2576 or WT mice.

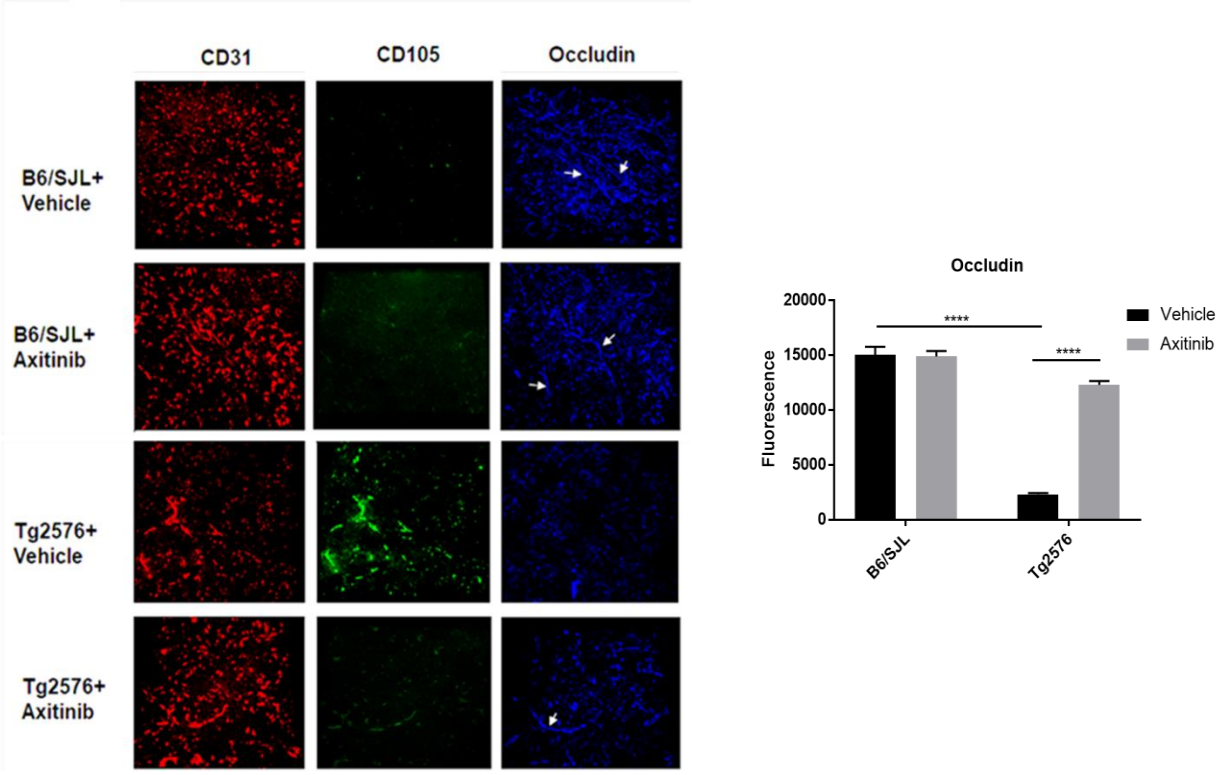

Figure 4.4: Immunofluorescence analysis shows Axitinib treatment reduces expression of Aβ, cerebral angiogenic vascular marker, CD105 in aged Tg2576 mice.

The data were pooled from 3 different trials and is represented as the mean± standard deviation with WT n= 6 and Tg2576 n= 6 per treatment group. Statistical analysis was carried out using unpaired Student's t test **(* p<0.03; ** p<0.002; *** p<0.0002; **** p<0.0001)**.
Brain sections of mice from different groups were stained for the combination of markers CD105, CD31 and the tight junction protein, occludin. The micrograph panels are representative of the cortical and hippocampal regions of the brains from the mice belonging to the different treatment groups. **White arrows indicate a normal occludin expression.** Significantly lower occludin expression was noted in the vehicle-treated Tg2576, as compared to WT (B6/SJL) or Axitinib-treated Tg2576 mice.

4.2.3 Axitinib treatment reduces the loss of tight junction structure and BBB integrity in aged Tg2576 mice

The physical seal of the BBB is maintained mainly by an intact and continuous arrangement of the tight junction proteins (TJP), ZO1, claudin and occludin, along with other components of the neurovascular unit. Their alteration can lead to disruption of the tight junctions between the endothelial cells and hence lead to increased permeability of the barrier, resulting in unhindered movement of toxic blood products into the brain, advancing AD pathology.

TJP disruption was analysed in the brains of Tg2576 mice and their WT littermates. A normal occludin expression pattern, as indicated by white arrows in Figure 4.5, is strong and continuous. It was observed that the WT mice showed a normal expression pattern of TJPs (as indicated with the white arrows in the micrographs) and thus a low percentage of disruption irrespective of Axitinib or vehicle treatment. In the vehicle-treated Tg2576 mice, however, there was a significant increase in the disruption of the TJPs. Tg2576 mice treated with Axitinib showed a lower percentage of the tight junction disruption, similar to the WT.

To prove that this intact arrangement of the TJP influenced the permeability of the BBB in the animals, we conducted an Evans Blue assay. Evans Blue dye binds to serum albumin, a protein to which the BBB is impermeable. A disrupted BBB allows albumin to enter the central nervous system (CNS), as indicated by the presence of the dye in the brain.

Figure 4.6 shows that when Evans Blue dye is injected in mice that have an intact BBB, the dye is unable to cross into and stain the brain. In Figure 4.6**b** the WT brain looks normal, while the vehicle-treated Tg2576 brain is stained blue. These brains (cortex alone) were assessed for the

extent to which the dye had crossed into the CNS. **Figure 4.6a.** illustrates Evans blue staining measured as absorbance in terms of optical density/unit mass of brain. Increased absorbance was noted in vehicle-treated Tg2576 mice, indicating substantial Evans Blue uptake in the brain, compared to WT littermates and Axitinib-treated Tg2576 mice.

In a separate experiment, brain sections of Tg2576 mice and WT littermates that were treated with Axitinib or vehicle were immunostained to look for the presence of albumin in the CNS. Representative micrographs of the cortical and hippocampal regions of the brain in **Figure 4.4c** show the presence of albumin in the CNS. Minimal amounts of albumin were seen in the WT brains, indicating an intact BBB, whereas substantial staining of albumin was seen in the vehicle-treated Tg2576 mice, implying a disrupted and highly permeable BBB. The brains of the Axitinib-treated Tg2576 mice showed less albumin in the brain, demonstrating a more functional BBB.

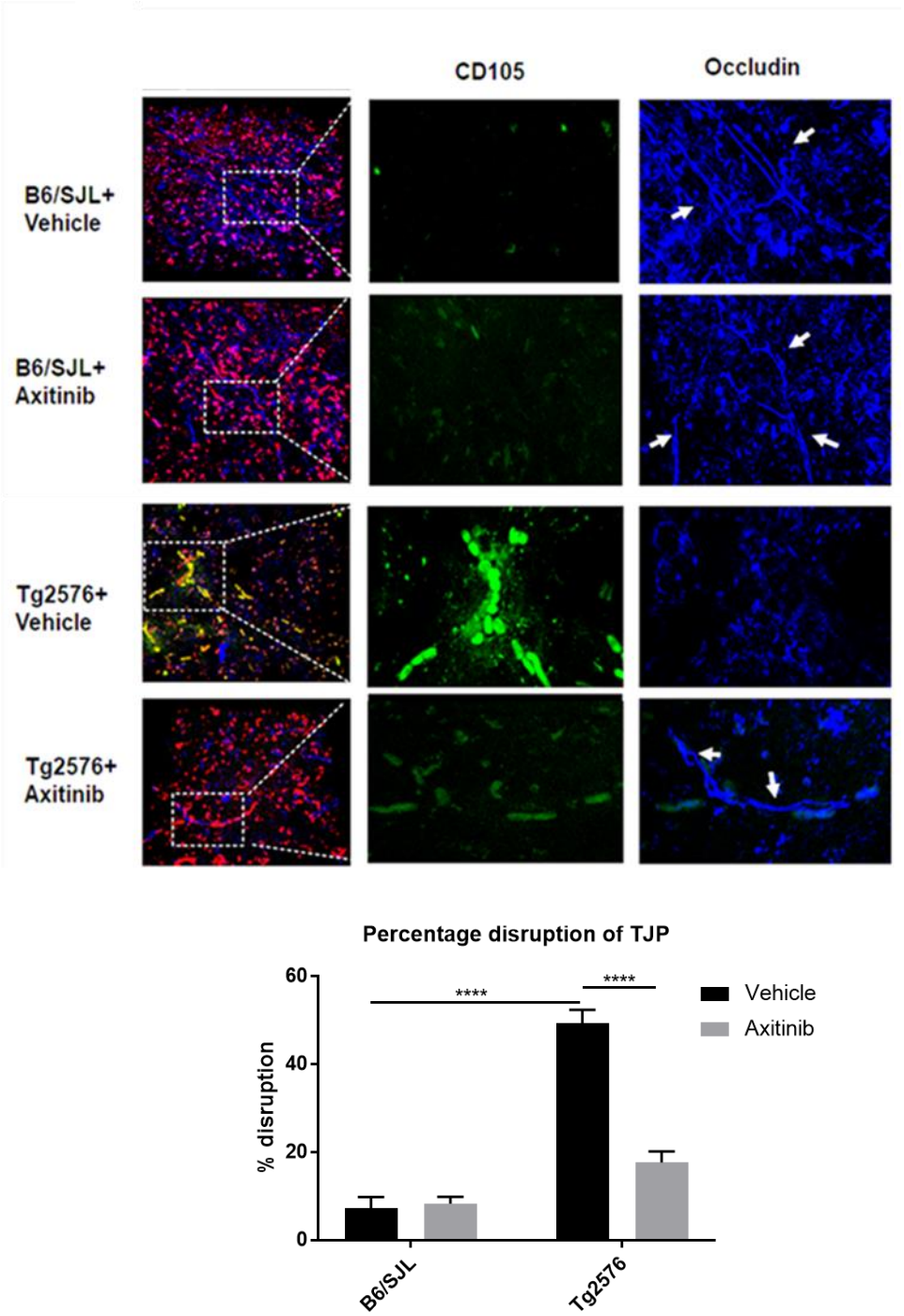

Figure 4.5: Axitinib reduces the loss of tight junction structure and BBB integrity in aged Tg2576 mice

Brains from perfused mice were used for immunofluorescence analysis of the BBB. Brain sections of mice from different groups were stained for the combination of markers CD105, CD31 and the tight junction protein, occludin. The CD31 was used as an indicator for intact vessels so that a discontinuity in occludin staining is not attributed to a discontinuous vessel and we avoid false positive for a broken tight junction. Only vessels of a continuous length were looked at for normal occludin expression pattern.

The micrograph panels shown are representative of the cortical and hippocampal regions of the brains from the mice belonging to the different treatment groups with WT n= 5 and Tg2576 n= 6. The data are representative of three separate experiments **(* p<0.03; ** p<0.002; *** p<0.0002; **** p<0.0001).**

The first panel shows the merged micrograph with CD31 (red), CD105 (green) and Occludin (blue) staining and the other two panels are CD105 and Occludin where the field of view was magnified, as indicated by the superimposed grid, to have a more detailed view of the structure of a normal Occludin expression pattern observed in the WT mice (indicated by white arrows) and an abnormal Occludin expression as seen in the vehicle-treated Tg2576 mice. Much lower occludin expression was noted in the vehicle-treated Tg2576 brain, as compared to WT (B6/SJL) and Axitinib-treated Tg2576 mice. The percentage of tight junction protein (TJP) disruption was significantly higher in vehicle-treated Tg2576 mice compared to Axitinib-treated Tg2576 mice or WT mice.

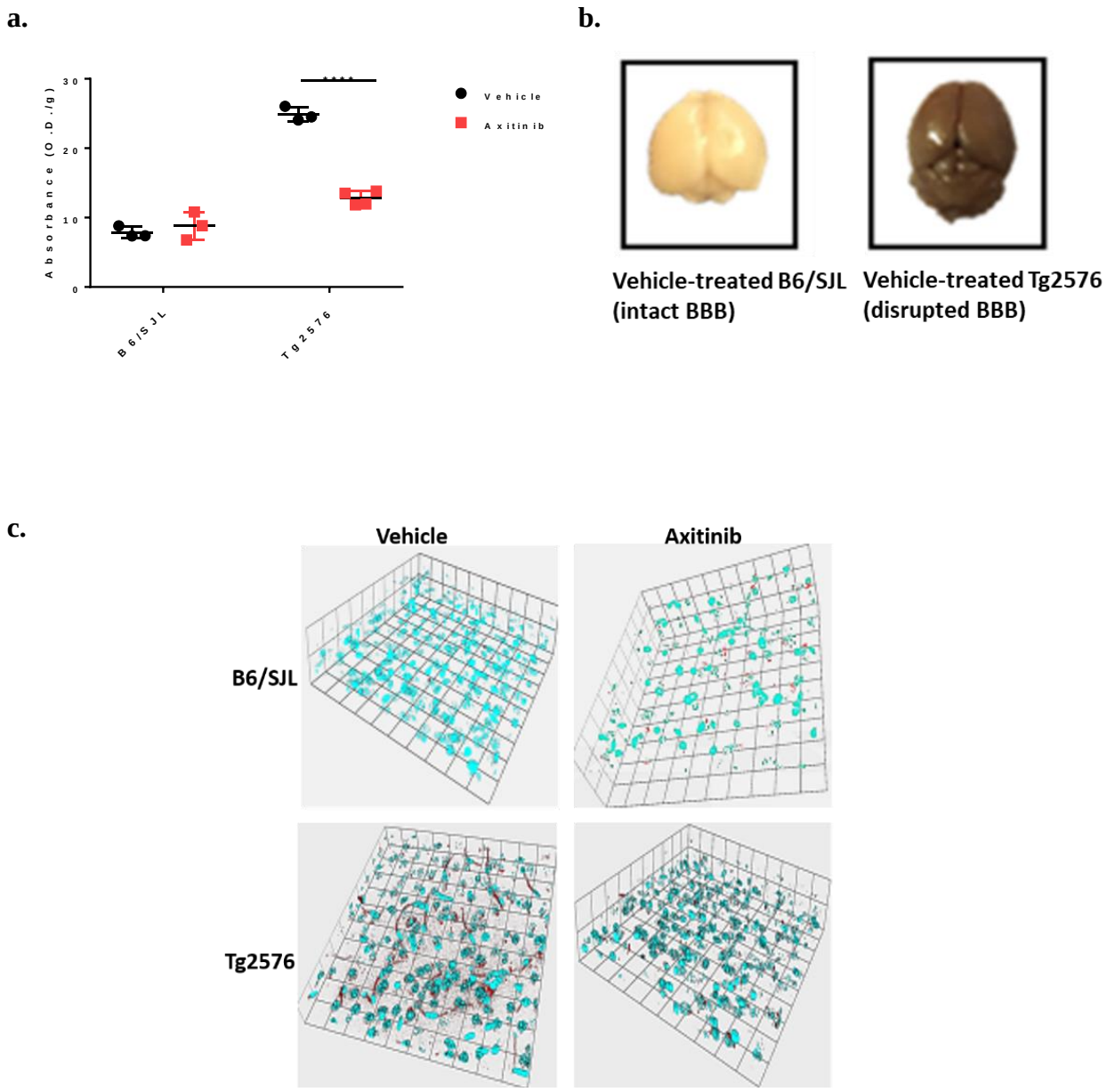

Figure 4.6: Functional BBB in aged Tg2576 mice after Axitinib treatment

Evans Blue dye was i.p. injected into mice from the treatment trial. Brains were harvested and homogenized with 50% trichloroacetic acid followed by dilution with ethanol.

a) The absorbance of the dye was read with an ELISA plate reader (Spectra Max 190; Molecular Devices, Sunnyvale, CA) at 620 nm. The readings were divided by the weight of the brain. This experiment was repeated twice. **(* *p*<0.03; ** *p*<0.002; *** *p*<0.0002; **** *p*<0.0001).**
An increase in the uptake of Evans Blue in the CNS of the vehicle-treated Tg2576 mice was indicated by the high absorbance of the dye present in the homogenates. This implied that an increased BBB permeability or leakiness in vehicle-treated Tg2576 animals compared to the WT (B6/SJL) mice. No difference was seen between the vehicle- and drug-treated B6/SJL mice. Axitinib treatment of the Tg2576 mice produced less Evans Blue staining than seen in the vehicle-treated animals, thereby indicating a functioning BBB.

b) The harvested brains from WT mice showed no colouration; however, vehicle-treated Tg2576 mice showed an overall bluish colouration of the brain.

c) The micrographs here show the voxels of the field of view of the imaged sections represented by the grid. The micrographs are representative of brain sections from mice from a separate experiment, where both Tg2576 and WT were treated with Axitinib or vehicle, were stained for albumin in the CNS. Representative immune-stained micrographs of 50µm thick coronal brain sections from mice. Red indicates immuno-stained albumin that has leaked into the brain, and cyan indicates cell nucleus (DAPI). Axitinib treatment is associated with less albumin leakage into the brain, indicative of a more functional BBB, in contrast to the greater albumin staining in the vehicle-treated Tg2576 mouse.

4.2.4 Pathological neo-angiogenic vessels co-localize with pathogenic Aβ and disrupted tight junction proteins

The co-localization of CD105 with Aβ and occludin is shown in **Figure 4.10**. Thresholded Pearson's Correlation Coefficients were calculated to assess the correlation between Aβ and CD105 expression and between CD105 and occludin expression in brain sections from vehicle-treated 11-month old Tg2576 and vehicle-treated age-matched WT littermates, where "+1" would indicate a positive correlation between the two events with an increase in one variable associated with a corresponding increase in the other, "0" would indicate no correlation, and "-1" would indicate a negative correlation with an increase in one variable associated with a corresponding decrease in the other.

A correlation coefficient of r = +0.62 (*p= 0.021*) in vehicle-treated Tg2576 mice, which have an overproduction of Aβ, indicated a positive correlation between Aβ and CD105, suggesting a relationship between the presence of excessive amounts of amyloid and an increase in the sprouting pathogenic vessels in the cerebral vasculature. On the other hand, a correlation coefficient of r = -0.73 (*p=0.006*) in the vehicle-treated Tg2576 mice indicates that CD105 and occludin expression are negatively correlated. WT brains show a low expression of Aβ and CD105 and have normal levels of tight junction proteins.

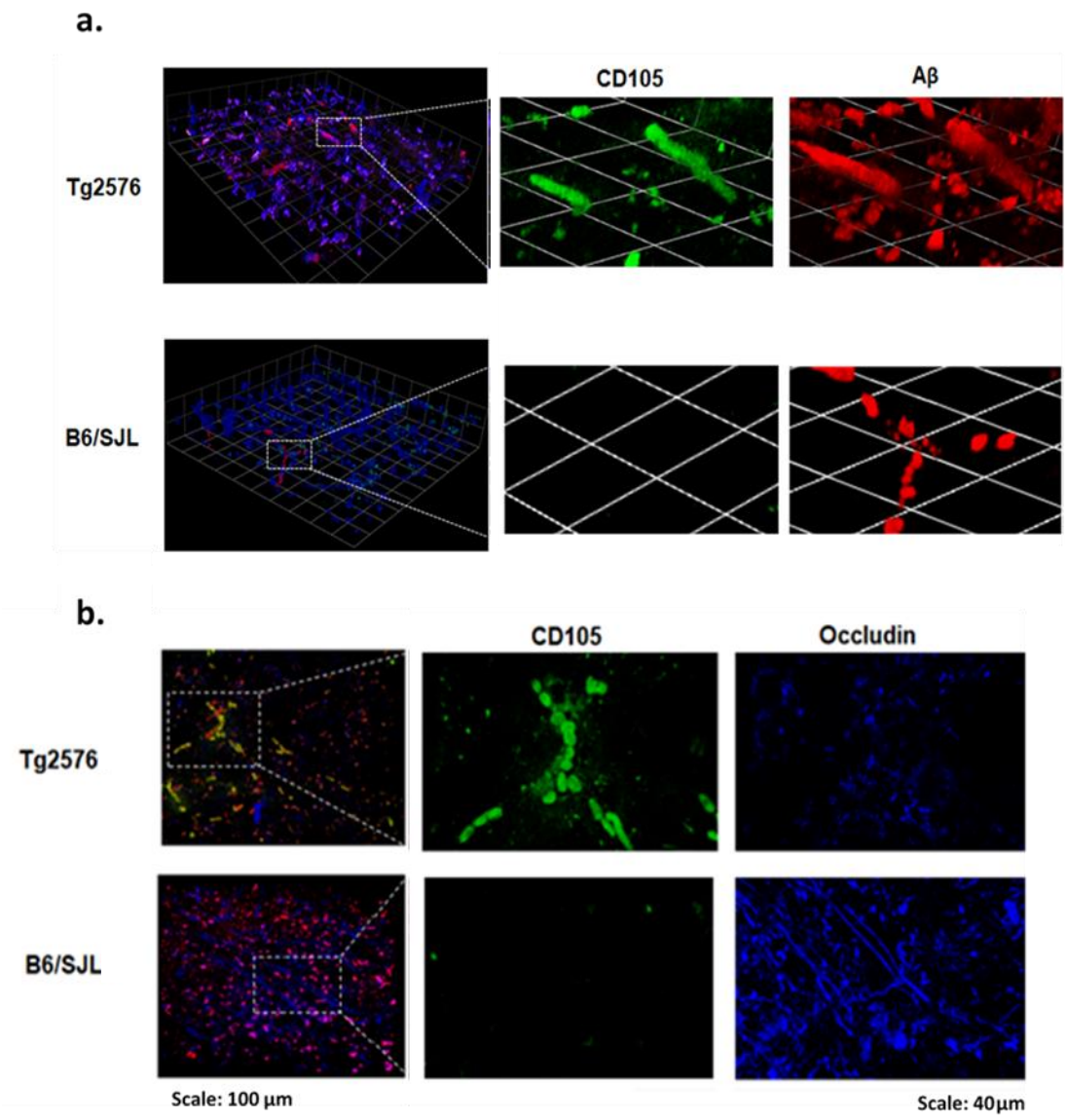

Figure 4.7: Angiogenesis is positively correlated with amyloid beta and negatively correlated with tight junction proteins

Micrographs representing hippocampal and cortical co-localization of **a)** CD105 (green) and Aβ (red), **b)** CD105 (green) and occludin (blue). The first column represents the micrographs showing the brain stained with a combination of antibody staining. The white overlay indicates the area in the field of view that was magnified and shown in the next two columns labeled either CD105 and Aβ or CD105 and Occludin.

Comparing the brain sections from 11-month-old vehicle-treated Tg2576 mice and vehicle-treated WT littermates using total fluorescence volume, the Thresholded Pearson's Correlation

Coefficient was calculated to assess the correlation between Aβ and neo-angiogenic marker, CD105 and between neo-angiogenic marker, CD105 and tight junction protein, Occludin. This indicated that in Tg2576 mice, a positive correlation coefficient of $r = +0.62$ was seen between Aβ and CD105 and a negative correlation coefficient of $r = -0.73$ was seen between CD105 and occludin.

4.2.5 Tg2576 mice show higher expression of pro-angiogenic proteins and downstream signalling effector proteins

To investigate protein expression of downstream signalling molecules and transcription factors implicated in amyloid overproducing Tg2576 mice, we conducted a phospho-kinase and angiogenesis proteome array analysis. The downstream signalling pathways MAPK, AKT, JAK/STAT and Wnt involved in cell proliferation, endothelial migration and cell survival were highly activated in 11 month-old untreated Tg2576 mice, as were transcription factors responsible for promoting vessel formation like STAT3, Hifα, c-fos, CREB and p53 **(Figure 4.8a)**. It was observed that in comparison to untreated WT littermates, the untreated Tg2576 mice showed upregulation of CD105, vascular endothelial growth factor (VEGF), fibroblast growth factor (FGF), Osteopontin, proliferin, platelet factor 4, angiogenin and IL-10, among other proangiogenic factors **(Figure 4.8b)**. The anti-angiogenic factor endostatin was also increased in untreated Tg2576 mice, possibly in compensation for the overall increased angiogenesis. The Tie-2 receptor ligand, Ang-1, was reduced in Tg2576 mice.

Western blot analysis was done on 11-month-old Tg2576 mice and WT littermates that were treated with either vehicle or Axitinib to look at various angiogenic effectors. It was noted **(Figure 4.8c)** that in the brains of vehicle-treated Tg2576 animals overexpressing Aβ, there were increases in APP, pERK-1, NOTCH-1 and p-FAK and that the expression of these effectors was lower in the Axitinib-treated Tg2576 mice.

Co-immunoprecipitation of Aβ with Tie-2 and VEGFR2 (**Figure 4.8d**) established their direct interaction with Aβ. Lastly, western blot analysis was done to look at the expression levels of the two ligands for the angiogenesis initiator receptor Tie2. It was shown that **(Figure 4.8e)** there was a lower expression of Ang-1 and a higher expression of Ang-2 in the 11-month-old vehicle-treated Tg2576 brain homogenates as compared to the vehicle-treated WT (B6/SJL) littermates.

a.

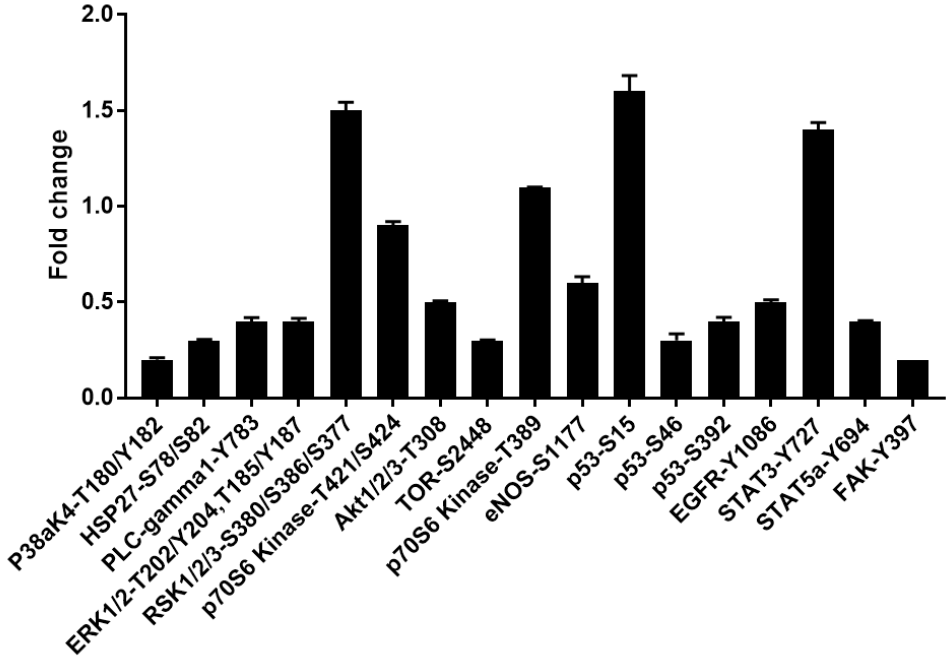
Fold change
2.0
1.5
1.0
0.5
0.0
P38aK4-T180/Y182
HSP27-S78/S82
PLC-gamma1-Y783
ERK1/2-T202/Y204,T185/Y187
RSK1/2/3-S380/S386/S377
p70S6 Kinase-T421/S424
Akt1/2/3-T308
TOR-S2448
p70S6 Kinase-T389
eNOS-S1177
p53-S15
p53-S46
p53-S392
EGFR-Y1086
STAT3-Y727
STAT5a-Y694
FAK-Y397

b.

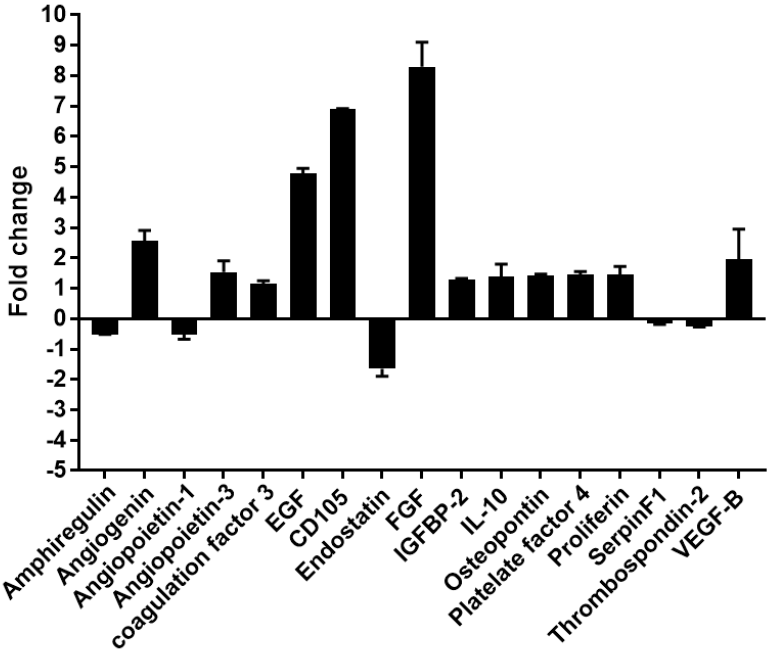
Fold change
10
9
8
7
6
5
4
3
2
1
0
-1
-2
-3
-4
-5
Amphiregulin
Angiogenin
Angiopoietin-1
Angiopoietin-3
coagulation factor 3
EGF
CD105
Endostatin
FGF
IGFBP-2
IL-10
Osteopontin
Platelate factor 4
Proliferin
SerpinF1
Thrombospondin-2
VEGF-B

c.

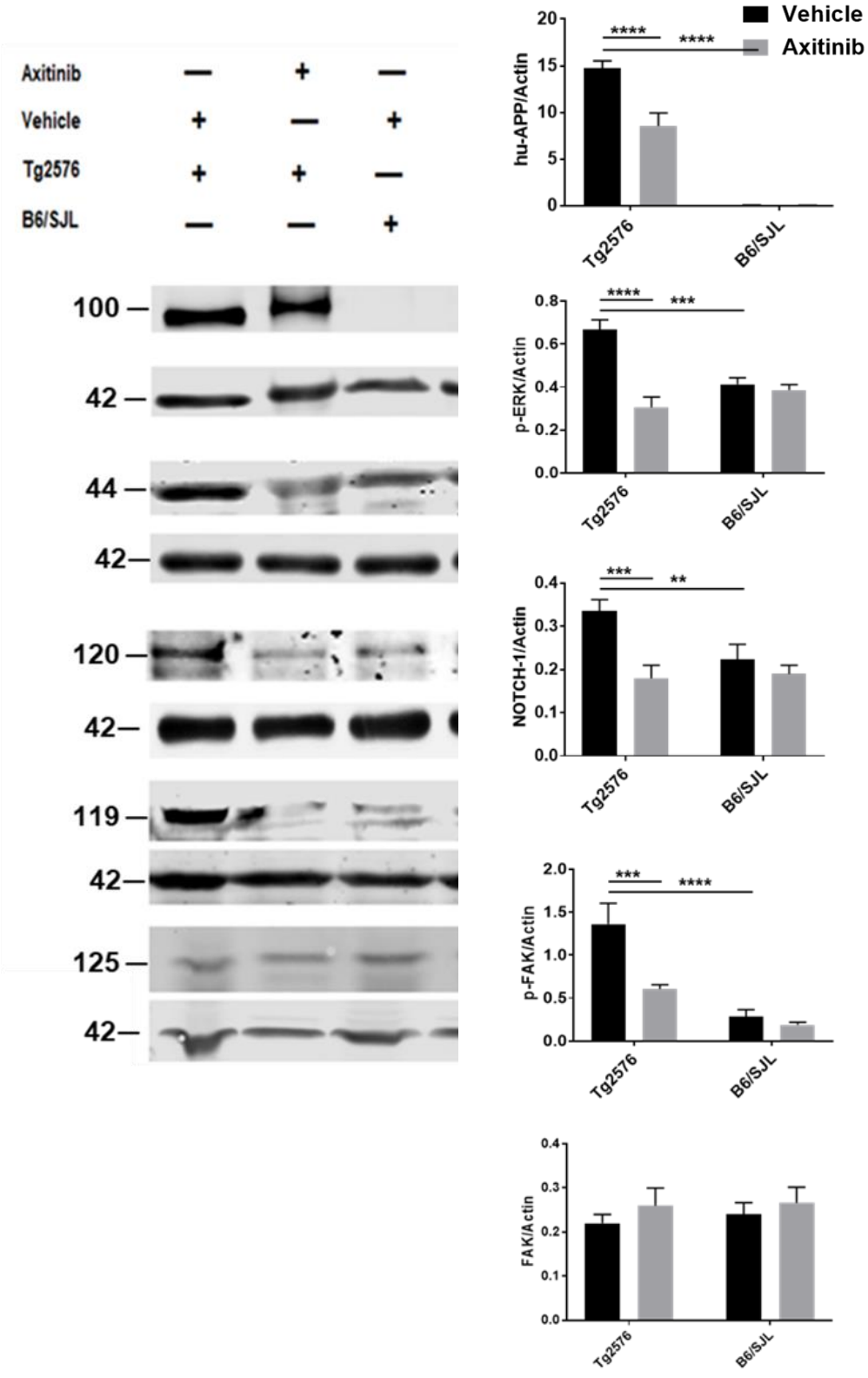
Axitinib
Vehicle
Tg2576
B6/SJL
100
42
44
42
120
42
119
42
125
42
Vehicle
Axitinib
hu-APP/Actin
p-ERK/Actin
NOTCH-1/Actin
p-FAK/Actin
FAK/Actin
Tg2576
B6/SJL

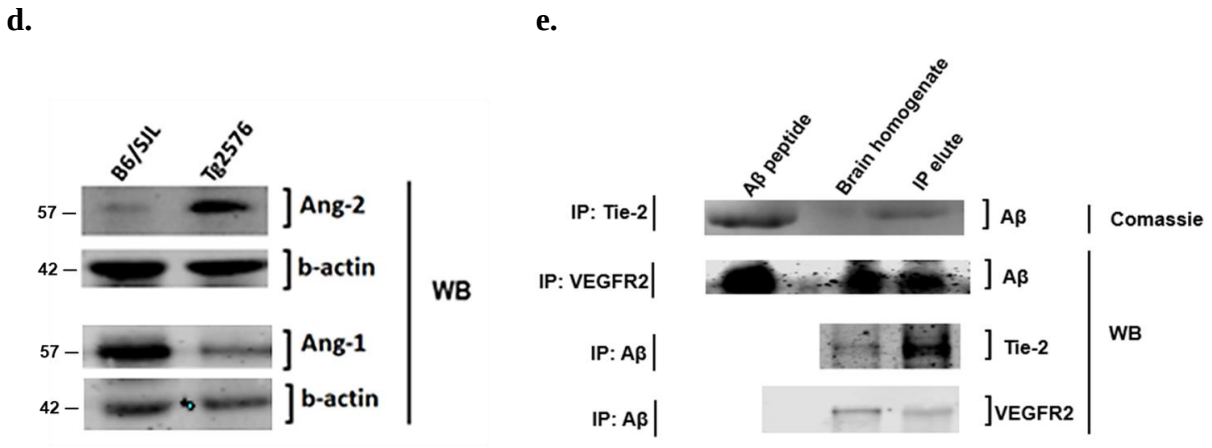

Figure 4.8: Amyloid overproduction in AD model mice is associated with increased angiogenic effector proteins and activation of downstream signaling pathways involved in cerebrovascular pathology and BBB disruption.

a, b) Level of phosphorylation of various kinases and expression levels of proteins involved in angiogenesis in 11-month-old untreated Tg2576 mice versus the untreated age-matched WT littermates, depicted as fold change. The data represent the mean fold change±S.E.M in the Tg2576 compared to the WT from three separate experiments.

Tg2576 mice showed upregulation of pro-angiogenic factors such as CD105, EGF, Osteopontin, proliferin, platelet factor 4, IL-10 and angiogenin. Anti-angiogenic effectors like endostatin, thrombospondin-2 and serpin-F1 were reduced, VEGF was upregulated, and Ang-1 was reduced in Tg2576 mice. The downstream signalling pathways for cell proliferation, endothelial migration and cell survival (MAPK/ERK/p38, AKT, JAK/STAT and Wnt pathways) were activated in Tg2576 mice.

c) Immunoblots for a few effector molecules involved in modulating angiogenesis.

d) Western blot analysis shows that Ang-1 expression is lower in 11-month-old vehicle-treated Tg2576 compared to age-matched vehicle-treated WT mice, whereas Ang-2 is seen increased in the vehicle-treated Tg2576 mice compared to the vehicle-treated WT mice.

e) This panel shows the co-immunoprecipitation of Aβ with the receptors that play a role in initiating angiogenesis using the brain homogenates of 11-month-old vehicle-treated Tg2576 mice and age-matched vehicle-treated WT mice.

IP: Tie2, IP: VEGFR2 and IP: Aβ indicate the pull down of the band by the anti-Tie2 antibody, anti-VEGFR2 antibody and anti-Aβ antibody respectively. The western blot is indicative of the western blotting that was performed by using antibodies for Aβ, Tie2 and VEGFR2. In the case of pull down with Tie2, the band was analyzed with Coomassie staining and confirmed with the help of loading of the positive control, i.e., Aβ peptide. A successful co-immunoprecipitation of Aβ (Tg2576 mouse brain homogenate) with Tie-2 and VEGFR2 established the direct interaction of these molecules.

4.2.6 Human brain endothelial cells (HBEC-5i) treated with amyloid beta demonstrate an increase in production and activity of VEGFR2 and Tie-2 receptors that are key initiators of angiogenesis

Human brain endothelial cells were grown to confluency and treated with either PBS, Aβ1-42 peptide, Aβ1-16 peptide, Ang-2 peptide or VEGFA-165 peptide for 24 hrs. The cell lysates were tested by western blot analysis for different proteins of interest.

Figure 4.9 shows representative blots from 3 different experiments. There was an increase in the expression of VEGFR2 when the cells were treated with the Aβ1-16 peptide as compared to the control (PBS-treated) cells. Aβ1-42 peptide did not exert a similar effect on the cells. There was a slight increase in the VEGFR2 expression when the cells were treated with VEGFA (the receptor ligand) and Ang-2 peptide but not to the level achieved with the Aβ1-16 peptide. Phosphorylated VEGFR2 was also increased after Aβ1-16 peptide treatment as compared to the other treatments (

Figure 4.9a). Similarly, the Tie-2 receptor was upregulated after treatment with the Aβ1-16 peptide as compared cells treated with PBS or to cells treated with the Aβ1-42 peptide. Ang-2 is a Tie-2 receptor ligand that initiates a dysregulated activity of Tie-2 [228-230]. Aβ1-16 peptide treatment demonstrated upregulation of Ang-2 more than the control cells or Aβ1-42 peptide-treated cells (

Figure 4.9b).

a.

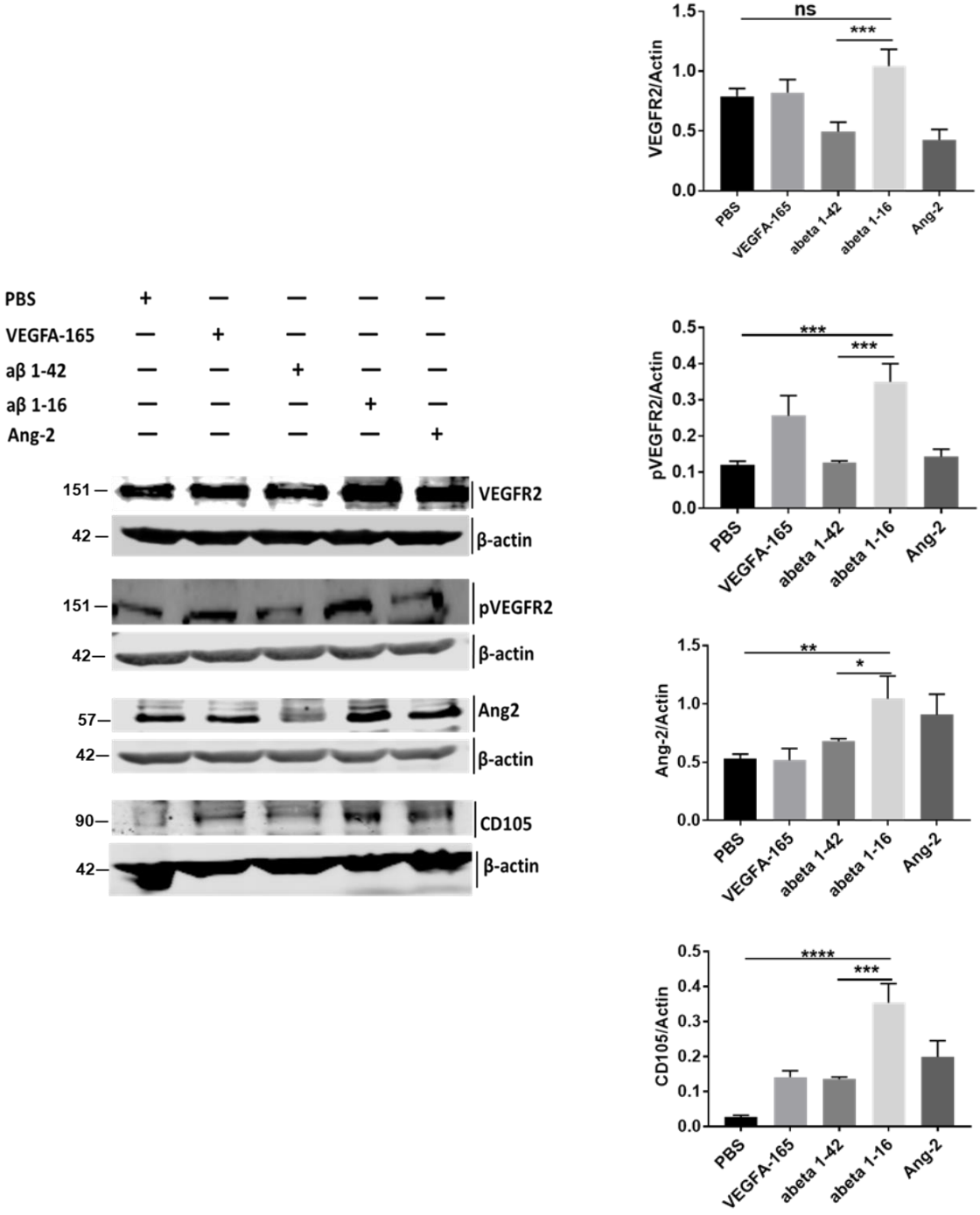
PBS
VEGFA-165
aβ 1-42
aβ 1-16
Ang-2
151
VEGFR2
42
β-actin
151
pVEGFR2
42
β-actin
57
Ang2
42
β-actin
90
CD105
42
β-actin
VEGFR2/Actin
ns
***
pVEGFR2/Actin
***
***
Ang-2/Actin
**
*
CD105/Actin
****
***
PBS
VEGFA-165
abeta 1-42
abeta 1-16
Ang-2

b

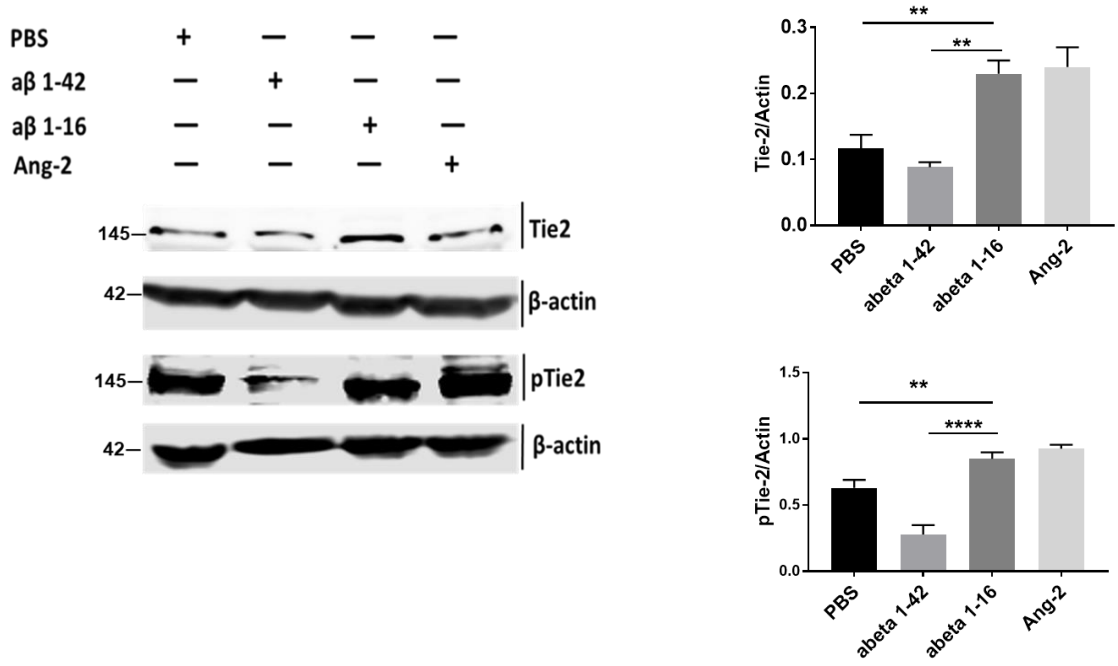

Figure 4.9: in vitro studies of HBEC-5i cells treated with Aβ1-16 peptide (soluble amyloid species) show an upregulation of key angiogenic receptors, Tie-2 and VEGFR2, and increased expression of Ang-2 and neoangiogenic marker CD105

a. shows the western blotting analysis of lysates from *in vitro* treatments. Increases in the expression levels of VEGFR2 and p-VEGFR2 are seen when cells were treated with Aβ1-16 as compared to PBS or Aβ1-42 treated cells. Similarly, increases in the CD105 and Ang-2 expression levels are noted with Aβ1-16 treatment.

b demonstrates the expression levels of Tie-2 and phosphorylated Tie-2, which seem to be unaffected by Aβ1-42 but increased with Aβ1-16 treatment.

4.3 Discussion

This Chapter assesses the role of angiogenesis in AD pathology. Changes in cerebral vessel growth are seen after treatment of 10-month-old Tg2576 mice with the anti-angiogenic, tyrosine kinase inhibitor, Axitinib for a period of one month. The Tg2576 AD-mouse model has been very well characterized for the development of plaques at 9-months of age and cognitive decline starting at 6 months of age and progressing until the animal's death [172]. A previous study showed that the vascular pathology and BBB disruption at 4 months of age preceded the formation of plaques [96]. I chose to use 10-month old Tg2576 mice for my studies as they would, by this age, be expected already to have substantial vascular pathology [231], BBB disruption [96, 118], amyloid load and cognitive decline [221, 232, 233].

In the previous Chapter, we saw the potential of anti-angiogenic molecules that alter the neo-angiogenic process and result in changes in vascular pathology, amyloid load and cognition in the aged Tg2576 mice. In this chapter we wanted to explore the effect of a second-generation anti-angiogenic small molecule TKI, Axitinib, that targets the VEGFR family and also attempt to understand the molecular mechanism of how amyloidgenesis leads to activation of pathological angiogenesis causing breakdown of the BBB.

10-month old pre-treatment Tg2576 mice and WT littermates along with 11-month old Axitinib and vehicle-treated Tg2576 mice and WT littermates were tested for different aspects of cognition. WT mice, as well as Axitinib, treated Tg2576 mice showed significantly higher cognition compared to the pre-treatment and vehicle-treated Tg2576 mice in respect to spatial awareness, exploration, associative memory, working memory and reference memory. The conclusion drawn

from these results is that one-month treatment with Axitinib can improve the above stated memory aspects in aged Tg2576 mice.

It was also noted that Axitinib treatment showed lower expression of angiogenic marker CD105, lower amyloid load, higher expression of TJPs like ZO1 and occludin, and a more functional BBB in aged Tg2576 mice. Thus, Axitinib has the ability to alter cerebral pathology, amyloid load and other pathological indications seen in the Tg2576 mouse model of AD and show a great potential as a proof of concept that with the inhibition of cerebral neo-angiogenesis cognitive decline can be treated as well as the molecular pathology seen in AD can be altered.

It can be concluded from the first part of this chapter that treatment with Axitinib improves cognition of the aged Tg2576 mice. Future studies of characterizing pre-treatment 10-month-old Tg2576 mice will help us address this question of whether Axitinib treatment forestalls the progression of the molecular pathology or reduces it. If the pathological changes seen in the Axitinib-treated Tg2576 mice at 11 months of age are similar to those seen in the pretreated Tg2576 mice at 10 months, then the drug will be considered preventative towards molecular pathology. However, if the Tg2576 mice show worse pathology and functional deficits before treatment than after one month of Axitinib treatment, then the drug will prove therapeutic towards molecular pathology. Similar to what was seen in the cognitive assessment, there may not be any significant difference in the molecular pathology between the 10-month old pre-treatment and the 11-month old vehicle-treated Tg2576 mice and there maybe a significant difference between drug-treated and vehicle-treated Tg2576 mice. Hence, it can be speculated that with respect to molecular

pathology, the drug treatment is more likely to also be therapeutic rather than being preventative, however further studies are needed to prove this aspect of the anti-angiogenic drug, Axitinib.

Angiogenesis is potentiated in AD [96]. To delve into the mechanism of vascular pathology in AD, we need to understand how the normal physiological process of angiogenesis becomes pathogenic. The adult vasculature is derived from a network of blood vessels created in the embryo by vasculogenesis [234]. The endothelial cell lattice that is created serves as a scaffold for angiogenesis, forming the primary capillary plexus which is remodelled by the sprouting and branching of new vessels from pre-existing ones in the process of angiogenesis [235]. Angiogenesis occurs in the adult during physiological repair processes such as wound healing. Vessel formation initiates with the activation of receptor Tie-2, leading to the removal of pericytes and causing vessel destabilization. The endothelial cells proliferate by activation of VEGFR2, and, as a result, the vessel starts sprouting [235].

Tie 2 has two ligands, Angiopoietin-1 (Ang-1) when the vessel is stable, and Angiopoietin-2 (Ang-2) when the vessel is destabilized. In the presence of excess VEGF, inflammatory cytokines (TNFα) and hypoxia, Tie-2 preferentially binds to Angiopoetin-2. Studies have shown that Ang-1 promotes strong activation of the Tie2/PI3K/AKT pathway in quiescent, mature vessels. When the Ang-1 is present, Ang-2 is a Tie-2 antagonist; however, when Ang-1 is absent, Ang-2 acts as a TIE2 agonist, though to a weaker extent than Ang-1 [228]. When Ang-1/Tie-2 signalling is weak, AKT level is reduced and transcription factor FOXO1 is activated, which results in an increase of Ang-2 expression. Ang-2 increases the phosphorylation of Tie-2, thereby compensating for the absence of a strong Ang-1 signal [229]. Ang-2 is known to promote tumour angiogenesis via

activation of Tie-2. While both ligands bind to Tie-2, Ang-1 binding to Tie-2 is altered by Tie-1. In the presence of the Tie-1 ectodomain, Ang-1 is unable to bind to Tie-2 [230]. However, the binding of Ang-2 to Tie-2 is unhindered by the presence or absence of Tie-1 [230].

Ang-2, although thought to be a Tie-2 antagonist, has recently been shown to play a more nuanced role in activating angiogenesis. Hypoxia, inflammatory cytokines and VEGFA regulate the interaction of Ang-2 with Tie-2. Ang2: Tie2 binding promotes destabilization of vessels and initiates neovascularization [229]. Increased VEGFA enables Ang-2 to promote endothelial cell migration and proliferation, while a lack of VEGFA leads to Ang-2 initiating endothelial cell death [229].

The case for vascular etiology of AD is strengthened by the close association of AD with cerebrovascular amyloid angiopathy (CAA), in which Aβ deposition is found in pial and intracerebral vessels [94]. This is seen in about 90% AD cases. CAA gradually causes vascular smooth muscle degeneration and increased vessel stiffness, eventually altering vascular function. It may also lead to blocking of the perivascular and BBB routes for drainage of Aβ [94]. Studies indicate that pathological angiogenesis and BBB disruption occur as a compensatory response to impaired CBF [100, 103].

A debated question is whether angiogenesis is a direct or an indirect initiator of BBB disruption in response to activation by Aβ or mechanisms such as oxidative stress and inflammation [100]. Aβ-induced neuroinflammatory responses facilitate the release of angiogenic activators like VEGF and thrombin. VEGF not only stimulates angiogenesis but also affects the permeability of the blood vessels. Thrombin is known to synergize with VEGF to increase endothelial cell

proliferation [236]. Thrombin induces the endothelial cells to further secrete Aβ, promoting the generation of reactive oxygen species and additional endothelial damage, causing a cycle of neurotoxic insult [100]. Aβ has been implicated as a modulator of blood vessel density and vascular remodelling through angiogenic mechanisms[96].

The BBB integrity in the Tg2576 mouse model has been shown to be compromised by hypervascularity as early as four months of age, preceding the formation of plaques [101]. Recently, it was demonstrated that TJ disruption is considerably higher in aged Tg2576 mice compared to age-matched WT littermates and young mice of both genotypes [96, 101]. In the same study, the cerebrovascular integrity of the Tg2576 mouse model was examined in conjunction with markers of angiogenesis and apoptosis. Aged Tg2576 mice, when compared to age-matched WT littermates, show a significant increase in the incidence of disrupted TJs that was directly linked to neoangiogenesis and an overall increase in microvascular density but not to apoptosis [101]. These observations in the AD mouse model parallel those seen in AD patients when compared to control groups[96].

Immunofluorescence co-localization analysis of the brains of 11-month-old vehicle-treated Tg2576 and WT mice showed a positive correlation between the neoangiogenic marker, CD105 and Aβ, and a negative correlation between CD105 and the tight junction protein, occludin. This suggests that the increase of Aβ will be associated with an increase in CD105 and an increase in CD105 will be associated with a decrease in occludin expression.

Upregulation of CD105, a marker of neoangiogenesis, is seen in the brains of Tg2576 mice. Increased proangiogenic signals like VEGF, Hypoxia inducible factor-1 (Hif-α) and decreased Ang-1 are also seen in 11-month-old Tg2576 mice, either vehicle-treated (Figure 4.8 c, d, e) or

untreated (Figure 4.8 b), compared to age-matched vehicle-treated or untreated WT littermates. These observations are consistent with studies in which angiogenesis is upregulated in the absence of Ang-1 and/or in the presence of VEGF [228-230]. Since the Tg2576 mouse strain has been shown to produce excessive amounts of Aβ, it can be speculated that Aβ itself has a role in the activation of the angiogenesis by either interacting with VEGFR-2 and/or Tie-2, recruiting VEGFA to activate VEGFR2, and mediating Ang-2-dependent activation of Tie2, ultimately leading to dysregulated neovascularization.

Another explanation for the role of Aβ in pathogenic angiogenesis could be the possibility that Aβ increases the transcription of VEGFA and Ang-2, thereby increasing the activation of VEGFR2 and Tie2 receptors. Lastly, Aβ might competitively inhibit VEGFA from binding its receptor, VEGFR2, and instead, Aβ itself binds the receptor and activates pathogenic constitutive angiogenic signalling.

Figure 4.10 shows one of the proposed pathway to explain how amyloid may initiate pathogenic angiogenesis and lead to the disruption of the BBB, a gateway to pathologies seen in AD. Increased levels of Aβ interacting with cerebral vessels in Tg2576 mouse brains in the presence of low levels of Ang-1 lead to recruitment of VEGF in the vicinity of the Tie-2 receptor. This assists Ang-2 to bind to Tie-2 and activates destabilized vessel formation, indicated by the increase in the downstream signalling pathways and activation of pro-angiogenic transcription factors for endothelial survival, proliferation, migration and production of VEGF. This VEGF effector moves out into the extracellular space, further facilitating Ang-2 in continuously binding to Tie-2 receptor molecules and constitutively activating endothelial cells to form pathogenically sprouting vessels. An increase in levels of the effector molecule, Focal Adhesion Kinase (FAK), leads to

rearrangement of the actin cytoskeleton that maintains the physical intactness of the tight junctions and thus destabilizes the vessels, thereby increasing vascular permeability. This allows for the toxic blood molecules to enter the CNS and cause inflammation, hypoxia and neuronal pathologies. In this way, angiogenesis would culminate in establishing AD pathology and cognitive decline.

To answer some of the questions surrounding the proposed mechanisms, human brain endothelial cells were treated with either Aβ (1-16), one of the more predominant sources of peripheral amyloid; Aβ (1-42), which is predominantly found in plaques; Ang2; VEGFA or PBS. It was noted that Aβ (1-16)-treated cells showed higher expression levels and higher phosphorylation levels of VEGFR2 and Tie2 receptors and higher expression of CD105 compared to PBS-treated cells or Aβ (1-42)-treated cells. This supports the idea that it is the soluble and circulating species of Aβ, and not the plaque-associated species that initiate angiogenesis. The Aβ (1-16)-treated cells also showed increased expression of Ang-2, supporting the proposed idea of Ang-2-dependent activation of dysregulated angiogenesis.

It is imperative to understand the pathophysiology of AD disease progression, and new research directions are needed. This is the first study which shows mechanistically that overabundance of amyloid leads to activation of destabilized and leaky vessels, resulting in a cascade of downstream signalling pathways, culminating in molecular pathologies seen in AD. My unique therapeutic approach directed at modulating cerebral angiogenesis, distinguished from targeting the amyloid cascade, may prove efficacious towards AD and related vascular diseases of the brain.

a.

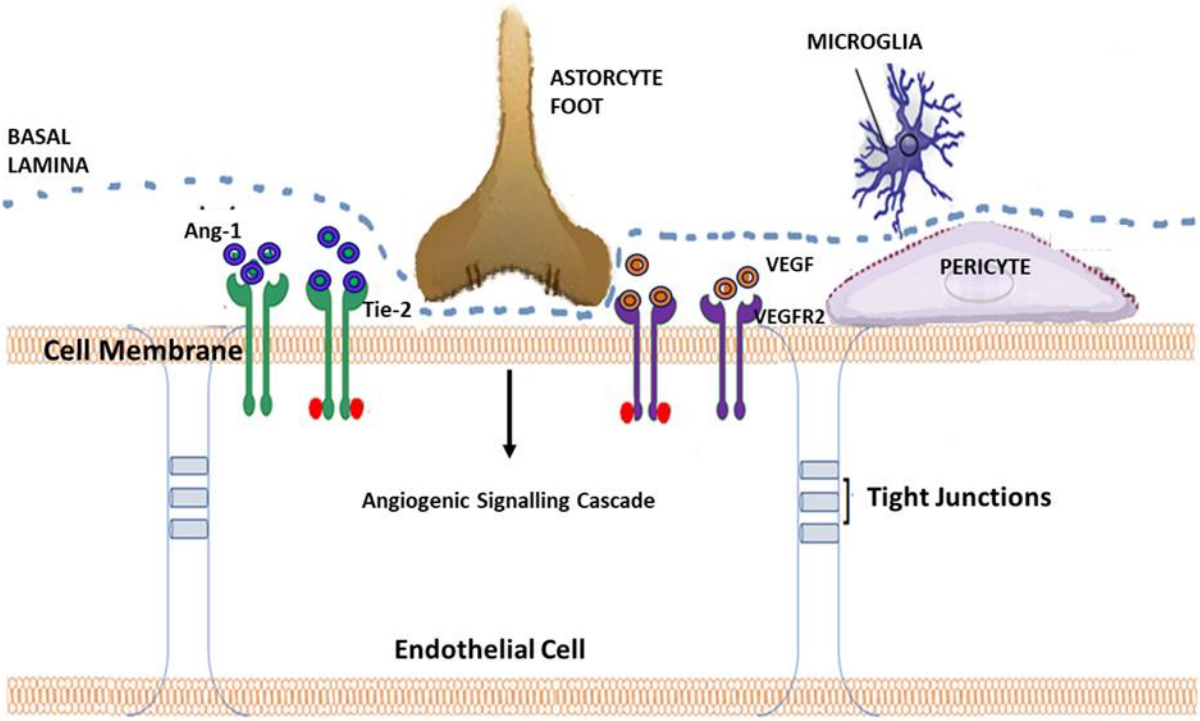
MICROGLIA
ASTORCYTE FOOT
BASAL LAMINA
Ang-1
Tie-2
VEGF
VEGFR2
PERICYTE
Cell Membrane
Angiogenic Signalling Cascade
Tight Junctions
Endothelial Cell

b.

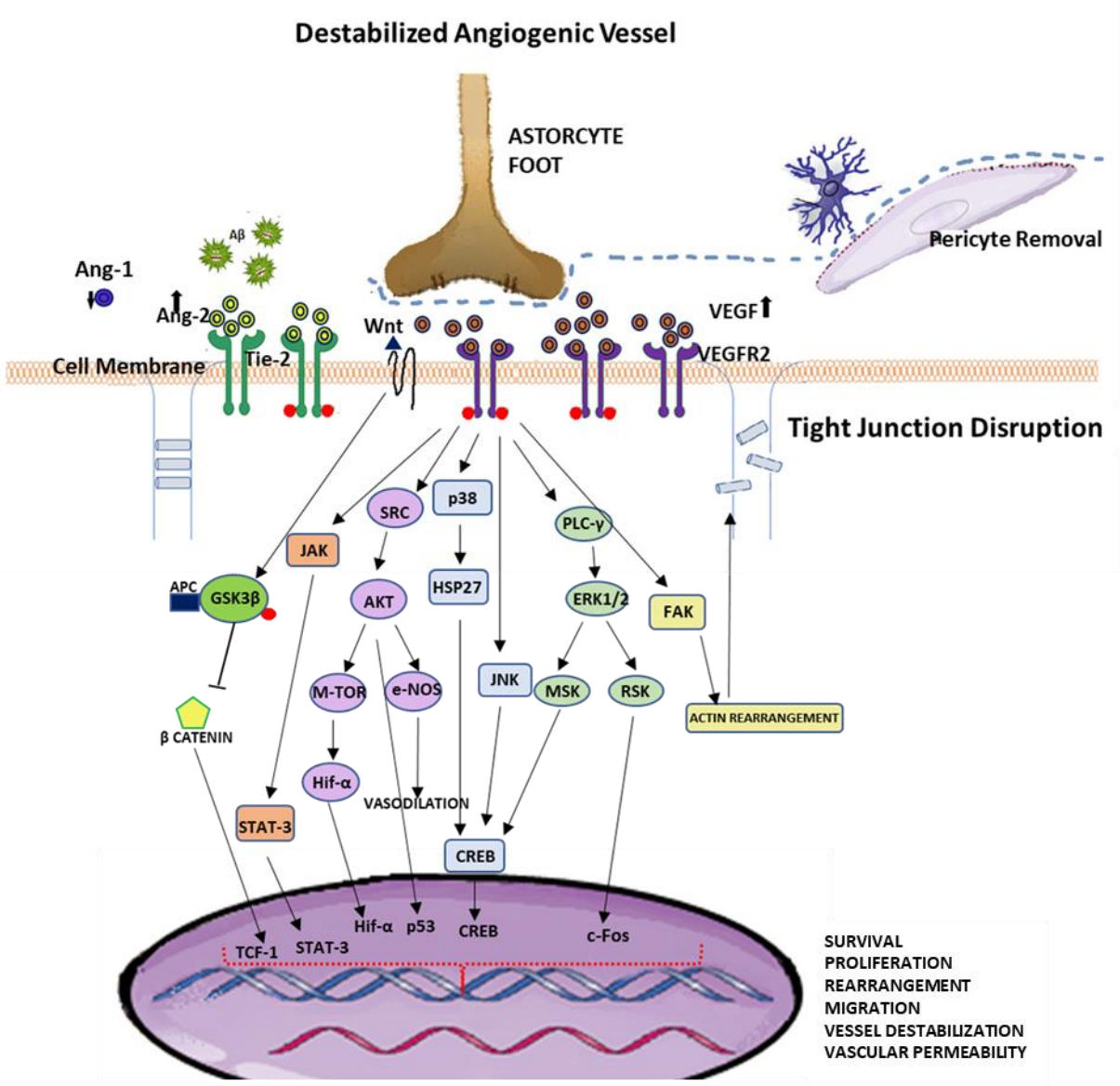

Figure 4.10: Schematic depicting a model mechanism for amyloid beta causing pathological angiogenesis and disruption of the tight junction proteins and the breakdown of the neurovascular unit

a) Normal physiological activation of blood vessel growth by Angiopoietin-1activating Tie-2.

b) The initiation of pathological and destabilized blood vessel growth. Increased levels of amyloid beta seen interacting with cerebral vessels, in the presence of hypoxic conditions and low levels of

Angiopoietin-1 recruits VEGF in the vicinity of the Tie-2 receptor. This assists Angiopoietin-2 to bind to Tie-2 and activate destabilized vessel formation, which is indicated by the increase in the downstream signaling pathways and activation of pro-angiogenic transcription factors for endothelial survival, proliferation, migration and production of VEGF. VEGF effector moves out into the extracellular space, further facilitating Ang-2 in continuously binding to Tie-2 receptor molecules and constitutively activating endothelial cells, leading to the formation of pathogenically sprouting vessels. Increases in certain effector molecules like FAK lead to rearrangement of the actin cytoskeleton that maintains the physical intactness of the tight junctions and thus destabilizes the vessels, thereby increasing vascular permeability. This allows for the toxic blood molecules to enter into the central nervous system and cause inflammation, hypoxia and neuronal pathologies. In this way, angiogenesis culminates in AD pathology and cognitive decline.

Chapter 5 Bone marrow cells from the Tg2576 AD mouse model can produce AD pathology in APP-KO mice, suggesting the role of soluble amyloid beta species in establishing AD pathogenesis

5.1 Introduction

Haematopoietic stem cells residing in the bone marrow of adult vertebrates are characterised as the cells that are responsible for the generation of all mature blood lineages via a process of stepwise commitment, which progressively restricts the differentiation potential of intermediate progenitors. Haematopoiesis refers to the commitment and differentiation processes that lead to the formation of all blood cells from haematopoietic stem cells. Self-renewing, long-term reconstituting hematopoietic stem cells (LT-HSC) first give rise to transiently reconstituting, short-term hematopoietic stem cells (ST-HSC). ST-HSC in turn, produce common myeloid progenitors (CMP) and common lymphoid progenitors (CLP). CLP are the source of committed progenitors that eventually give rise to T and B lymphocytes. CMPs further give rise to megakaryocyte-erythroid progenitors (MEP) and granulocyte-macrophage progenitors (GMP). MEPs are the source of committed progenitors that eventually give rise to erythrocytes and megakaryocytes whereas GMPs are the source of committed progenitors that eventually give rise to mast-cells, neutrophils, eosinophils and monocytes.

In recent times many studies have employed the use of haematopoietic stem cells (HSCs) as a therapeutic strategy towards various aspects of AD pathology. One study suggested that blood-derived microglia and not their resident counterparts have the ability to eliminate amyloid from the brain [204]. Another group showed that the HSC-derived monocytic cells displayed

inflammatory responses comparable to microglia and contributed to the reduction of amyloid. These easily genetically-modifiable cells may have therapeutic potential for AD [205]. Current advances in cell-based therapies have shown that transplanted exogenous stem cells are efficacious in recapitulating pathological features in human patients [237]. HSCs have also been used to study neurogenesis and reduction in amyloid production to counter the neuronal loss and increased amyloid in AD brains [237].

All these cell-based therapies have great potential; however, there is a looming concern around their safety. In recent years, the idea of AD spreading through plasma like the infamous prion disease has arisen. The idea that misfolded amyloid peptides are 'proteinaceous infectious particles' is being investigated. In one case, four patients died of iatrogenic Creutzfeldt-Jakob disease after childhood treatment for short stature, with prion-contaminated cadaveric pituitary extract. Upon investigation, it was reported that these patients also had substantial immunoreactive amyloid and increased microvessels in the brain [238]. The pituitary glands of AD patients are known to have amyloid deposits. This provided evidence of human to human transmission of amyloid seeds. This raises concern for many of the cell-based therapies of AD.

In this chapter, we wanted to try and tackle this key concern regarding whether AD pathology can be produced by the transfer of HSCs from the amyloid-overproducing Tg2576 AD mouse model.

It would also facilitate us to move away from the conventional central dogma of around AD pathology. The conventional idea of AD pathogenesis is that the accumulation of brain derived amyloid, specifically produced by dying neurons, is the cause of the disease. Over the years most

therapeutics developed have been around this dogma, and several spotlighted trials using these therapeutics have failed to improve cognition or altering disease progression in patients [93, 239, 240] Most therapeutics based around either lessening the production of amyloid or increasing its clearance have been successful in reducing the overall amyloid load, but some immunotherapies have also resulted in deleterious outcomes like inducing inflammatory insults that have resulted in patient deaths [92]. This tells us that successful elimination of amyloid in animal models, which typically overexpress *APP* or presenilin (*PS1*, *PS2*) genes, does not guarantee successful cognitive restoration in human patients.

Conventionally, amyloid that is deposited in the brain, a hallmark of AD, has been thought to originate from the brain itself. Recent studies have shown that circulating amyloid species are able to cross the blood brain barrier [241, 242], but the contribution of these peripherally derived peptides toward AD pathology is unexplored. The primary source of the peripheral APP is the platelets [21, 243]. Upon platelet activation, β secretase enzyme activity increases in their membranes, resulting in the production of soluble amyloid species [244]. Although platelets are the leading source of peripheral amyloid, other sources like skin fibroblasts, skeletal muscles and cerebrovascular smooth muscle cells can also produce Aβ [241]. In this chapter, we wanted to see if the APP being transported and amyloid being produced by platelets that originate from HSCs of donor Tg2576 mice and WT littermates after a bone marrow transplant are able to establish AD pathology in APP-KO mice. This will help us understand whether a bone marrow transplant can potentially spread a disease like AD and also help us understand the contribution of amyloid being generated outside the brain in establishing the disease.

5.2 Results

To establish that circulating amyloid beta can cause AD pathology, we undertook the transfer of hematopoietic stem cells expressing large amounts of the mutant human APP into mice that do not express murine APP (APP-KO mice). If such transfer causes deposition of amyloid in the brains of the recipients, establishing Alzheimer's disease, brain-derived APP may not be required for the formation of plaques. If this experiment does produce Alzheimer's disease pathology in the recipient mice, it may help us to understand the pathogenesis of the disease better.

Bone marrow cells from Tg2576 or B6/SJL donor mice were injected via the tail vein into recipient APP-KO mice that had received X-irradiation in a dose sufficient to ablate the marrow. The presence of a donor bone marrow cell population from Tg2576 or B6/SJL mice used to demonstrate a successful reconstitution. This was established by FACS analysis. **Figure 5.1** shows the representative scatter plot and histogram of the FACS analysis of the CD45 type of the lymphocyte population. The recipient APP-KO mice exhibit CD45.2. Figure 1a demonstrates that the donor Tg2576 female mouse is type 1 (CD45.1). Two months after initial injection of the donor bone marrow, FACS analysis on the lymphocyte population of the recipient showed a successful reconstitution of the donor lymphocytes, with 91.6% being type 1 **(Figure 5.1b)** and 6.8%, CD45.2 type. The major population was derived from the donor, but there was a small residual population of recipient cells that had not been removed completely with the irradiation. This was seen across the different groups.

a.

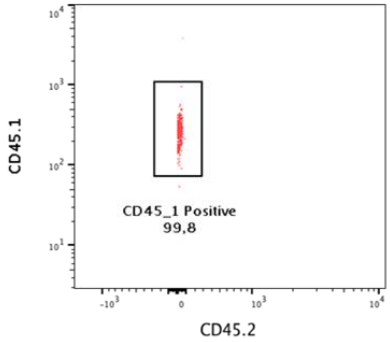

SampleID	Subset Name	Count
CD45.1 Transgenic Donor	lymphocytes	992

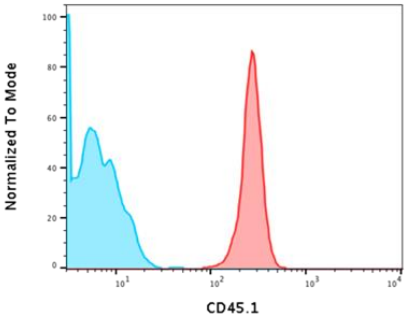

SampleID	Subset Name	Count
CD45.1 Transgenic Donor	lymphocytes	992
CD45.2 Recipient	lymphocytes	687

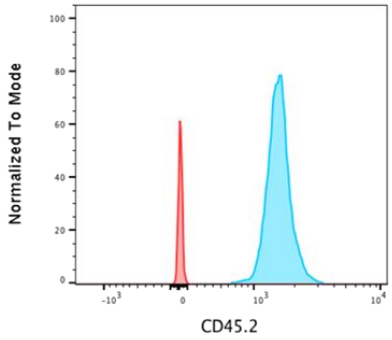

SampleID	Subset Name	Count
CD45.1 Transgenic Donor	lymphocytes	992
CD45.2 Recipient	lymphocytes	687

b.

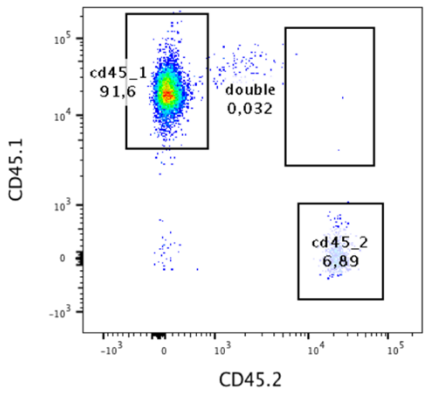

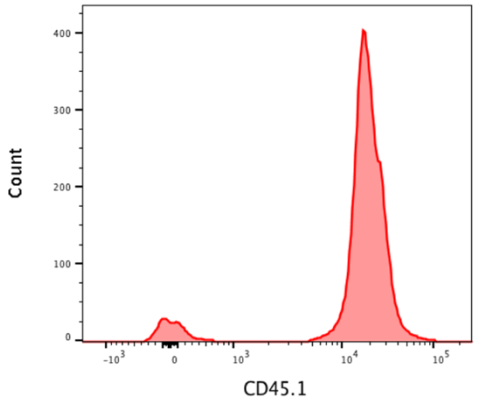

SampleID	Subset Name	Count
Reconstituted Recipient with Donor Bone Marrow	Lymphocytes	9277

Figure 5.1: Successful reconstitution of the donor bone marrow cell population in the recipient

a. representative scatter plot for the donor mice showing the gating strategy and histograms of both the recipient and donor mice. Lymphocytes were gated based on size and shape, and gating was consistent among all samples. The x-axis indicates the level of fluorescence of the CD45.1 or CD45.2 marker using antibodies specific for the isotype CD45.1 or CD45.2.

All the donor mice (Tg2576 and B6/SJL) were positive for CD 45.1 and negative for CD 45.2, as indicated by the red peaks. All the recipient APP-KO mice were positive for CD 45.2 and negative for CD 45.1, indicated by the blue peaks, prior to irradiation and reconstitution.

The graph was normalized to mode, which allows us to visualize the relative percentage of a cell population expressing the marker fluorescence. This compensates for the visual difference in cell count.

b. representative scatter plot and histogram of the APP-KO recipient mice two months after transplant with donor mouse bone marrow (Tg256 or B6/SJL), showing successful reconstitution of the donor bone marrow CD45 type (CD45.1). The recipient APP-KO mice that were previously CD45.2 positive are now CD45.1 positive, indicating successful reconstitution.

The scatter plot shows CD45.1 on the Y axis and CD45.2 on the x axis and indicates that in the newly reconstituted recipient mice 91.6% lymphocytes originated from the donor bone marrow cells (CD45.1) and the remainder (6.89%) originated from the recipient's resident bone marrow cells (CD45.2).

5.2.1 APP-KO recipient mice that received haematopoietic stem cell transfers from Tg2576 mice exhibit impaired cognitive status

APP-KO recipient mice that were reconstituted with Tg2576 marrow containing the mutant human APP transgene performed poorly in the open field test **(Figure 5.2a)**, spending significantly more time exploring the central region of the field as compared to the APP-KO mice that received WT bone marrow cells. Mice that were reconstituted with Tg2576 marrow also had low spatial awareness when tested on the Y- maze, with a significantly lower percentage of alternation than APP-KO mice, reconstituted with WT marrow **(Figure 5.2b)**. A significantly lower percentage of freezing in the contextual fear conditioning test indicated that the APP-KO mice reconstituted with Tg2576 marrow had a poorer associative memory than APP-KO mice reconstituted with WT marrow **(Figure 5.2c)**. **Figure 5.2d and e** show the latency time and the total number of memory errors made in the Radial Arm Water Maze test. APP-KO mice reconstituted with Tg2576 marrow had diminished working and reference memories, showing no learning over the 5-day test trial, as compared to APP-KO mice reconstituted with WT marrow. These cognitive analyses indicate that cognitive impairment associated with AD can be established by transferring hematopoietic stem cells from Tg2576 animals that express high levels of a mutant human APP.

a.

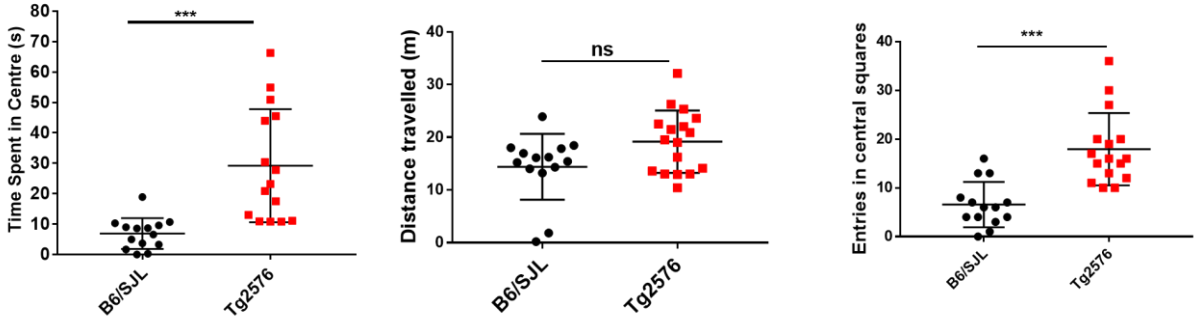
Time Spent in Centre (s)
***
B6/SJL
Tg2576
Distance travelled (m)
ns
B6/SJL
Tg2576
Entries in central squares
***
B6/SJL
Tg2576

b.

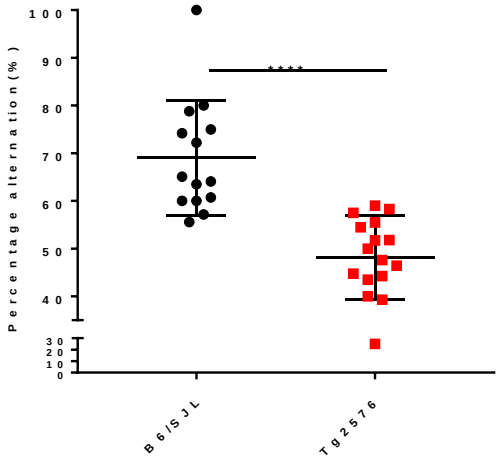
Percentage alternation (%)
****
B6/SJL
Tg2576

c.

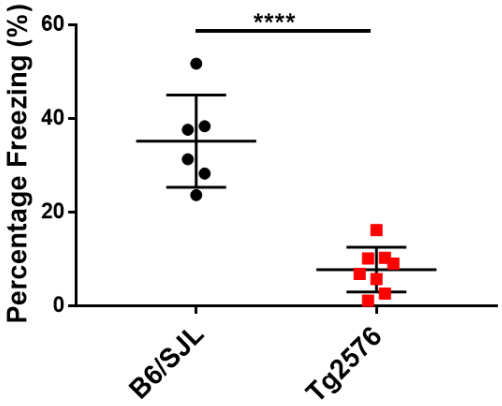
Percentage Freezing (%)
****
B6/SJL
Tg2576

d.

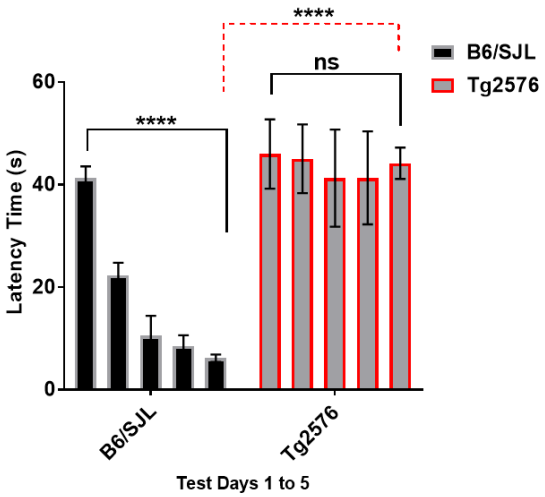
Latency Time (s)
****
ns
B6/SJL
Tg2576
Test Days 1 to 5

e.

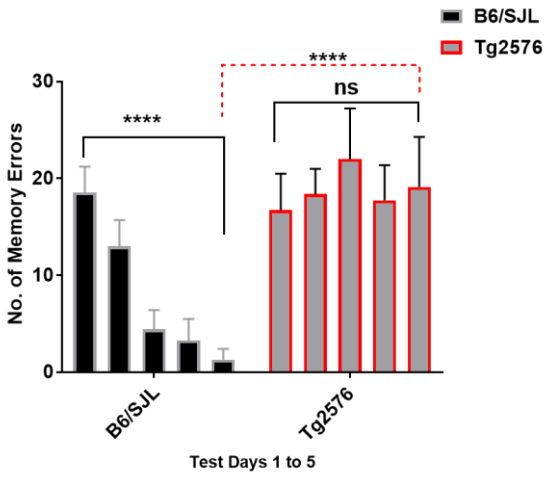
No. of Memory Errors
B6/SJL
Tg2576
****
ns
****
B6/SJL
Tg2576
Test Days 1 to 5

Figure 5.2 Bone marrow transfer from an AD model mouse, Tg2576, produces cognitive deficits in APP-KO recipient mice.

APP-KO recipient mice 6-months after reconstitution with Tg2576 bone marrow cells were assessed for cognitive deficits as compared to recipient mice that received bone marrow cells from B6/SJL (wildtype) mice **(* p<0.03; ** p<0.002; *** p<0.0002; **** p<0.0001).** The data were pooled from 3 different trials for statistical analysis (WT, n =14; Tg2576, n = 17, unless otherwise stated) APP-KO mice that received WT bone marrow are labelled as 'B6/SJL', and APP-KO mice that received Tg2576 bone marrow are labelled as 'Tg2576' in the graphs above. The data are expressed as the mean of individual animals in each group ± standard deviation. Statistical analysis was done using unpaired Student's t test unless otherwise stated.

a) Open Field Test. recipient mice reconstituted with WT (B6/SJL) bone marrow cells spend less in the center of the field, whereas mice that were given Tg2576 bone marrow spend more time exploring the center. There was no significant difference noted between the APP-KO mice that received WT bone marrow and APP-KO mice that received Tg2576 bone marrow in the overall distance travelled in the field; however, there was a significant increase in the number of entries made in the center by the Tg2576-reconstituted mice as compared to WT-reconstituted mice

b) Spontaneous alternation (Y-maze) Test. Cognitively aware mice show a high percentage of alternation, as was seen in APP-KO mice that received WT bone marrow; APP-KO mice that received Tg2576 bone marrow exhibited poor performance on the test, with a significantly lower percentage of alternation.

c) Contextual Fear conditioning. APP-KO mice that received WT bone marrow showed good associative memory with high freezing percentages. The APP-KO mice that received Tg2576 bone marrow displayed a significantly lower freezing percentage. (Data for this test are only from two different mouse trials; B6/SJL, n=6; Tg2576, n=8)

e, f) Radial arm water maze. Panel e shows the time it takes for the mice to locate the escape platforms, and Panel f shows the number of errors (working and reference memory errors) made by the mice when locating the escape platforms. APP-KO mice that received WT bone marrow showed an overall decrease in the latency time and number of errors made over the 5-day trial. APP-KO mice that received Tg2576 bone marrow showed significantly higher latency time and a number of errors, with no improvement over the 5 days.
The data in **e** and **f** are expressed as the mean of the latency time or a total number of errors made in single trial per day by individual animals in each group. The data were pooled from 3 different trials and is represented as the mean± standard deviation. Statistical analysis was carried out using a 2-way ANOVA with correction for multiple comparisons using the Bonferroni's test **(* p<0.03; ** p<0.002; *** p<0.0002; **** p<0.0001).**

5.3 Molecular and histological analysis of the mice receiving Tg2576 haematopoietic stem cells demonstrate AD pathology

The APP-KO mice that received bone marrow cell transfers from Tg2576 or WT donors were terminally anesthetized with ketamine/xylazine, perfused with PBS, and their brains harvested. **Figure 5.3a** and **b** show the immunofluorescence analysis. Heavy amyloid staining and an increase in the angiogenic vessels can be seen in the brains of APP-KO mice that received Tg2576 bone marrow but not in the brains of the APP-KO mice that received WT bone marrow. CD31 staining was done to look for the expression of mature vessels. Panel b shows that expression of ZO1 is low in the brains of APP-KO mice that received Tg2576 bone marrow but high in APP-KO mice that received WT bone marrow. Western blot analysis shows that there was increased expression of the amyloid beta protein (from the combined SDS membrane bound fraction and formic acid fraction) in the brains of APP-KO mice that received Tg2576 bone marrow but no apparent amyloid expression in the brains of APP-KO mice that received WT bone marrow **(Figure 5.3c)**.

To examine whether the presence of this amyloid had any functional implications on the vasculature and BBB integrity, we looked at the expression of VEGFA, a factor that is crucial for angiogenesis initiation extracted from the cytosolic fraction, and the tight junction protein ZO1 extracted from the SDS membrane bound fraction. Higher expression of VEGFA and lower expression of ZO1 were seen in the APP-KO mice that received Tg2576 bone marrow compared to the APP-KO mice that received WT bone marrow. This implies that there is not only transfer of disease-associated mutant human APP to the recipient mouse brain but also that this amyloid can induce AD pathology in mice that have no endogenous APP expression in their brains.

a.

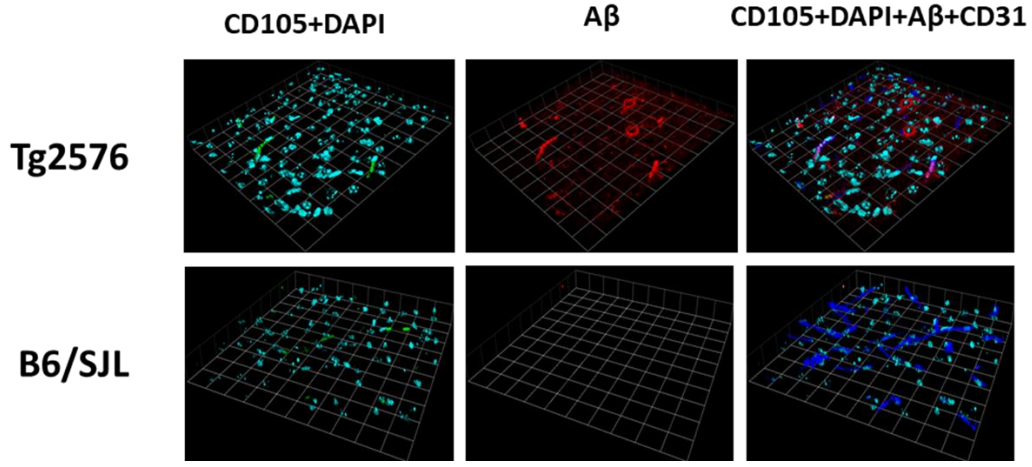
CD105+DAPI
Aβ
CD105+DAPI+Aβ+CD31
Tg2576
B6/SJL

b.

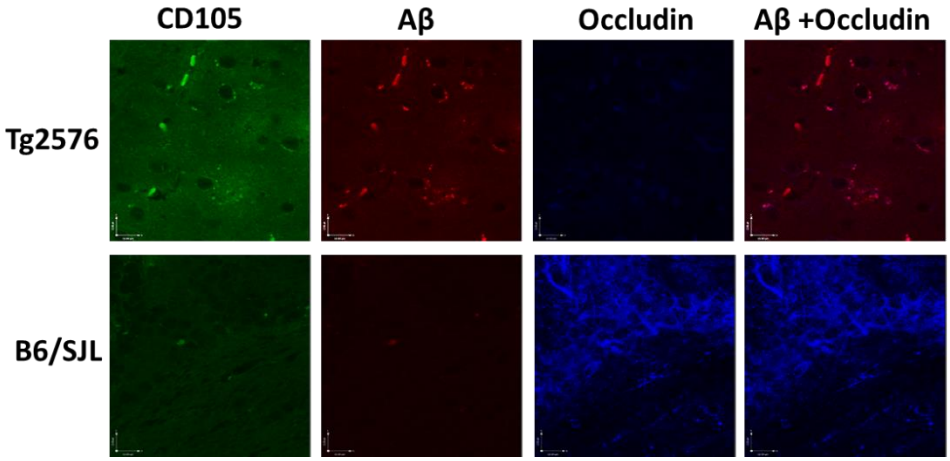
CD105
Aβ
Occludin
Aβ +Occludin
Tg2576
B6/SJL

c.

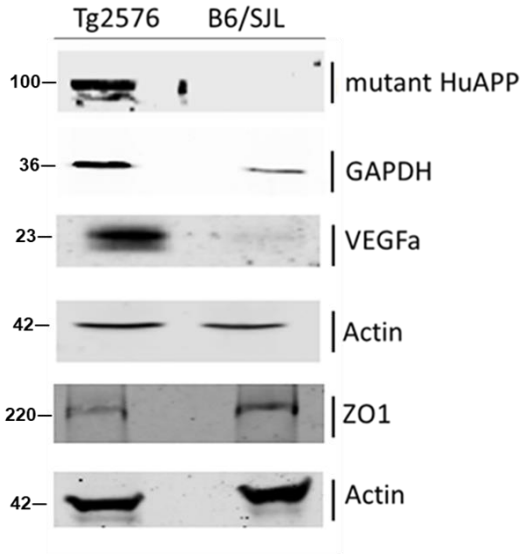
Tg2576
B6/SJL
100—
mutant HuAPP
36—
GAPDH
23—
VEGFa
42—
Actin
220—
ZO1
42—
Actin

Figure 5.3: Immunofluorescence and western blotting analysis show evidence of AD pathology in the brains of APP-KO mice reconstituted with Tg2576 marrow.

5.3**a and b.** Representative micrographs of cortical and hippocampal brain sections from APP-KO mice that received bone marrow cells either from either a wildtype (B6/SJL) donor or a transgenic Tg2576 donor mouse. Recipients of Tg2576 marrow show increased Aβ and increased CD105 expression but decreased expression of occludin. Panel **a** is a 3D image representation of the field of view (as indicated by the grid) and Panel **b** is a 2D image representation of the field of view.

5.3**c** demonstrates similar findings by western blotting analysis. The brains of APP-KO recipients of Tg2576 marrow exhibit an increased presence of APP protein and of VEGFA. A decrease in the expression levels of ZO1 was observed in brains of APP-KO mice that were reconstituted with Tg2576 marrow, consistent with the breakdown of the BBB.

5.4 Discussion

In this Chapter, we have discussed the potential of haematopoietic stem cells from Tg2576 AD model mice to produce AD pathology in recipient animals. A successful reconstitution of Tg2576 bone marrow into APP-KO mice, which do not produce any endogenous amyloid, was recorded. 6-months after transfer of the amyloid overproducing Tg2576 HSCs, the transplanted APP-KO mice showed cognitive impairment compared to the WT-bone marrow-transplanted APP-KO mice. Upon molecular assessment of various effectors related to AD pathology, it was noted that the Tg2576-bone marrow-transplanted APP-KO mice showed an increased expression of APP protein, increased amyloid expression in the brain, increased expression of the neoangiogenic marker CD105, and decreased expression of the tight junction proteins, occludin and ZO1. We conclude from these observations that transplantation of HSCs from a mouse that overproduces mutant human amyloid can cause AD pathology in a recipient animal that does not make the endogenous APP.

The APP-KO mice do not produce endogenous amyloid in their body. If the central dogma that brain-derived amyloid is what causes AD pathology were correct, then the reconstitution of the APP-KO mice with Tg2576 HSCs should not have induced AD pathology. Since we observed that Tg2576 HSCs did, in fact, induce AD pathology in the APP-KO mice, we have shown that amyloid produced outside the brain can contribute to the development of AD pathology.

The majority of the peripheral amyloid is found in circulating platelets, and we speculate that megakaryocytes derived from the Tg2576 HSCs give rise to the platelets that carry the peripheral amyloid. Aβ molecules that are carried and generated from activated platelets are known to be

soluble [244, 245] and this property may enable them to be transported into the CNS through the cerebral vessels. The disruption of the BBB seen in these mice could be a result of a normal age-related phenomenon that permits transfer of the soluble amyloid into the brain. This process would occur much more in the Tg2576 recipients because they make much more amyloid. It could also be triggered by the platelets that circulate in the cerebral vessels. The excess collagen around the tight junctions activates the platelets and releases the amyloid. More the amyloid produced more is the activation of vasculogenesis leading to the breakdown in BBB integrity. Once the AD pathology gets started, it might further trigger vasculogenesis and further breakdown of the BBB in a vicious cycle. The findings in this chapter establish that peripherally derived amyloid can initiate vascular pathology, BBB disruption and AD pathology.

The production of AD pathology in Tg2576-bone marrow-transplanted APP-KO mice also supports the idea that the transfer of AD from individual to individual. This suggests the importance of screening individuals carefully for potentially transferable disease before using them as donors for cell-based therapies.

For future studies, it would be interesting to use this cell-based technique to see if HSCs from a WT animal can revert AD pathology in the Tg2576 mice to assess the therapeutic potential of haematopoietic stem cells in AD.

Chapter 6 Conclusions and Future Directions

AD is the most prevalent form of dementia, affecting millions of people worldwide. It has been over a century since the disease was first discovered. Over the years billions of dollars have been spent on disease intervention, management and research on AD: however, our understanding of the pathophysiology and progression of the disease is still very limited.

One of the most prevalent ideas in the field is the amyloid cascade hypothesis where Aβ is thought to be central to the pathology of the disease. However, the exact mechanisms that link Aβ to the various pathologies associated with AD are yet to be clarified. A strong relationship between the cerebral vasculature and AD neuropathology exists. The vascular link to AD has been shown to extend to the level of BBB where vascular dysfunction has been noted in both humans and various AD mouse models.

6.1 Anti-angiogenic therapeutics can modulate cerebral vessel growth and AD pathology

The overall goal of this thesis was to characterize the relationship between Aβ and its role in the initiation of dysregulated cerebral angiogenesis that leads to the observed BBB dysfunction in AD using the Tg2576 mouse model. The idea was to show that pathological cerebral vessel growth lies in the center, where many of the pathways involved in AD pathology converge. The first initiator of vascular pathology in AD is not known. The possible mechanisms that initiate vascular pathology are the activation of inflammatory pathways, as a result of normal aging, in response to hypoxia, impaired cerebral blood flow or the genesis of Aβ which itself is vasculotropic. The

different pathways mentioned above may also be working in concert with one another to cause cerebral vascular pathology.

This was achieved by modulating the growth of cerebral vessels in Tg2576 AD mouse model with the help of small molecule tyrosine kinase inhibitors and biologics with anti-angiogenic properties. Aged Tg2576 mice (10-months old) have been very well characterized for the presence of AD pathology and impaired cognition. The maintenance of cognition and prevention of progression of disease suggested a therapeutic potential for these TKIs and antibodies in human patients.

The role of angiogenesis in AD pathology was further established through molecular studies of the brains of vehicle-treated and drug/antibody-treated Tg2576 and control WT mice. The decreased amyloid load in the brains of drug/antibody-treated Tg2576 mice indicated the possibility of amyloid clearance or inhibition of disease progression.

The next aspect of brain health assessed was the morphology of the TJs in the brain vasculature of this mouse. Aged Tg2576 mice have been noted to have TJ-related vascular pathologies, which are absent in age-matched controls and young mice [96]. The observed brain vascular pathologies appeared to be associated with the presence of Aβ. This association was further strengthened by the fact that Tg2576 mice treated with Aβ immunotherapy have reduced brain Aβ levels [246-248]. In a previous study, 11-month old Tg2576 mice actively immunized with Aβ had normal TJ morphology in the capillary cerebral vasculature. However, the larger vessels in the Aβ-immunized Tg2576 mice displayed TJ pathology that appeared to be related to vascular deposition of Aβ. This unique pathology has not been fully characterized *in vivo* [212].

This thesis attempted to directly correlate Aβ-induced vascular leakage with the presence of TJ abnormalities in the Tg2576 AD mice. The presence of the Evans Blue dye in the CNS of the vehicle-treated 11-month old Tg2576 mice indicated a disrupted BBB. The drug/antibody-treated Tg2576 mice showed much lower Evans Blue staining, indicating a functional BBB. This implied the possibility that dysregulated vessel growth affects BBB intactness, leading to vascular leakage.

In the future, various studies can be done to address the potential of anti-angiogenic therapeutics further. Molecular pathology assessment of the brains of 10-month-old Tg2576 mice pre-treatment will help us understand whether the difference seen in the data in this thesis is due to the improvement of the disease pathology or the prevention of its progression. Although looking at the data from cognitive analysis, it can be speculated that the anti-angiogenics used in this thesis may be therapeutic. However, it would be interesting to see if these anti-angiogenics have the potential to prevent the formation of pathology in the first place when administered to animals much before the establishment of the disease. Another question is to analyze dose, schedule and frequency of administering the therapeutic and to see how long normal levels of cognition can be maintained. Scenarios exploring the effect of varying dosages and scheduling would only increase our knowledge in treating AD with anti-angiogenic therapeutics.

A technical limitation of the work is presented with respect to the morphologic and immunohistochemical parameters. Higher magnification and lager panels may provide more information. The semiquantitative analysis of tight junction morphology convey an impression of their integrity however ultrastructural analyses with electron microscopy would provide the necessary resolution to assess structural integrity or pathology leading to leakage.

6.2 Amyloidgenesis promotes dysregulated neoangiogenesis leading to BBB disruption and other AD pathologies

An RNA-microarray analysis (*data not shown*) conducted with samples derived from brain homogenates of 12-month-old vehicle-treated Tg2576 mice and age-matched vehicle-treated WT mice showed global changes in gene expression between the two groups that were related to processes like memory, endothelial proliferation, response to hypoxia and survival. These data provide candidates that could be potential targets to help understand the mechanisms of pathophysiology in AD. To further delve into this, a proteome array was performed on brain protein homogenates from 11-month-old untreated Tg2576 mice and homogenates from age-matched WT mice to look for various effector proteins involved in angiogenesis. In comparison to the WT, the Tg2576 mice showed an overall increase in the pro-angiogenic effectors and a decrease in the anti-angiogenic effectors, with the exception of the anti-angiogenic endostatin, which could be upregulated as a compensatory mechanism for the overall increase in angiogenesis.

The process of vessel formation is initiated by the activation of the Tie2 receptor, which is involved in pericyte removal to prepare the endothelial layer for proliferation. The other very important initiator of the pathway is the VEGFR2 receptor that activates the downstream signalling for endothelial proliferation and survival, among other things. We have studied the activity and status of these two prominent receptors of angiogenesis with respect to the over production of Aβ in the Tg2576 mouse brains as well as the human brain endothelial cells in Chapter 4. At first, we demonstrated an increased angiogenic state with BBB disruption in the Tg2576 mice, which overproduce Aβ. Our next question was whether this Aβ interacts with molecules that initiate the angiogenesis pathway. This was followed by a successful co-immunoprecipitation of Tie2 and

VEGFR2 with Aβ and visa versa indicated that a physical interaction exists between Aβ and the receptor molecules.

We then asked whether this interaction was functional or not. This was answered in a few different ways: Brain homogenates from 11-month-old untreated Tg2576 mice and age-matched WT mice were used to analyse the phosphorylation status of different kinases that are involved in the signalling cascade for endothelial proliferation, endothelial survival, rearrangement and migration of endothelial cells. It was observed that downstream signalling molecules as indicated in **Figure 4.8a** showed increased phosphorylation status in the Tg2576 mice compared to the WT. *In vitro* analysis of human brain endothelial cells treated with Aβ (1-16) showed increased phosphorylation of both the Tie2 and VEGFR2 receptors. These data indicate that Aβ not only binds to the key activators of the angiogenesis pathway but also leads to the activation of those receptors and an increased activity of downstream signalling molecules. This suggests that Aβ has a functional interaction with the receptors Tie2 and VEGFR2.

6.3 Aβ initiates Ang-2-mediated activation of Tie2 receptor resulting in a dysregulated angiogenesis in Tg2576 mice

It is known that in the presence of decreased Ang-1 and increased VEGFA, the ligand Ang-2 binds to Tie2 and activates it to result in a dysregulated vessel formation [228, 229]. We showed that decreased Ang-1, increased VEGFA and increased Ang-2 expression occur in the Tg2576 mice. One of the overriding differences between the WT and Tg2576 is the overproduction of Aβ.

HBEC-5i cells treated with Aβ (1-16) showed both an increased expression of Ang-2 and Tie-2 as well as increased phosphorylation of Tie-2. This suggests that Aβ directly or indirectly promotes the Ang-2 mediated activation of Tie2.

6.4 Soluble Aβ and its interaction with the vascular endothelial growth factor receptor

The Aβ (1-16) species is predominantly found as peripherally circulating Aβ, whereas Aβ (1-42) is mainly a component of the aggregated form of Aβ found in the brain. After a 24-hour treatment of HBEC5i cells with these Aβ species, it was noted that Aβ (1-16) not only greatly increased the expression of VEGFR2 but also was highly phosphorylated as compared to PBS-treated cells. This increase in protein expression and phosphorylation was not observed in cells treated with Aβ (1-42). These data imply that soluble Aβ species, rather than Aβ species that form aggregates, might have a role in the initiation of pathological angiogenesis.

In the future, experiments need to be conducted to see whether Aβ (1-16) imodulates vessel growth by increasing the transcription of VEGF or can also recruit VEGF to the vicinity of VEGFR2 to further increase its activity. This investigation can be done by first treating cells with actinomycin-D, which blocks new transcription, and then treating them with the Aβ (1-16). If the same levels of phosphorylation are seen in VEGFR2 under both conditions, it would imply that soluble Aβ both increases the transcription of VEGFR2 and positively modulates its activity.

Another possible mechanism of Aβ modulating angiogenesis is by competitively inhibiting the binding of VEGFA to VEGFR2 and instead binding itself to the receptor to initiate a pathogenic angiogenesis pathway.

6.5 Circulating Aβ originating from HSC transfer can produce AD pathology

Moving away from the central dogma of AD in which brain-derived Aβ is seen as the cause for AD pathology comes the story of peripheral Aβ as an alternate explanation for the pathogenesis.

Platelets are the major source of the peripheral Aβ [21, 243, 244]. In Chapter 4 and Chapter 5 we showed how a soluble Aβ species, as opposed to an Aβ species associated with the brain aggregates, can induce changes in the vasculature. HSC-derived megakaryocytes give rise to the platelets. It is known in that in AD there is an excessive formation of mini-strokes or clots [249]. These clots are abnormal structurally and resistant to degradation [155]. Whole blood from Tg2576 mice clots faster than whole blood from wild-type animals, suggesting that coagulation is intrinsically accelerated in the Tg2576 [249]. It is possible that Aβ may influence platelet biology to account for this rapid clotting anomaly. Several initial experiments investigating Aβ and platelet interactions in the Tg2576 mouse could be performed. Expression of the human APP on circulating platelets in the Tg2576 mouse should be confirmed. This can be done by western blot for the human APP protein using a specific anti-human APP antibody on isolated circulating mouse platelets.

Aβ has also been shown to enhance human platelet aggregation *in vitro* [250, 251]. Platelets upon activation release Aβ into the circulating blood. This Aβ could then travel and reach the brain and other organs. These vascular changes may provide important clues to understanding the environment of cerebral vessels and how interactions of various molecules affect AD pathology.

It was shown that successful reconstitution of APP-KO mice with Tg2576 bone marrow induced AD pathology in the recipients. This observation not only suggests a possible role of Aβ from sources other than the brain in AD but also reiterates to the importance of scrutinizing the donor for any cell-based therapy.

6.6 Concluding Statement

To conclude, the work done in this thesis provides mechanistic insight into a possible role of soluble Aβ in the vascular pathology in a familial mouse model of AD. In a field that is constantly striving to find new therapeutics, we have shown the potential of anti-angiogenic therapeutics, one of the very few approaches that do not target any aspect of the amyloid cascade hypothesis. Most of the anti-angiogenic therapies used in this thesis have been approved as anti-cancer interventions; hence the repurposing these well-characterized candidates can expedite the translation from the pre-clinical to the clinical stage.

This work is a drop in the vast Ocean of knowledge that still needs to be uncovered to help us understand AD and to alleviate this societal burden that is ever increasing.

Bibliography

1. WHO_international, *Dementia factsheet* http://www.who.int/mediacentre/factsheets/fs362/en/, 2015.
2. Wimo, A., et al., *The worldwide costs of dementia 2015 and comparisons with 2010.* Alzheimers Dement, 2017. **13**(1): p. 1-7.
3. Alzheimer, A., *About a peculiar disease of the cerebral cortex. By Alois Alzheimer, 1907 (Translated by L. Jarvik and H. Greenson).* Alzheimer Dis Assoc Disord, 1987. **1**(1): p. 3-8.
4. Glenner, G.G. and C.W. Wong, *Alzheimer's disease: initial report of the purification and characterization of a novel cerebrovascular amyloid protein. 1984.* Biochem Biophys Res Commun, 2012. **425**(3): p. 534-9.
5. Glenner, G.G. and C.W. Wong, *Alzheimer's disease: initial report of the purification and characterization of a novel cerebrovascular amyloid protein.* Biochem Biophys Res Commun, 1984. **120**(3): p. 885-90.
6. Gorevic, P.D., et al., *Isolation and partial characterization of neurofibrillary tangles and amyloid plaque core in Alzheimer's disease: immunohistological studies.* J Neuropathol Exp Neurol, 1986. **45**(6): p. 647-64.
7. Zanetti, O., S.B. Solerte, and F. Cantoni, *Life expectancy in Alzheimer's disease (AD).* Arch Gerontol Geriatr, 2009. **49 Suppl 1**: p. 237-43.
8. Minati, L., et al., *Current concepts in Alzheimer's disease: a multidisciplinary review.* Am J Alzheimers Dis Other Demen, 2009. **24**(2): p. 95-121.
9. Alzheimer, A., *Über eine eigenartige Erkrankung der Hirnrinde.* Centralblatt für Nervenheilkunde und Psychiatrie 1907. **18**: p. 177-179.
10. Masters, C.L., et al., *Amyloid plaque core protein in Alzheimer disease and Down syndrome.* Proc Natl Acad Sci U S A, 1985. **82**(12): p. 4245-9.
11. Glenner, G.G. and C.W. Wong, *Alzheimer's disease and Down's syndrome: sharing of a unique cerebrovascular amyloid fibril protein.* Biochem Biophys Res Commun, 1984. **122**(3): p. 1131-5.
12. Hardy, J.A. and G.A. Higgins, *Alzheimer's disease: the amyloid cascade hypothesis.* Science, 1992. **256**(5054): p. 184-5.
13. Thinakaran, G. and E.H. Koo, *Amyloid precursor protein trafficking, processing, and function.* J Biol Chem, 2008. **283**(44): p. 29615-9.
14. Citron, M., et al., *Mutation of the beta-amyloid precursor protein in familial Alzheimer's disease increases beta-protein production.* Nature, 1992. **360**(6405): p. 672-4.
15. Haass, C., et al., *The Swedish mutation causes early-onset Alzheimer's disease by beta-secretase cleavage within the secretory pathway.* Nat Med, 1995. **1**(12): p. 1291-6.
16. Haass, C. and B. De Strooper, *The presenilins in Alzheimer's disease--proteolysis holds the key.* Science, 1999. **286**(5441): p. 916-9.
17. Chow, V.W., et al., *An overview of APP processing enzymes and products.* Neuromolecular Med, 2010. **12**(1): p. 1-12.

18. Kang, J., et al., *The precursor of Alzheimer's disease amyloid A4 protein resembles a cell-surface receptor.* Nature, 1987. **325**(6106): p. 733-6.
19. Jacobsen, K.T. and K. Iverfeldt, *Amyloid precursor protein and its homologues: a family of proteolysis-dependent receptors.* Cell Mol Life Sci, 2009. **66**(14): p. 2299-318.
20. Bush, A.I., et al., *The amyloid precursor protein of Alzheimer's disease is released by human platelets.* J Biol Chem, 1990. **265**(26): p. 15977-83.
21. Li, Q.X., et al., *Proteolytic processing of Alzheimer's disease beta A4 amyloid precursor protein in human platelets.* J Biol Chem, 1995. **270**(23): p. 14140-7.
22. Dyrks, T., et al., *Identification, transmembrane orientation and biogenesis of the amyloid A4 precursor of Alzheimer's disease.* EMBO J, 1988. **7**(4): p. 949-57.
23. Van Nostrand, W.E., et al., *Immunopurification and protease inhibitory properties of protease nexin-2/amyloid beta-protein precursor.* J Biol Chem, 1990. **265**(17): p. 9591-4.
24. Smith, R.P., D.A. Higuchi, and G.J. Broze, Jr., *Platelet coagulation factor XIa-inhibitor, a form of Alzheimer amyloid precursor protein.* Science, 1990. **248**(4959): p. 1126-8.
25. Schmaier, A.H., et al., *Protease nexin-2/amyloid beta protein precursor. A tight-binding inhibitor of coagulation factor IXa.* J Clin Invest, 1993. **92**(5): p. 2540-5.
26. Mahdi, F., W.E. Van Nostrand, and A.H. Schmaier, *Protease nexin-2/amyloid beta-protein precursor inhibits factor Xa in the prothrombinase complex.* J Biol Chem, 1995. **270**(40): p. 23468-74.
27. Wasco, W., et al., *Identification of a mouse brain cDNA that encodes a protein related to the Alzheimer disease-associated amyloid beta protein precursor.* Proc Natl Acad Sci U S A, 1992. **89**(22): p. 10758-62.
28. Wasco, W., et al., *Isolation and characterization of APLP2 encoding a homologue of the Alzheimer's associated amyloid beta protein precursor.* Nat Genet, 1993. **5**(1): p. 95-100.
29. De Strooper, B., R. Vassar, and T. Golde, *The secretases: enzymes with therapeutic potential in Alzheimer disease.* Nat Rev Neurol, 2010. **6**(2): p. 99-107.
30. Hiltunen, M., T. van Groen, and J. Jolkkonen, *Functional roles of amyloid-beta protein precursor and amyloid-beta peptides: evidence from experimental studies.* J Alzheimers Dis, 2009. **18**(2): p. 401-12.
31. Mattson, M.P., et al., *Evidence for excitoprotective and intraneuronal calcium-regulating roles for secreted forms of the beta-amyloid precursor protein.* Neuron, 1993. **10**(2): p. 243-54.
32. Ring, S., et al., *The secreted beta-amyloid precursor protein ectodomain APPs alpha is sufficient to rescue the anatomical, behavioral, and electrophysiological abnormalities of APP-deficient mice.* J Neurosci, 2007. **27**(29): p. 7817-26.
33. Herms, J., et al., *Cortical dysplasia resembling human type 2 lissencephaly in mice lacking all three APP family members.* EMBO J, 2004. **23**(20): p. 4106-15.
34. Haass, C., et al., *Amyloid beta-peptide is produced by cultured cells during normal metabolism.* Nature, 1992. **359**(6393): p. 322-5.
35. Seubert, P., et al., *Isolation and quantification of soluble Alzheimer's beta-peptide from biological fluids.* Nature, 1992. **359**(6393): p. 325-7.

36. Shoji, M., et al., *Production of the Alzheimer amyloid beta protein by normal proteolytic processing.* Science, 1992. **258**(5079): p. 126-9.
37. Cruts, M., J. Theuns, and C. Van Broeckhoven, *Locus-specific mutation databases for neurodegenerative brain diseases.* Hum Mutat, 2012. **33**(9): p. 1340-4.
38. Van Broeck, B., C. Van Broeckhoven, and S. Kumar-Singh, *Current insights into molecular mechanisms of Alzheimer disease and their implications for therapeutic approaches.* Neurodegener Dis, 2007. **4**(5): p. 349-65.
39. Cai, X.D., T.E. Golde, and S.G. Younkin, *Release of excess amyloid beta protein from a mutant amyloid beta protein precursor.* Science, 1993. **259**(5094): p. 514-6.
40. Harrison, R.S., et al., *Amyloid peptides and proteins in review.* Rev Physiol Biochem Pharmacol, 2007. **159**: p. 1-77.
41. Jarrett, J.T., E.P. Berger, and P.T. Lansbury, Jr., *The carboxy terminus of the beta amyloid protein is critical for the seeding of amyloid formation: implications for the pathogenesis of Alzheimer's disease.* Biochemistry, 1993. **32**(18): p. 4693-7.
42. Roher, A.E., et al., *beta-Amyloid-(1-42) is a major component of cerebrovascular amyloid deposits: implications for the pathology of Alzheimer disease.* Proc Natl Acad Sci U S A, 1993. **90**(22): p. 10836-40.
43. Iwatsubo, T., et al., *Visualization of A beta 42(43) and A beta 40 in senile plaques with end-specific A beta monoclonals: evidence that an initially deposited species is A beta 42(43).* Neuron, 1994. **13**(1): p. 45-53.
44. Sakono, M. and T. Zako, *Amyloid oligomers: formation and toxicity of Abeta oligomers.* FEBS J, 2010. **277**(6): p. 1348-58.
45. Robert D. Terry, E.M., Lawrence A. Hansen, *The neuropathology of Alzheimer disease and the structural basis of its cognitive alterations*, in *Alzheimer disease*, R.D. Terry, Editor. 1999, Lippincott Williams & Wilkins: Philadelphia. p. 187–206.
46. Lambert, M.P., et al., *Diffusible, nonfibrillar ligands derived from Abeta1-42 are potent central nervous system neurotoxins.* Proc Natl Acad Sci U S A, 1998. **95**(11): p. 6448-53.
47. Lesne, S., et al., *A specific amyloid-beta protein assembly in the brain impairs memory.* Nature, 2006. **440**(7082): p. 352-7.
48. Walsh, D.M., et al., *Naturally secreted oligomers of amyloid beta protein potently inhibit hippocampal long-term potentiation in vivo.* Nature, 2002. **416**(6880): p. 535-9.
49. Wang, H.W., et al., *Soluble oligomers of beta amyloid (1-42) inhibit long-term potentiation but not long-term depression in rat dentate gyrus.* Brain Res, 2002. **924**(2): p. 133-40.
50. Bird, T.D., *Alzheimer Disease Overview*, in *GeneReviews((R))*, M.P. Adam, et al., Editors. 2015: Seattle (WA).
51. Victor A. McKusick, A.H., *ALZHEIMER DISEASE 2 # 104310*
1988 (updated:2016).
52. Nilsberth, C., et al., *The 'Arctic' APP mutation (E693G) causes Alzheimer's disease by enhanced Abeta protofibril formation.* Nat Neurosci, 2001. **4**(9): p. 887-93.
53. Cruts, M., et al., *Molecular genetic analysis of familial early-onset Alzheimer's disease linked to chromosome 14q24.3.* Hum Mol Genet, 1995. **4**(12): p. 2363-71.

54. Basun, H., et al., *Clinical and neuropathological features of the arctic APP gene mutation causing early-onset Alzheimer disease.* Arch Neurol, 2008. **65**(4): p. 499-505.
55. Di Fede, G., et al., *A Recessive Mutation in the APP Gene with Dominant-Negative Effect on Amyloidogenesis.* Science (New York, N.Y.), 2009. **323**(5920): p. 1473-1477.
56. Roks, G., et al., *Presentation of amyloidosis in carriers of the codon 692 mutation in the amyloid precursor protein gene (APP692).* Brain, 2000. **123 (Pt 10)**: p. 2130-40.
57. Van Broeckhoven, C., et al., *Mapping of a gene predisposing to early–onset Alzheimer's disease to chromosome 14q24.3.* Nature Genetics, 1992. **2**: p. 335.
58. Campion, D., et al., *A large pedigree with early-onset Alzheimer's disease: clinical, neuropathologic, and genetic characterization.* Neurology, 1995. **45**(1): p. 80-5.
59. Sherrington, R., et al., *Cloning of a gene bearing missense mutations in early-onset familial Alzheimer's disease.* Nature, 1995. **375**: p. 754.
60. Crook, R., et al., *A variant of Alzheimer's disease with spastic paraparesis and unusual plaques due to deletion of exon 9 of presenilin 1.* Nat Med, 1998. **4**(4): p. 452-5.
61. Miklossy, J., et al., *Two novel presenilin-1 mutations (Y256S and Q222H) are associated with early-onset Alzheimer's disease.* Neurobiol Aging, 2003. **24**(5): p. 655-62.
62. Jayadev, S., et al., *Alzheimer's disease phenotypes and genotypes associated with mutations in presenilin 2.* Brain, 2010. **133**(Pt 4): p. 1143-54.
63. Cruchaga, C., et al., *Rare variants in APP, PSEN1 and PSEN2 increase risk for AD in late-onset Alzheimer's disease families.* PLoS One, 2012. **7**(2): p. e31039.
64. Jofre-Monseny, L., A.M. Minihane, and G. Rimbach, *Impact of apoE genotype on oxidative stress, inflammation and disease risk.* Mol Nutr Food Res, 2008. **52**(1): p. 131-45.
65. van der Flier, W.M., et al., *Early-onset versus late-onset Alzheimer's disease: the case of the missing APOE varepsilon4 allele.* Lancet Neurol, 2011. **10**(3): p. 280-8.
66. Pitas, R.E., et al., *Lipoproteins and their receptors in the central nervous system. Characterization of the lipoproteins in cerebrospinal fluid and identification of apolipoprotein B,E(LDL) receptors in the brain.* J Biol Chem, 1987. **262**(29): p. 14352-60.
67. Pfrieger, F.W., *Cholesterol homeostasis and function in neurons of the central nervous system.* Cell Mol Life Sci, 2003. **60**(6): p. 1158-71.
68. Nickerson, D.A., et al., *Sequence diversity and large-scale typing of SNPs in the human apolipoprotein E gene.* Genome Res, 2000. **10**(10): p. 1532-45.
69. Roses, A.D., *Apolipoprotein E alleles as risk factors in Alzheimer's disease.* Annu Rev Med, 1996. **47**: p. 387-400.
70. Tokuda, T., et al., *Lipidation of apolipoprotein E influences its isoform-specific interaction with Alzheimer's amyloid beta peptides.* Biochem J, 2000. **348 Pt 2**: p. 359-65.
71. Ma, J., et al., *Amyloid-associated proteins alpha 1-antichymotrypsin and apolipoprotein E promote assembly of Alzheimer beta-protein into filaments.* Nature, 1994. **372**(6501): p. 92-4.

72. Cam, J.A. and G. Bu, *Modulation of beta-amyloid precursor protein trafficking and processing by the low density lipoprotein receptor family.* Mol Neurodegener, 2006. **1**: p. 8.
73. Sagare, A., et al., *Clearance of amyloid-beta by circulating lipoprotein receptors.* Nat Med, 2007. **13**(9): p. 1029-31.
74. Jonsson, T., et al., *A mutation in APP protects against Alzheimer's disease and age-related cognitive decline.* Nature, 2012. **488**(7409): p. 96-9.
75. Blass, J.P. and G.E. Gibson, *Cerebrometabolic aspects of delirium in relationship to dementia.* Dement Geriatr Cogn Disord, 1999. **10**(5): p. 335-8.
76. Blass, J.P., R.K. Sheu, and G.E. Gibson, *Inherent abnormalities in energy metabolism in Alzheimer disease. Interaction with cerebrovascular compromise.* Ann N Y Acad Sci, 2000. **903**: p. 204-21.
77. Maurer, I., S. Zierz, and H.J. Moller, *A selective defect of cytochrome c oxidase is present in brain of Alzheimer disease patients.* Neurobiol Aging, 2000. **21**(3): p. 455-62.
78. Keith Crutcher, S.R., *Challenging Views of Alzheimer's Disease.* https://www.alzforum.org/news/conference-coverage/challenging-views-alzheimers-disease-meeting-notes, 2001.
79. Mattson, M.P., *Pathways towards and away from Alzheimer's disease.* Nature, 2004. **430**(7000): p. 631-9.
80. Grant, W.B., et al., *The significance of environmental factors in the etiology of Alzheimer's disease.* J Alzheimers Dis, 2002. **4**(3): p. 179-89.
81. Lahiri, D.K., K. Sambamurti, and D.A. Bennett, *Apolipoprotein gene and its interaction with the environmentally driven risk factors: molecular, genetic and epidemiological studies of Alzheimer's disease.* Neurobiol Aging, 2004. **25**(5): p. 651-60.
82. Van Duijn, C.M., et al., *Interaction between genetic and environmental risk factors for Alzheimer's disease: a reanalysis of case-control studies.* Genet Epidemiol, 1994. **11**(6): p. 539-51.
83. Chouliaras, L., et al., *Gene-environment interaction research and transgenic mouse models of Alzheimer's disease.* Int J Alzheimers Dis, 2010. **2010**.
84. Veerappan, C.S., S. Sleiman, and G. Coppola, *Epigenetics of Alzheimer's disease and frontotemporal dementia.* Neurotherapeutics, 2013. **10**(4): p. 709-21.
85. Selkoe, D.J., *The molecular pathology of Alzheimer's disease.* Neuron, 1991. **6**(4): p. 487-98.
86. Pimplikar, S.W., *Reassessing the amyloid cascade hypothesis of Alzheimer's disease.* Int J Biochem Cell Biol, 2009. **41**(6): p. 1261-8.
87. Hardy, J., *The amyloid hypothesis for Alzheimer's disease: a critical reappraisal.* J Neurochem, 2009. **110**(4): p. 1129-34.
88. de la Torre, J.C., *Alzheimer's disease: how does it start?* J Alzheimers Dis, 2002. **4**(6): p. 497-512.
89. Mielke, R., et al., *Regional cerebral glucose metabolism and postmortem pathology in Alzheimer's disease.* Acta Neuropathol, 1996. **91**(2): p. 174-9.
90. Davis, D.G., et al., *Alzheimer neuropathologic alterations in aged cognitively normal subjects.* J Neuropathol Exp Neurol, 1999. **58**(4): p. 376-88.

91. Jansen, W.J., et al., *Prevalence of cerebral amyloid pathology in persons without dementia: a meta-analysis.* JAMA, 2015. **313**(19): p. 1924-38.
92. Abbott, A. and E. Dolgin, *Failed Alzheimer's trial does not kill leading theory of disease.* Nature, 2016. **540**(7631): p. 15-16.
93. Cummings, J.L., T. Morstorf, and K. Zhong, *Alzheimer's disease drug-development pipeline: few candidates, frequent failures.* Alzheimers Res Ther, 2014. **6**(4): p. 37.
94. Claassen, J.A. and R. Zhang, *Cerebral autoregulation in Alzheimer's disease.* J Cereb Blood Flow Metab, 2011. **31**(7): p. 1572-7.
95. Pfeifer, M., et al., *Cerebral hemorrhage after passive anti-Abeta immunotherapy.* Science, 2002. **298**(5597): p. 1379.
96. Biron, K.E., et al., *Amyloid triggers extensive cerebral angiogenesis causing blood brain barrier permeability and hypervascularity in Alzheimer's disease.* PLoS One, 2011. **6**(8): p. e23789.
97. Chaahat Singh, C.G.P.a.W.A.J., *Pathogenic Angiogenic Mechanisms in Alzheimer's Disease*, in *Physiologic and Pathologic Angiogenesis*, D. Simionescu, Editor. 2017, IntechOpen. p. 93-109.
98. Jefferies, W.A., et al., *Adjusting the compass: new insights into the role of angiogenesis in Alzheimer's disease.* Alzheimers Res Ther, 2013. **5**(6): p. 64.
99. Desai, B.S., et al., *Evidence of angiogenic vessels in Alzheimer's disease.* J Neural Transm (Vienna), 2009. **116**(5): p. 587-97.
100. Vagnucci, A.H., Jr. and W.W. Li, *Alzheimer's disease and angiogenesis.* Lancet, 2003. **361**(9357): p. 605-8.
101. Ujiie, M., et al., *Blood-brain barrier permeability precedes senile plaque formation in an Alzheimer disease model.* Microcirculation, 2003. **10**(6): p. 463-70.
102. Iadecola, C., *Neurovascular regulation in the normal brain and in Alzheimer's disease.* Nat Rev Neurosci, 2004. **5**(5): p. 347-60.
103. Ruitenberg, A., et al., *Cerebral hypoperfusion and clinical onset of dementia: the Rotterdam Study.* Ann Neurol, 2005. **57**(6): p. 789-94.
104. Attems, J. and K.A. Jellinger, *The overlap between vascular disease and Alzheimer's disease - lessons from pathology.* BMC Medicine, 2014. **12**(1): p. 206.
105. Kövari, E., et al., *The relationship between cerebral amyloid angiopathy and cortical microinfarcts in brain ageing and Alzheimer's disease.* Neuropathology and applied neurobiology, 2013. **39**(5): p. 498-509.
106. Brenowitz, W.D., et al., *Cerebral amyloid angiopathy and its co-occurrence with Alzheimer's disease and other cerebrovascular neuropathologic changes.* Neurobiology of aging, 2015. **36**(10): p. 2702-2708.
107. Buée, L., et al., *Pathological alterations of the cerebral microvasculature in Alzheimer's disease and related dementing disorders.* Acta Neuropathologica, 1994. **87**(5): p. 469-480.
108. BuÉE, L.U.C., P.R. Hof, and A. Delacourte, *Brain Microvascular Changes in Alzheimer's Disease and Other Dementias.* Annals of the New York Academy of Sciences. **826**(1 cerebrovascul): p. 7-24.
109. Bouras, C., et al., *Stereologic Analysis of Microvascular Morphology in the Elderly: Alzheimer Disease Pathology and Cognitive Status.* Journal of Neuropathology and Experimental Neurology, 2006. **65**(3): p. 235-244.

110. Li, D., et al., *Mutations of Presenilin Genes in Dilated Cardiomyopathy and Heart Failure.* American Journal of Human Genetics, 2006. **79**(6): p. 1030-1039.
111. Jefferies, W.A., et al., *Reactive microglia specifically associated with amyloid plaques in Alzheimer's disease brain tissue express melanotransferrin.* Brain Research, 1996. **712**(1): p. 122-126.
112. Sala, R., et al., *The human melanoma associated protein melanotransferrin promotes endothelial cell migration and angiogenesis in vivo.* European journal of cell biology, 2002. **81**(11): p. 599-607.
113. Yamada, T., et al., *Possible roles of transglutaminases in Alzheimer"s disease.* Dementia and geriatric cognitive disorders, 1998. **9**(2): p. 103-110.
114. Martin, A., G. De Vivo, and V. Gentile, *Possible role of the transglutaminases in the pathogenesis of Alzheimer's disease and other neurodegenerative diseases.* Int J Alzheimers Dis, 2011. **2011**: p. 865432.
115. Zlokovic, B.V., *The blood-brain barrier in health and chronic neurodegenerative disorders.* Neuron, 2008. **57**(2): p. 178-201.
116. Begley, D.J. and M.W. Brightman, *Structural and functional aspects of the blood-brain barrier.* Prog Drug Res, 2003. **61**: p. 39-78.
117. Cecchelli, R., et al., *Modelling of the blood-brain barrier in drug discovery and development.* Nat Rev Drug Discov, 2007. **6**(8): p. 650-61.
118. Kook, S.Y., et al., *Disruption of blood-brain barrier in Alzheimer disease pathogenesis.* Tissue Barriers, 2013. **1**(2): p. e23993.
119. Erickson, M.A. and W.A. Banks, *Blood-brain barrier dysfunction as a cause and consequence of Alzheimer's disease.* J Cereb Blood Flow Metab, 2013. **33**(10): p. 1500-13.
120. Banks, W.A., et al., *Lipopolysaccharide-induced blood-brain barrier disruption: roles of cyclooxygenase, oxidative stress, neuroinflammation, and elements of the neurovascular unit.* J Neuroinflammation, 2015. **12**: p. 223.
121. Abbott, N.J., et al., *Structure and function of the blood-brain barrier.* Neurobiol Dis, 2010. **37**(1): p. 13-25.
122. Armulik, A., et al., *Pericytes regulate the blood-brain barrier.* Nature, 2010. **468**(7323): p. 557-61.
123. Abbott, N.J., L. Ronnback, and E. Hansson, *Astrocyte-endothelial interactions at the blood-brain barrier.* Nat Rev Neurosci, 2006. **7**(1): p. 41-53.
124. Arai, T., et al., *Thrombin and prothrombin are expressed by neurons and glial cells and accumulate in neurofibrillary tangles in Alzheimer disease brain.* J Neuropathol Exp Neurol, 2006. **65**(1): p. 19-25.
125. Zipser, B.D., et al., *Microvascular injury and blood-brain barrier leakage in Alzheimer's disease.* Neurobiol Aging, 2007. **28**(7): p. 977-86.
126. Lewczuk, P., et al., *Prothrombin concentration in the cerebrospinal fluid is not altered in Alzheimer's disease.* Neurochem Res, 1999. **24**(12): p. 1531-4.
127. L. Shinde, R., A. Jindal, and P. Devarajan, *Microemulsions and Nanoemulsions for Targeted Drug Delivery to the Brain*. Vol. 7. 2011. 119-133.
128. Benarroch, E.E., *Blood–brain barrier.* Recent developments and clinical correlations, 2012. **78**(16): p. 1268-1276.

129. Rosenberg, G.A., *Blood-Brain Barrier Permeability in Aging and Alzheimer's Disease.* J Prev Alzheimers Dis, 2014. **1**(3): p. 138-139.
130. Ujiie, M., et al., *Blood-brain barrier permeability precedes senile plaque formation in an Alzheimer disease model.* Microcirculation, 2003. **10**: p. 463-70.
131. Desai, B.S., et al., *Evidence of angiogenic vessels in Alzheimer's disease.* J Neural Transm, 2009. **116**(5): p. 587-97.
132. Austin, B.P., et al., *Effects of hypoperfusion in Alzheimer's disease.* J Alzheimers Dis, 2011. **26 Suppl 3**: p. 123-33.
133. Thomas, T., S. Miners, and S. Love, *Post-mortem assessment of hypoperfusion of cerebral cortex in Alzheimer's disease and vascular dementia.* Brain, 2015. **138**(Pt 4): p. 1059-69.
134. Olichney, J.M., et al., *The apolipoprotein E epsilon 4 allele is associated with increased neuritic plaques and cerebral amyloid angiopathy in Alzheimer's disease and Lewy body variant.* Neurology, 1996. **47**(1): p. 190-6.
135. Verghese, P.B., J.M. Castellano, and D.M. Holtzman, *Apolipoprotein E in Alzheimer's disease and other neurological disorders.* Lancet Neurol, 2011. **10**(3): p. 241-52.
136. D'Esposito, M., W. Jagust, and A. Gazzaley, *Methodological and conceptual issues in the study of the aging brain*. Imaging of the Aging Brain. 2009: Oxford University Press.
137. Selkoe, D.J., *Toward a comprehensive theory for Alzheimer's disease. Hypothesis: Alzheimer's disease is caused by the cerebral accumulation and cytotoxicity of amyloid beta-protein.* Ann N Y Acad Sci, 2000. **924**: p. 17-25.
138. Kara, F., et al., *Monitoring blood flow alterations in the Tg2576 mouse model of Alzheimer's disease by in vivo magnetic resonance angiography at 17.6 T.* Neuroimage, 2012. **60**(2): p. 958-66.
139. Beckmann, N., et al., *Age-dependent cerebrovascular abnormalities and blood flow disturbances in APP23 mice modeling Alzheimer's disease.* J Neurosci, 2003. **23**(24): p. 8453-9.
140. Thal, D.R., et al., *Capillary cerebral amyloid angiopathy is associated with vessel occlusion and cerebral blood flow disturbances.* Neurobiol Aging, 2009. **30**(12): p. 1936-48.
141. Pfeifer, L.A., et al., *Cerebral amyloid angiopathy and cognitive function: the HAAS autopsy study.* Neurology, 2002. **58**(11): p. 1629-34.
142. de la Torre, J.C. and T. Mussivand, *Can disturbed brain microcirculation cause Alzheimer's disease?* Neurol Res, 1993. **15**(3): p. 146-53.
143. de la Torre, J.C., *How do heart disease and stroke become risk factors for Alzheimer's disease?* Neurol Res,, 2006. **28**(6): p. 637-44.
144. Rose, J.A., S. Erzurum, and K. Asosingh, *Biology and flow cytometry of proangiogenic hematopoietic progenitors cells.* Cytometry A, 2015. **87**(1): p. 5-19.
145. Patan, S., *Vasculogenesis and angiogenesis.* Cancer Treat Res, 2004. **117**: p. 3-32.
146. Herbert, S.P. and D.Y. Stainier, *Molecular control of endothelial cell behaviour during blood vessel morphogenesis.* Nat Rev Mol Cell Biol, 2011. **12**(9): p. 551-64.

147. Chiarini, A., et al., *Amyloid-beta(25-35), an amyloid-beta(1-42) surrogate, and proinflammatory cytokines stimulate VEGF-A secretion by cultured, early passage, normoxic adult human cerebral astrocytes.* J Alzheimers Dis, 2010. **21**(3): p. 915-26.
148. Pogue, A.I. and W.J. Lukiw, *Angiogenic signaling in Alzheimer's disease.* Neuroreport, 2004. **15**(9): p. 1507-10.
149. Meyer, E.P., et al., *Altered morphology and 3D architecture of brain vasculature in a mouse model for Alzheimer's disease.* Proc Natl Acad Sci U S A, 2008. **105**(9): p. 3587-92.
150. Schultheiss, C., et al., *In vivo characterization of endothelial cell activation in a transgenic mouse model of Alzheimer's disease.* Angiogenesis, 2006. **9**(2): p. 59-65.
151. Selkoe, D.J., *The cell biology of beta-amyloid precursor protein and presenilin in Alzheimer's disease.* Trends Cell Biol, 1998. **8**(11): p. 447-53.
152. Selkoe, D.J., *Translating cell biology into therapeutic advances in Alzheimer's disease.* Nature, 1999. **399**(6738 Suppl): p. A23-31.
153. Morris, G.P., I.A. Clark, and B. Vissel, *Inconsistencies and controversies surrounding the amyloid hypothesis of Alzheimer's disease.* Acta Neuropathol Commun, 2014. **2**: p. 135.
154. Biron, K.E., et al., *Cessation of neoangiogenesis in Alzheimer's disease follows amyloid-beta immunization.* Sci Rep, 2013. **3**: p. 1354.
155. Cortes-Canteli, M., et al., *Fibrinogen and beta-amyloid association alters thrombosis and fibrinolysis: a possible contributing factor to Alzheimer's disease.* Neuron, 2010. **66**(5): p. 695-709.
156. Zamolodchikov, D. and S. Strickland, *Abeta delays fibrin clot lysis by altering fibrin structure and attenuating plasminogen binding to fibrin.* Blood, 2012. **119**(14): p. 3342-51.
157. Paul, J., S. Strickland, and J.P. Melchor, *Fibrin deposition accelerates neurovascular damage and neuroinflammation in mouse models of Alzheimer's disease.* J Exp Med, 2007. **204**(8): p. 1999-2008.
158. Fioravanzo, L., et al., *Involvement of rat hippocampal astrocytes in beta-amyloid-induced angiogenesis and neuroinflammation.* Curr Alzheimer Res, 2010. **7**(7): p. 591-601.
159. Boulton, M.E., J. Cai, and M.B. Grant, *gamma-Secretase: a multifaceted regulator of angiogenesis.* J Cell Mol Med, 2008. **12**(3): p. 781-95.
160. Boscolo, E., et al., *Beta amyloid angiogenic activity in vitro and in vivo.* Int J Mol Med, 2007. **19**(4): p. 581-7.
161. Schreitm, et al., *Elevated Angiopoietin-1 Serum Levels in Patients with Alzheimer’s Disease.* International Journal of Alzheimer’s Disease, 2012. **2012**: p. 5.
162. Johnston, H., H. Boutin, and S.M. Allan, *Assessing the contribution of inflammation in models of Alzheimer's disease.* Biochem Soc Trans, 2011. **39**(4): p. 886-90.
163. Yan, S.D., et al., *RAGE and amyloid-beta peptide neurotoxicity in Alzheimer's disease.* Nature, 1996. **382**(6593): p. 685-91.
164. Mackic, J.B., et al., *Human blood-brain barrier receptors for Alzheimer's amyloid-beta 1- 40. Asymmetrical binding, endocytosis, and transcytosis at the apical side of*

brain microvascular endothelial cell monolayer. J Clin Invest, 1998. **102**(4): p. 734-43.
165. Stern, D., et al., *Receptor for advanced glycation endproducts: a multiligand receptor magnifying cell stress in diverse pathologic settings.* Adv Drug Deliv Rev, 2002. **54**(12): p. 1615-25.
166. Deane, R., et al., *RAGE mediates amyloid-beta peptide transport across the blood-brain barrier and accumulation in brain.* Nat Med, 2003. **9**(7): p. 907-13.
167. McMichael, M., *New models of hemostasis.* Top Companion Anim Med, 2012. **27**(2): p. 40-5.
168. Versteeg, H.H., et al., *New fundamentals in hemostasis.* Physiol Rev, 2013. **93**(1): p. 327-58.
169. Alzforum, https://www.alzforum.org/research-models/alzheimers-disease.
170. Games, D., et al., *Alzheimer-type neuropathology in transgenic mice overexpressing V717F beta-amyloid precursor protein.* Nature, 1995. **373**(6514): p. 523-7.
171. Moechars, D., et al., *Early phenotypic changes in transgenic mice that overexpress different mutants of amyloid precursor protein in brain.* J Biol Chem, 1999. **274**(10): p. 6483-92.
172. Hsiao, K., et al., *Correlative memory deficits, Abeta elevation, and amyloid plaques in transgenic mice.* Science, 1996. **274**(5284): p. 99-102.
173. Sturchler-Pierrat, C., et al., *Two amyloid precursor protein transgenic mouse models with Alzheimer disease-like pathology.* Proc Natl Acad Sci U S A, 1997. **94**(24): p. 13287-92.
174. Chishti, M.A., et al., *Early-onset amyloid deposition and cognitive deficits in transgenic mice expressing a double mutant form of amyloid precursor protein 695.* J Biol Chem, 2001. **276**(24): p. 21562-70.
175. Herzig, M.C., et al., *Abeta is targeted to the vasculature in a mouse model of hereditary cerebral hemorrhage with amyloidosis.* Nat Neurosci, 2004. **7**(9): p. 954-60.
176. Davis, J., et al., *Early-onset and robust cerebral microvascular accumulation of amyloid beta-protein in transgenic mice expressing low levels of a vasculotropic Dutch/Iowa mutant form of amyloid beta-protein precursor.* J Biol Chem, 2004. **279**(19): p. 20296-306.
177. Lord, A., et al., *The Arctic Alzheimer mutation facilitates early intraneuronal Abeta aggregation and senile plaque formation in transgenic mice.* Neurobiol Aging, 2006. **27**(1): p. 67-77.
178. Oddo, S., et al., *Triple-transgenic model of Alzheimer's disease with plaques and tangles: intracellular Abeta and synaptic dysfunction.* Neuron, 2003. **39**(3): p. 409-21.
179. Oakley, H., et al., *Intraneuronal beta-amyloid aggregates, neurodegeneration, and neuron loss in transgenic mice with five familial Alzheimer's disease mutations: potential factors in amyloid plaque formation.* J Neurosci, 2006. **26**(40): p. 10129-40.
180. Philipson, O., et al., *Animal models of amyloid-beta-related pathologies in Alzheimer's disease.* FEBS J, 2010. **277**(6): p. 1389-409.

181. Mullan, M., et al., *A pathogenic mutation for probable Alzheimer's disease in the APP gene at the N-terminus of beta-amyloid.* Nat Genet, 1992. **1**(5): p. 345-7.
182. Chávez-Gutiérrez, L., et al., *The mechanism of γ-Secretase dysfunction in familial Alzheimer disease.* The EMBO journal, 2012. **31**(10): p. 2261-2274.
183. Vassar, R., et al., *Beta-secretase cleavage of Alzheimer's amyloid precursor protein by the transmembrane aspartic protease BACE.* Science, 1999. **286**(5440): p. 735-41.
184. Reaume, A.G., et al., *Enhanced amyloidogenic processing of the beta-amyloid precursor protein in gene-targeted mice bearing the Swedish familial Alzheimer's disease mutations and a "humanized" Abeta sequence.* J Biol Chem, 1996. **271**(38): p. 23380-8.
185. Flood, D.G., et al., *FAD mutant PS-1 gene-targeted mice: increased A beta 42 and A beta deposition without APP overproduction.* Neurobiol Aging, 2002. **23**(3): p. 335-48.
186. Van Dam, D., et al., *Age-dependent cognitive decline in the APP23 model precedes amyloid deposition.* Eur J Neurosci, 2003. **17**(2): p. 388-96.
187. Winkler, D.T., et al., *Spontaneous hemorrhagic stroke in a mouse model of cerebral amyloid angiopathy.* J Neurosci, 2001. **21**(5): p. 1619-27.
188. Hsiao, K.K., et al., *Age-related CNS disorder and early death in transgenic FVB/N mice overexpressing Alzheimer amyloid precursor proteins.* Neuron, 1995. **15**(5): p. 1203-18.
189. Domnitz, S.B., et al., *Progression of cerebral amyloid angiopathy in transgenic mouse models of Alzheimer disease.* J Neuropathol Exp Neurol, 2005. **64**(7): p. 588-94.
190. Dickstein, D.L., et al., *A{beta} peptide immunization restores blood-brain barrier integrity in Alzheimer disease.* Faseb J, 2006. **20**(3): p. 426-33.
191. Lee, E.B., et al., *Meningoencephalitis associated with passive immunization of a transgenic murine model of Alzheimer's amyloidosis.* FEBS Lett, 2005. **579**(12): p. 2564-8.
192. Kumar-Singh, S., et al., *Dense-core plaques in Tg2576 and PSAPP mouse models of Alzheimer's disease are centered on vessel walls.* Am J Pathol, 2005. **167**(2): p. 527-43.
193. Irizarry, M.C., et al., *APPSw transgenic mice develop age-related A beta deposits and neuropil abnormalities, but no neuronal loss in CA1.* J Neuropathol Exp Neurol, 1997. **56**(9): p. 965-73.
194. Frautschy, S.A., et al., *Microglial response to amyloid plaques in APPsw transgenic mice.* Am J Pathol, 1998. **152**(1): p. 307-17.
195. Pappolla, M.A., et al., *Evidence of oxidative stress and in vivo neurotoxicity of beta-amyloid in a transgenic mouse model of Alzheimer's disease: a chronic oxidative paradigm for testing antioxidant therapies in vivo.* Am J Pathol, 1998. **152**(4): p. 871-7.
196. Hsiao, K., et al., *Correlative Memory Deficits, Aβ Elevation, and Amyloid Plaques in Transgenic Mice.* Science, 1996. **274**(5284): p. 99-103.
197. Powles, T., et al., *Sunitinib and other targeted therapies for renal cell carcinoma.* Br J Cancer, 2011. **104**(5): p. 741-5.

198. Grammas, P., et al., *A new paradigm for the treatment of Alzheimer's disease: targeting vascular activation.* J Alzheimers Dis, 2014. **40**(3): p. 619-30.
199. Barrascout, E., et al., *[Angiogenesis inhibition: review of the activity of sorafenib, sunitinib and bevacizumab]*. Bull Cancer, 2010. **97**: p. 29-43.
200. Kazazi-Hyseni, F., J.H. Beijnen, and J.H.M. Schellens, *Bevacizumab.* The oncologist, 2010. **15**(8): p. 819-825.
201. Pavletic, S.Z., et al., *Unrelated Donor Marrow Transplantation for B-Cell Chronic Lymphocytic Leukemia After Using Myeloablative Conditioning: Results From the Center for International Blood and Marrow Transplant Research.* Journal of Clinical Oncology, 2005. **23**(24): p. 5788-5794.
202. Rashidi, A., M. Ebadi, and A.F. Cashen, *Allogeneic hematopoietic stem cell transplantation in Hodgkin lymphoma: a systematic review and meta-analysis.* Bone marrow transplantation, 2016. **51**(4): p. 521-528.
203. Liu, M., et al., *Hematopoietic Stem Cell Transplantation for Treatment of Patients with Leukemia Concomitant with Active Tuberculosis Infection.* Medical Science Monitor : International Medical Journal of Experimental and Clinical Research, 2014. **20**: p. 2484-2488.
204. Lampron, A., D. Gosselin, and S. Rivest, *Targeting the hematopoietic system for the treatment of Alzheimer's disease.* Brain, Behavior, and Immunity, 2011. **25**: p. S71-S79.
205. Magga, J., et al., *Production of monocytic cells from bone marrow stem cells: therapeutic usage in Alzheimer's disease.* Journal of Cellular and Molecular Medicine, 2012. **16**(5): p. 1060-1073.
206. Lee, J.K., H.K. Jin, and J.-s. Bae, *Bone marrow-derived mesenchymal stem cells reduce brain amyloid-β deposition and accelerate the activation of microglia in an acutely induced Alzheimer's disease mouse model.* Neuroscience Letters, 2009. **450**(2): p. 136-141.
207. Lee, J.K., et al., *Soluble CCL5 Derived from Bone Marrow-Derived Mesenchymal Stem Cells and Activated by Amyloid β Ameliorates Alzheimer's Disease in Mice by Recruiting Bone Marrow-Induced Microglia Immune Responses.* STEM CELLS, 2012. **30**(7): p. 1544-1555.
208. Dobson, K.R., et al., *Centrifugal Isolation of Bone Marrow from Bone: An Improved Method for the Recovery and Quantitation of Bone Marrow Osteoprogenitor Cells from Rat Tibiae and Femurae.* Calcified Tissue International, 1999. **65**(5): p. 411-413.
209. Volocity_user_guide, *Volocity User Guide.* http://cellularimaging.perkinelmer.com/pdfs/manuals/VolocityUserGuide.pdf, 2011.
210. Chen, P.C., et al., *Activation of multiple signaling pathways causes developmental defects in mice with a Noonan syndrome-associated Sos1 mutation.* J Clin Invest, 2010. **120**(12): p. 4353-65.
211. O'Hara, S.D. and R.L. Garcea, *Murine Polyomavirus Cell Surface Receptors Activate Distinct Signaling Pathways Required for Infection.* MBio, 2016. **7**(6).
212. Dickstein, D.L., et al., *Abeta peptide immunization restores blood-brain barrier integrity in Alzheimer disease.* FASEB J, 2006. **20**(3): p. 426-33.

213. Zlokovic, B.V., *Neurovascular pathways to neurodegeneration in Alzheimer's disease and other disorders.* Nat Rev Neurosci, 2011. **12**(12): p. 723-38.
214. Aparicio-Gallego, G., et al., *New Insights into Molecular Mechanisms of Sunitinib-Associated Side Effects.* Molecular Cancer Therapeutics, 2011. **10**(12): p. 2215-2223.
215. Verheul, H.M. and H.M. Pinedo, *The role of vascular endothelial growth factor (VEGF) in tumor angiogenesis and early clinical development of VEGF-receptor kinase inhibitors.* Clin Breast Cancer, 2000. **1 Suppl 1**: p. S80-4.
216. Carmeliet, P., *VEGF as a key mediator of angiogenesis in cancer.* Oncology, 2005. **69 Suppl 3**: p. 4-10.
217. Bruns, C.J., et al., *Effect of the vascular endothelial growth factor receptor-2 antibody DC101 plus gemcitabine on growth, metastasis and angiogenesis of human pancreatic cancer growing orthotopically in nude mice.* Int J Cancer, 2002. **102**(2): p. 101-8.
218. Franco, M., et al., *Targeted anti-vascular endothelial growth factor receptor-2 therapy leads to short-term and long-term impairment of vascular function and increase in tumor hypoxia.* Cancer Res, 2006. **66**(7): p. 3639-48.
219. Miller, D.W., et al., *Rapid vessel regression, protease inhibition, and stromal normalization upon short-term vascular endothelial growth factor receptor 2 inhibition in skin carcinoma heterotransplants.* Am J Pathol, 2005. **167**(5): p. 1389-403.
220. Falcon, B.L., et al., *Antagonist antibodies to vascular endothelial growth factor receptor 2 (VEGFR-2) as anti-angiogenic agents.* Pharmacol Ther, 2016. **164**: p. 204-25.
221. Kawarabayashi, T., et al., *Age-Dependent Changes in Brain, CSF, and Plasma Amyloid β Protein in the Tg2576 Transgenic Mouse Model of Alzheimer's Disease.* The Journal of Neuroscience, 2001. **21**(2): p. 372-381.
222. Lee, K.-W., et al., *Behavioral stress accelerates plaque pathogenesis in the brain of Tg2576 mice via generation of metabolic oxidative stress.* Journal of Neurochemistry, 2009. **108**(1): p. 165-175.
223. Matsumoto, T., et al., *VEGF receptor-2 Y951 signaling and a role for the adapter molecule TSAd in tumor angiogenesis.* EMBO J, 2005. **24**(13): p. 2342-53.
224. Shalaby, F., et al., *Failure of blood-island formation and vasculogenesis in Flk-1-deficient mice.* Nature, 1995. **376**(6535): p. 62-6.
225. Sakurai, Y., et al., *Essential role of Flk-1 (VEGF receptor 2) tyrosine residue 1173 in vasculogenesis in mice.* Proc Natl Acad Sci U S A, 2005. **102**(4): p. 1076-81.
226. BC_Cancer_Agency. *Drug Index (Professional): The BC Cancer Agency's Cancer Drug Manual*. 2015; Available from: http://www.bccancer.bc.ca/HPI/DrugDatabase/DrugIndexPro/default.htm.
227. Wikipedia_contributors, *Axitinib.* https://en.wikipedia.org/wiki/Axitinib, 2018.
228. Yuan, H.T., et al., *Angiopoietin 2 is a partial agonist/antagonist of Tie2 signaling in the endothelium.* Mol Cell Biol, 2009. **29**(8): p. 2011-22.
229. Thurston, G. and C. Daly, *The complex role of angiopoietin-2 in the angiopoietin-tie signaling pathway.* Cold Spring Harb Perspect Med, 2012. **2**(9): p. a006550.

230. Hansen, T.M., et al., *Effects of angiopoietins-1 and -2 on the receptor tyrosine kinase Tie2 are differentially regulated at the endothelial cell surface.* Cell Signal, 2010. **22**(3): p. 527-32.
231. Gama Sosa, M.A., et al., *Age-Related Vascular Pathology in Transgenic Mice Expressing Presenilin 1-Associated Familial Alzheimer's Disease Mutations.* The American Journal of Pathology, 2010. **176**(1): p. 353-368.
232. Westerman, M.A., et al., *The Relationship between Aβ and Memory in the Tg2576 Mouse Model of Alzheimer's Disease.* The Journal of Neuroscience, 2002. **22**(5): p. 1858-1867.
233. Stewart, S., F. Cacucci, and C. Lever, *Which memory task for my mouse? A systematic review of spatial memory performance in the Tg2576 Alzheimer's mouse model.* Journal Of Alzheimer's Disease: JAD, 2011. **26**(1): p. 105-126.
234. Bell, R.D., et al., *Pericytes control key neurovascular functions and neuronal phenotype in the adult brain and during brain aging.* Neuron, 2010. **68**(3): p. 409-27.
235. Papetti, M. and I.M. Herman, *Mechanisms of normal and tumor-derived angiogenesis.* Am J Physiol Cell Physiol, 2002. **282**(5): p. C947-70.
236. *https://en.wikipedia.org/wiki/Vascular_endothelial_growth_factor*. 2018.
237. Fang, Y., et al., *Recent Advances: Decoding Alzheimer's Disease With Stem Cells.* Frontiers in Aging Neuroscience, 2018. **10**: p. 77.
238. Jaunmuktane, Z., et al., *Evidence for human transmission of amyloid-β pathology and cerebral amyloid angiopathy.* Nature, 2015. **525**: p. 247.
239. Doody, R.S., et al., *A Phase 3 Trial of Semagacestat for Treatment of Alzheimer's Disease.* New England Journal of Medicine, 2013. **369**(4): p. 341-350.
240. Salloway, S., et al., *Two Phase 3 Trials of Bapineuzumab in Mild-to-Moderate Alzheimer's Disease.* The New England journal of medicine, 2014. **370**(4): p. 322-333.
241. Deane, R. and B.V. Zlokovic, *Role of the blood-brain barrier in the pathogenesis of Alzheimer's disease.* Curr Alzheimer Res, 2007. **4**(2): p. 191-7.
242. Zlokovic, B.V., et al., *Brain uptake of circulating apolipoproteins J and E complexed to Alzheimer's amyloid beta.* Biochem Biophys Res Commun, 1994. **205**(2): p. 1431-7.
243. Evin, G., et al., *Proteolytic processing of the Alzheimer's disease amyloid precursor protein in brain and platelets.* J Neurosci Res, 2003. **74**(3): p. 386-92.
244. Chen, M., et al., *Platelets are the primary source of amyloid beta-peptide in human blood.* Biochem Biophys Res Commun, 1995. **213**(1): p. 96-103.
245. MATSUBARA, E., et al., *Platelet Microparticles as Carriers of Soluble Alzheimer's Amyloid β (sAβ).* Annals of the New York Academy of Sciences, 2002. **977**(1): p. 340-348.
246. Schenk, D., et al., *Immunization with amyloid-beta attenuates Alzheimer-disease-like pathology in the PDAPP mouse.* Nature, 1999. **400**(6740): p. 173-7.
247. Bard, F., et al., *Peripherally administered antibodies against amyloid beta-peptide enter the central nervous system and reduce pathology in a mouse model of Alzheimer disease.* Nat Med, 2000. **6**(8): p. 916-9.

248. Nicoll, J.A., et al., *Neuropathology of human Alzheimer disease after immunization with amyloid-beta peptide: a case report.* Nat Med, 2003. **9**(4): p. 448-52.
249. Ho, L., *Altered clot formation and anticoagulation in a familial Alzheimer's disease mouse model*, in *Microbiology and Immunology*. 2013, University of British Columbia: Vancouver. p. 101.
250. Wolozin, B., et al., *Beta-amyloid augments platelet aggregation: reduced activity of familial angiopathy-associated mutants.* Mol Psychiatry, 1998. **3**(6): p. 500-7.
251. Kowalska, M.A. and K. Badellino, *beta-Amyloid protein induces platelet aggregation and supports platelet adhesion.* Biochem Biophys Res Commun, 1994. **205**(3): p. 1829-35.